AD-A065 735 VARIAN ASSOCIATES BEVERLY MASS F/G 9/1
CFA DESIGN IMPROVEMENT PROGRAM. VOLUME I. INSTRUMENTED CFA STUD--ETC(U)
JUN 78 G K FARNEY N00123-75-C-1294
UNCLASSIFIED NL

1 OF 2
AD
AD 65735

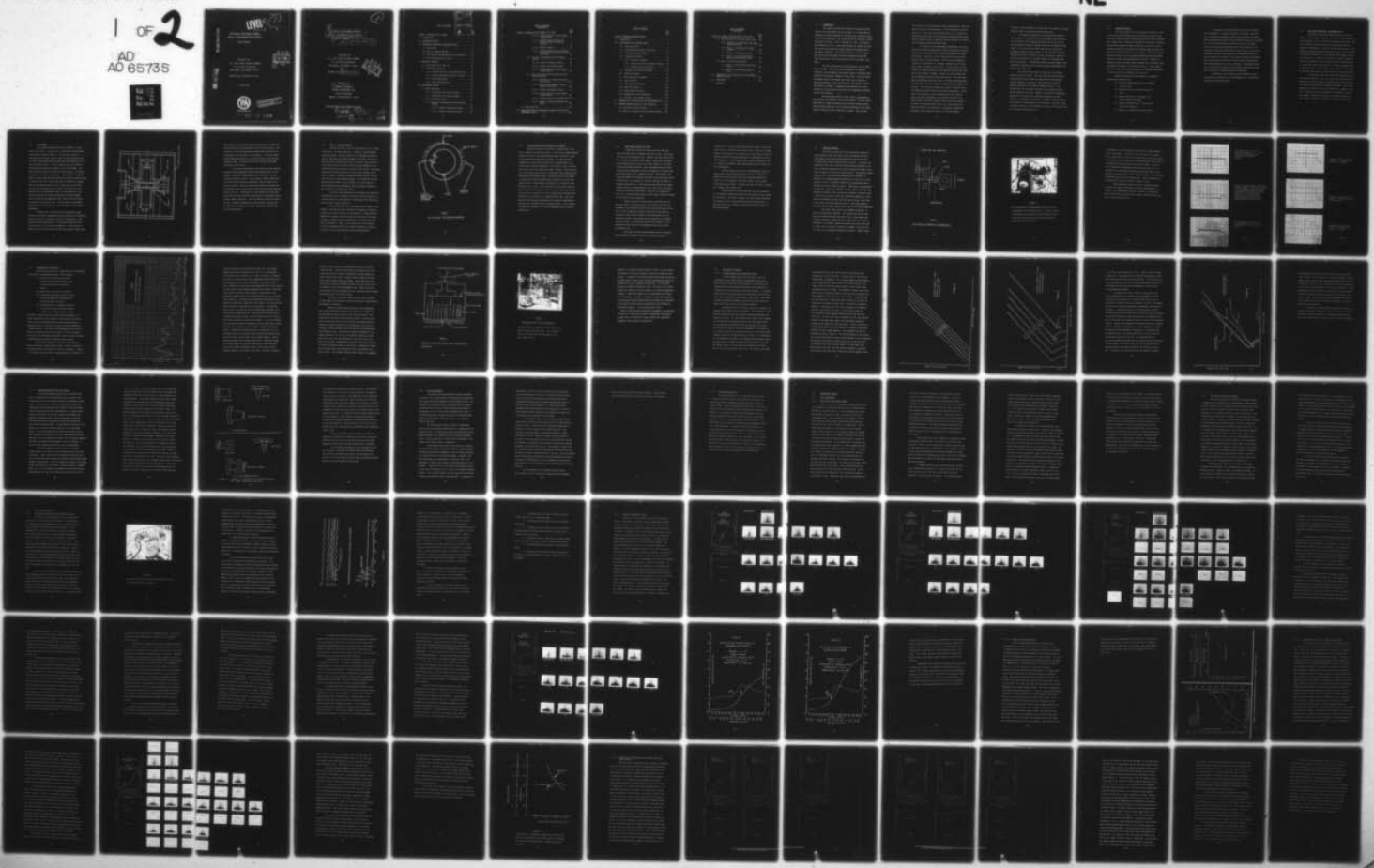

CFA Design Improvement Program
Volume I--Instrumented CFA Studies

-Final Report-

Prepared For:

U.S. Navy Ocean Systems Command

271 Catalina Boulevard

San Diego, California 92152

Contract No. N00123-75-C-1294

2 June 1978

VARIAN/BEVERLY

1.

(6)

CFA DESIGN IMPROVEMENT PROGRAM.
VOLUME I--INSTRUMENTED CFA STUDIES.

(9) FINAL REPORT.
1 Jul 75-31 Dec 77

PREPARED FOR:

U.S. NAVY OCEAN SYSTEMS COMMAND

271 CATALINA BOULEVARD

SAN DIEGO, CALIFORNIA 92152

(15) CONTRACT NO. N00123-75-C-1294

(10) PREPARED BY:

GEORGE K. FARNEY

VARIAN ASSOCIATES, INC.

EIGHT SALEM ROAD

BEVERLY, MASSACHUSETTS 01915

(11) 2 JUNE 1978

(12) 188p.

364070

TABLE OF CONTENTS

TABLE OF CONTENTS
(continued)

TABLE OF CONTENTS

TABLE OF CONTENTS
(continued)

1.0 INTRODUCTION

This report describes the technical objectives and summarizes the accomplishments during one phase of a program aimed at improving the design techniques for emitting sole, reentrant stream crossed-field amplifiers. The program efforts in this phase covered the period from July 1, 1975, to December 31, 1977. The program was sponsored by the U. S. Navy under Contract No. N00123-75-C-1294. The contract was issued by the Naval Regional Procurement Office, Long Beach, California. The technical direction of the program was initially from the Naval Electronics Laboratory Center and later from the Naval Ocean System Center, both of San Diego, California.

The total program was divided essentially into two time-phased portions. This first portion consisted of a combined theoretical and experimental investigation aimed at improving understanding of the internal workings of these tubes. From this effort new design concepts have emerged that should lead to devices of improved performance. The second portion of the program to follow will consist of attempts to demonstrate the validity of the new concepts by incorporating these features into experimental vehicles for test and evaluation.

The investigative phase to obtain better understanding of these devices was composed of two broad activities. One uses instrumented tubes to measure experimentally the actual RF power growth, noise and phase properties, and the thermal dissipation on the anode along the slow wave circuit from input to output. This was done

for a variety of interaction space design configurations. The basic vehicle used for these measurements is the SFD-261 CFA and derivatives of it. This tube was selected because it is a forward wave amplifier that has been built in sufficient numbers and been extensively evaluated so that a large data base is available for comparison as changes and modifications are made.

In addition to the experimental measurements, the second activity was aimed at developing a computer program that accurately simulates the electron/RF wave interaction throughout the length of the tube. Heretofore, RF power measurements have been made of only the input and output signals. This has not been enough to confirm fully the details of a computer simulation of the interaction along the length of the circuit. For this reason the true validity of computer simulation of a reentrant, emitting sole tube has not been properly assessed. However, the data obtained from the instrumented tube has altered this situation. The new experimental measurements show much of what is actually occurring within the tube, and this can be compared in detail with the computer predictions. Corrections and changes can be made if necessary until the computer simulation agrees with measured performance. At this point a new design tool will be available that can do much to permit more rapid development of new forward wave CFA's with improved gain, efficiency, reduced noise, better phase stability, and that can ultimately operate from a d.c. power supply with complete RF keyed, self-modulation. Considerable progress has been made in simulating what occurs in a CFA with uniform

interaction space parameters, but more effort is required to properly duplicate tubes with non-uniform interaction areas.

Following the completion of the investigative phase of this program, it is planned that the new insight to CFA operation and the validity of the computer simulation will be put to test. New instrumented tubes with improved design will be fabricated and tested. It is expected that these tubes will use some form of programmed interaction space design. It has long been known that emitting sole CFA's can benefit by using non-uniform, electrical interaction parameters, but specific designs for optimizing this have not been known. A satisfactory computer program together with confirmatory measurement and evaluation using an instrumented test vehicle will change this.

The format of this report is such that it is divided essentially into two parts. The first part discusses the experimental portion of this effort including background information, technical approach, and results. The second part contains a similar discussion of the computer simulation effort. It is believed that this will make it easier for the reader to follow the two phases of the effort. However, in each of the discussions reference will be made to the other when results of one show support or corroboration of the other. Because of the size of the total report, it has been bound into two volumes. The first volume is devoted primarily to the experimental effort and the second volume to the computer simulation effort.

2.0 PROGRAM OBJECTIVES

The broad objectives of this program were twofold: first, to obtain improved understanding of the internal electronic interaction and energy conversion processes in reentrant stream, emitting sole, forward wave, crossed-field amplifiers; and second, to develop new and better analytical design methods for these tubes so that improved capabilities with greater performance margin and more reliability for system utilization can be obtained. Particular emphasis was placed initially upon increasing amplifier gain and efficiency, reduction of noise, and improving phase stability. Methods for reducing arc rates and power supply shutdowns will be explored later to increase reliability of CFA operation with d.c. power supplies. This will permit improved RF modulation to be obtained using quench electrode turn-off or, preferably, self turn-off.

Specific objectives for improvements to the SFD-261 crossed-field amplifier were:

(a) increase the amplifier gain from a nominal 12 dB to 20 dB.

(b) reduce the noise and spurious outputs by 20 dB.

(c) improve efficiency to a minimum in the 50-60% range over the band.

(d) reduce arc/shutdown rate to only one per 100 hours of operation.

(e) obtain d.c. operation with self turn-off.

The methods for obtaining these results was to be based upon development of a computer simulation of reentrant, emitting sole, crossed-field amplifiers together with evaluation of results from an experimental program using instrumented versions of the SFD-261 CFA. The tube instrumentation consisted of the use of thermal couples for temperature measurements and RF probe sensors for RF measurements distributed along the slow wave circuit. Direct intercomparison of results from experiments and calculations could be used to indicate the validity of the computer simulation techniques. It was planned that this would be verified further by generating new designs intended for improved performance. Instrumented tubes are to be fabricated employing these new design concepts and evaluated to confirm the computer simulation predictions.

Experimental tubes employing these new design concepts and suitable for operation in an electromagnet will be delivered to the Navy for further evaluation.

3.0 BACKGROUND INFORMATION--INSTRUMENTED TUBE

The SFD-261 crossed-field amplifier used as the basic vehicle for this design improvement study is a forward wave amplifier developed by the U. S. Navy for an advanced radar system. The tube performance and specifications for system application are classified "CONFIDENTIAL." However, the exploratory nature of this program investigating physical principles did not require divulgence of classified information to be meaningful. Experimental results are presented in a normalized or coded form in order to keep this document unclassified. This is feasible since the objectives are to evaluate and improve performance in a relative sense more than in absolute values. In this way the results should be applicable to many other emitting sole, reentrant stream, forward wave CFA's.

Two semiannual reports have been submitted previously on this program (Reference 1, 2). The reports were lengthy and contained much detailed historical information about CFA's and about the origins of the program for computer simulation. All of this background information will not be repeated here. However, some will be described for the completeness of this summary report of this program. Reference can be made to the earlier reports for more extensive background information if desired by the reader.

3.1 The SFD-261

The standard design SFD-261 CFA is assumed to be well known to the reader. The tube uses a forward wave, helix-coupled, vane circuit as shown in Figure 1. The slow wave circuit is uniform along its length, but the anode-to-cathode spacing varies in a non-uniform manner which has been found experimentally to produce the desired results. It was recognized that the cathode-to-anode spacing variation may, however, be far from optimum. The drift space is uniform as a function of axial height. It occupies 60 degrees of the anode circumference. Approximately 70 identical models of these tubes have been fabricated and tested, thus producing a large data base that could be employed for comparison of results with the instrumented tubes that were constructed on this effort and with any new designs that are tested. In this way we could make sure that our instrumented tubes are representative of the SFD-261 design and that design improvements are making changes that are statistically significant when compared with the spread of results of the standard tubes. The data base of the standard tubes would also be of great use in the validation of our computer simulations.

Although most of the electrical and mechanical design features of the basic instrumented tube were like that of the SFD-261, there was, however, one change of electrical significance. This change involved a modification to the matching sections from the slow wave circuit to the external waveguides. A choke section to isolate the match from the drift section was included in these tubes.

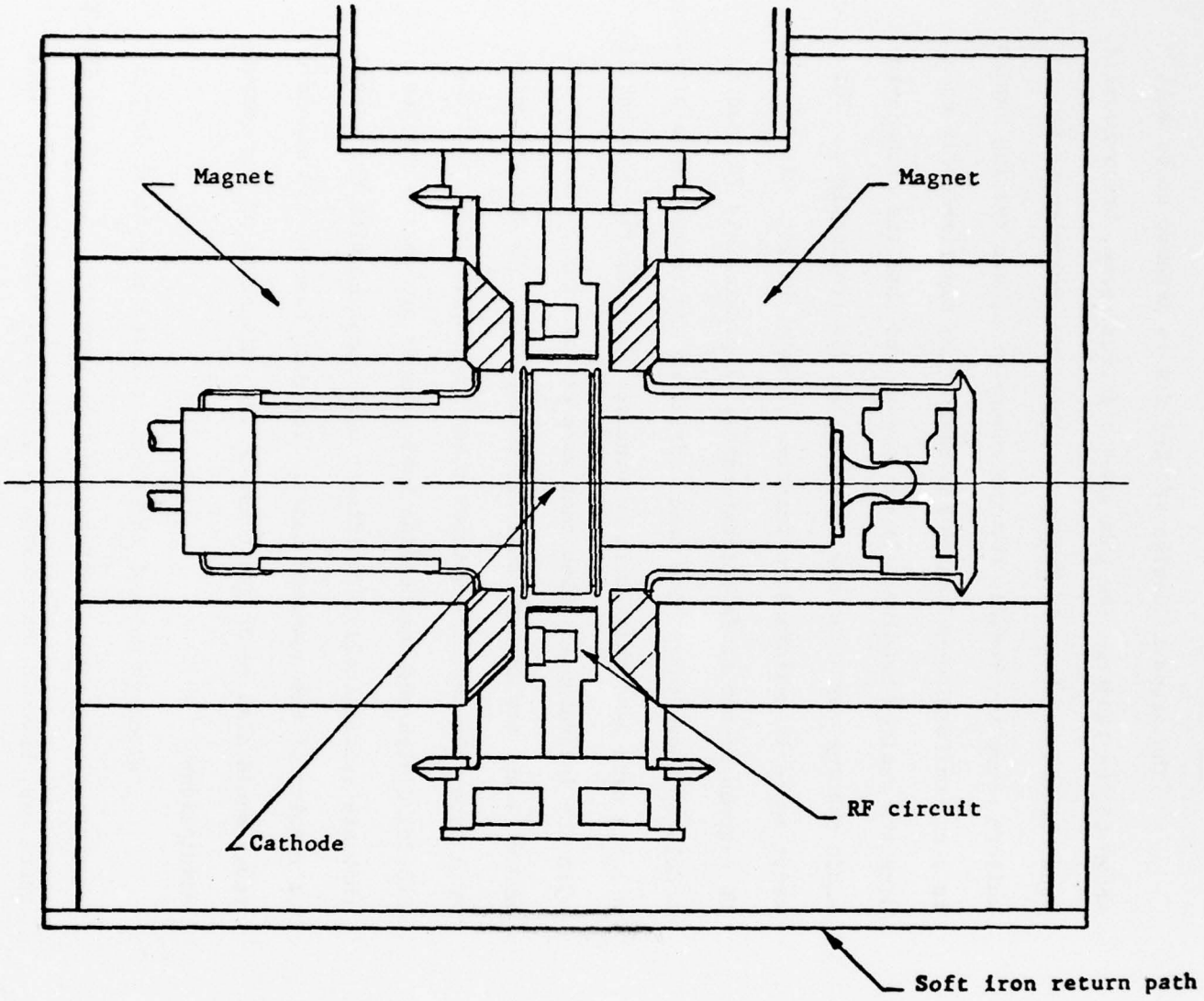

FIGURE 1--SKETCH OF SFD-261 CFA

This appears to reduce the fast mode excitation in the interaction space and thus the unwanted feedback across the drift space. This version of the CFA has demonstrated improved phase linearity as a consequence of the reduction of the feedback. It has also demonstrated improved efficiency in the lower portion of the operating frequency range. The details of how the efficiency improvement comes about are not clear.

To facilitate comparison of the results from the computer simulation with measurements from the instrumented tubes, it was planned to make early measurements using a tube with a circular cathode on mechanical center. This provides a uniform interaction space and uniform interaction parameters along the length of the slow wave circuit. This was planned even though it was known that this geometry did not function well across the full design operating band for the tube. Nevertheless, it was believed that this would permit the most rapid comparison between actual experimental results and the computer simulation. Once the computer program was shown to provide a reasonable simulation for this geometry, it would then be modified to correspond to the more complicated, tapered interaction configurations.

3.2 The D.C. Operated SFD-261

Forward wave CFA's have also been operated in a d.c. mode of operation. For these tubes a d.c. voltage is applied between anode and cathode. Cathode current flow and subsequent amplification are initiated by an input RF signal to the tube. For most of these tubes the cathode current flow is terminated after removal of the RF input signal by pulsing a quench electrode imbedded in the cathode positive with respect to the rest of the cathode. The quench electrode is located typically in the drift space between the RF input and output. The quench voltage is often as much as, or more than, half of the anode-cathode voltage. It is desirable that the quench voltage be made as low as possible. One of the goals of this program using the instrumented tubes and computer simulation was to learn how to reduce this voltage.

It has also been demonstrated that complete, RF controlled self-modulation can be obtained by locating an electrode similar to a quench electrode in the cathode but located under the RF structure near the input as seen in Figure 2.

This electrode has a d.c. bias applied with respect to the cathode. Self-modulation was obtained at the expense of some gain reduction and a small reduction in efficiency; i.e. higher RF drive signals were required, and some current is collected by the biased electrode. Complete RF keyed amplification is desirable for some system applications. Hence, it was another goal of this program to use the instrumented tubes and computer simulation to arrive at a design for a more effective bias electrode configuration.

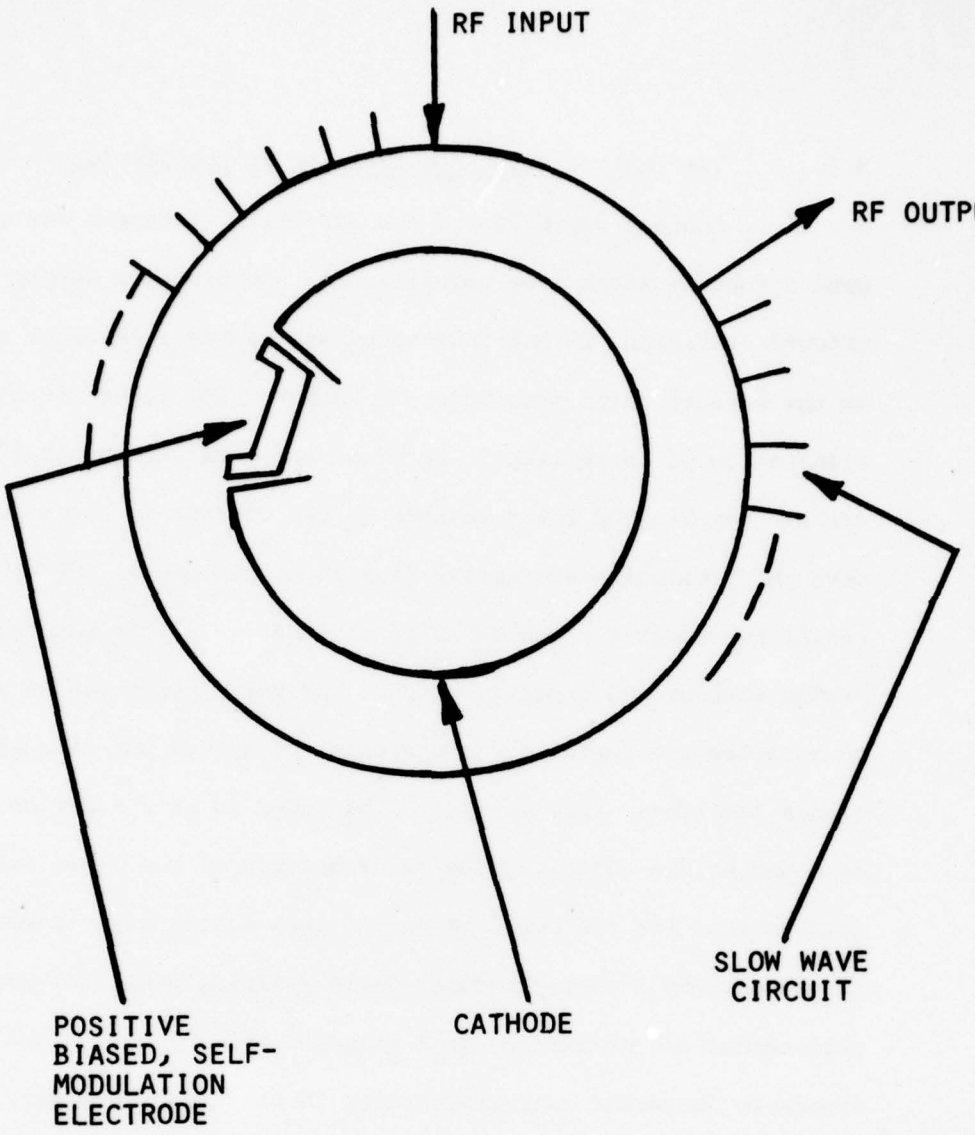

FIGURE 2

CFA WITH BIASED, SELF-MODULATION ELECTRODE

3.3 The Tapered Pitch Modification to the SFD-261

Another variation of the SFD-261 of interest was a tube with a tapered pitch slow wave circuit. On previous company-sponsored efforts at Varian, we had fabricated and tested a CFA with a taper in the circuit pitch from input to output. The taper involved elimination of three circuit sections and a uniform taper of the circuit pitch along the remainder of the circuit by about 10 percent with phase velocity decreasing from input to output. Other than the use of the tapered pitch circuit, the CFA was of the standard SFD-261 design without the isolated match. The pitch taper was an attempt to optimize the degree of asynchronism of spokes and circuit wave around the tube. This optimum is believed to be a function of the RF power on the circuit. The incorporation of the taper raised the gain so that the CFA could be driven with a peak input power of less than one-fifth of normal drive, while yielding about the same noise performance and efficiency as a standard SFD-261 CFA. This corresponds to increased gain approaching 20 dB, which is significantly more than that available from the standard SFD-261. It was planned to explore this approach in a fully instrumented tube for further understanding.

3.4 Noise Characteristics of CFA's

Crossed-field amplifiers historically have been more noisy than beam tubes of comparable peak power output. The reasons for this are not completely clear. However, very little effort has been directed specifically toward making a significant improvement in the signal-to-noise ratio for the output signal of a reentrant stream crossed-field amplifier. Most development effort has been directed toward improvement of the basic parameters of greater peak and average power output, bandwidth and gain. Nevertheless, some ideas have existed for obtaining reduction in the noise power output of these tubes. For instance, it has been observed that some d.c. operated tubes with a d.c. bias electrode have shown better signal-to-noise output than cathode-pulsed tubes. This led to much speculation but no definite conclusions. Therefore, one thought was that a d.c. biased electrode mounted in the cathode should be studied for its effect on noise reduction.

Another concept for noise reduction was based upon the idea that much of the noise coupled to the slow wave circuit was contained in the reentrant electron stream near the RF input to the tube. It was thought that removal of some of the recirculating current by a beam scraper attached to the anode would lead to a reduction of noise. This had been tested previously on a company-sponsored effort, and encouraging results were obtained. It was planned that this concept be investigated further using a fully instrumented tube.

Other ideas for noise reduction were also to be explored. These included using shaped end hats and contoured cathodes to

change the d.c. electric field pattern near the edges of the interaction space to provide a more constant ratio of E/B over the whole region. The rationale for this was that the wide range of values of E/B that now exists in these tubes may be a contributing factor to noise generation. It was expected that computer simulation of the d.c. electric and magnetic field distributions would be helpful in this investigation.

Another concept was the use of shaped magnetic fields to reduce noise. This was based upon the fact that a significant reduction in noise has been obtained in injected beam CFA's by using a tilt in the magnetic field with respect to the cathode in the electron gun region. Emitting sole tubes are quite different, but a similar effect might occur.

Some speculation has been made also that the variability of the secondary emission properties over the surface of the cathode may contribute to the noise. However, this effect may be masked by the presence of the circulating hub above the cathode surface. A detailed study of this effect was considered beyond the scope of the present program.

4.0 TECHNICAL APPROACH

The technical approach for the experimental position of this program was based upon using a fully instrumented CFA that would measure the RF power growth through the tube and the vane tip temperature variation from RF input to output. To do this, the experimental CFA's were equipped with thermocouples imbedded in the vanes to measure temperatures and coaxial connectors attached to the vanes to sense the localized RF field intensity. Thermocouple instrumentation has in the past been implemented in the SFD-261. In addition, on a company-sponsored program prior to the start of this program, we built a preliminary SFD-261 tube incorporating twelve RF probes of the sort shown in Figure 3. There were no thermocouples in this tube. The probes consisted of small coaxial lines that came through the backwall of the tube and were attached to selected vanes. A contact of the probes to the vanes is believed necessary to insure that we are sampling the wave on the slow wave circuit, rather than a fast wave in the space above the circuit. The probes employed were made from the output coaxial line of one of our beacon magnetrons.

The initial probe tube was put together principally to verify the measurement technique. The coupling from the CFA input port to the probes was down only about 20 dB, a value higher than we liked. There was a slight change in the RF match as a result of incorporating the probes. Rather than modify this first probe tube to correct this, we decided to proceed to assemble it and hot test it to see if any unforeseen problems would develop. Figure 4 shows

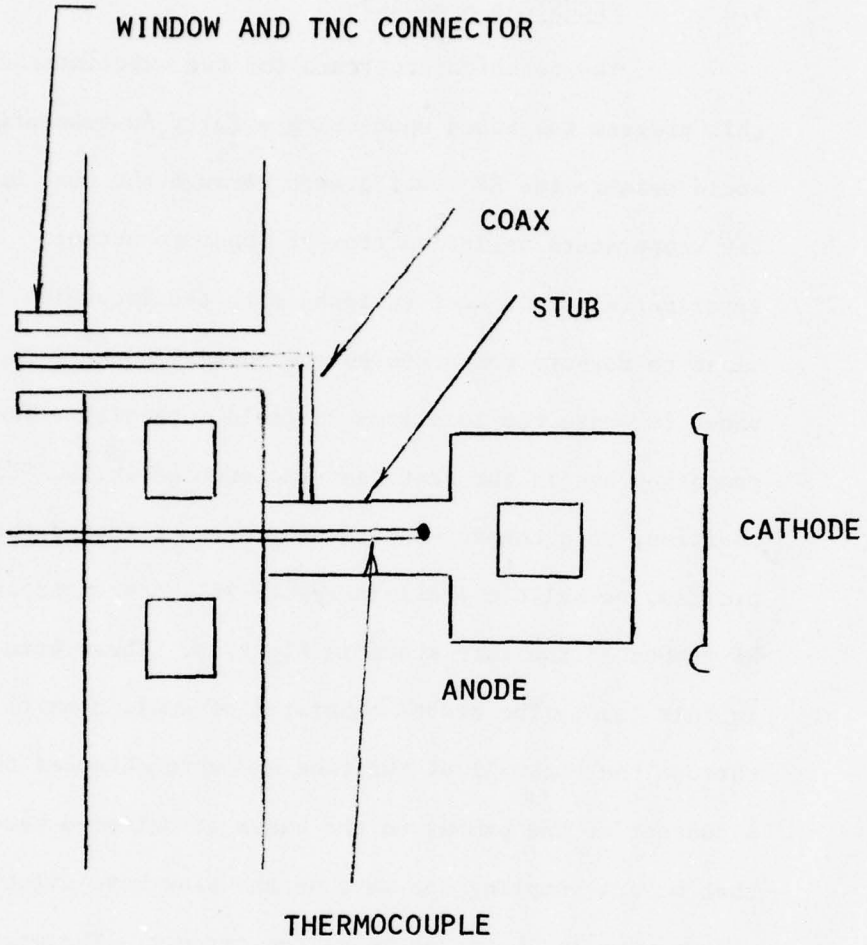

FIGURE 3

THE RF PROBE AND THERMOCOUPLE INSTRUMENTATION

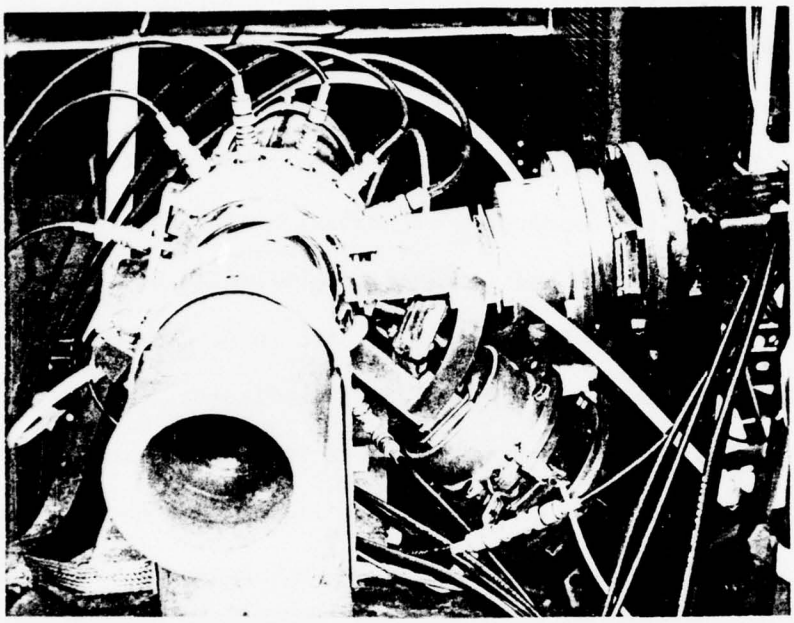

FIGURE 4

THIS FIGURE SHOWS THE INSTRUMENTED S-BAND CFA IN THE ELECTROMAGNET OF THE MASTER TEST SET. THE SMALL COAXIAL TRANSMISSION LINES CONNECTED TO THE RF SAMPLING PROBES DISTRIBUTED ALONG THE SLOW WAVE CIRCUIT ARE VISIBLE AROUND THE BODY OF THE TUBE.

a photograph of the resulting tube with the probe outputs mounted in the electromagnet. The initial RF tests results did, indeed, show a growing wave on the circuit as monitored at the probe outputs. By using a drive pulse longer than the cathode pulse, it was possible to determine the electronic gain at each probe output. This was done by measuring the necessary attenuation level that had to be inserted in the connecting transmission line between the probe and detector to reduce the level of the amplified portion. The electronic gain in dB is equal to this insertion loss. Typical photographs of preliminary test results are shown in Figures 5 and 6.

These preliminary results with CFA's with thermocouples and with a CFA with RF probes were limited but established the validity of the experimental approach. However, it was apparent that the experimental technique would require revision and improvement to obtain meaningful data.

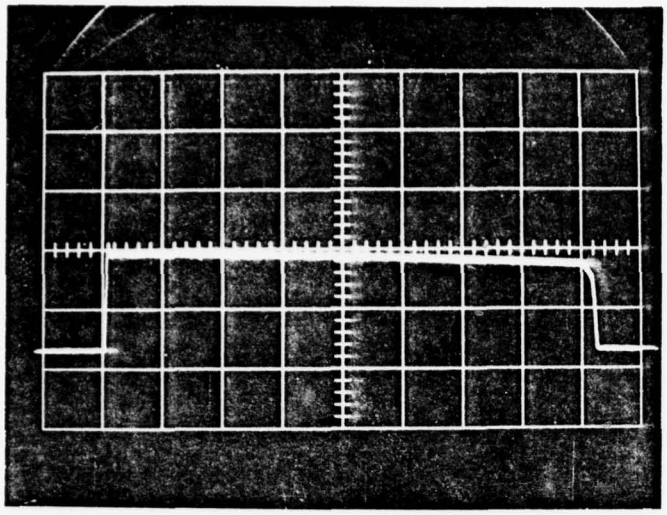

INPUT DRIVE SIGNAL - F1 GHz
PEAK INPUT DRIVE POWER - 0.75 Pi
FIGURE SHOWS DETECTED INPUT
PULSE AT 16 MICROSECONDS
DURATION.

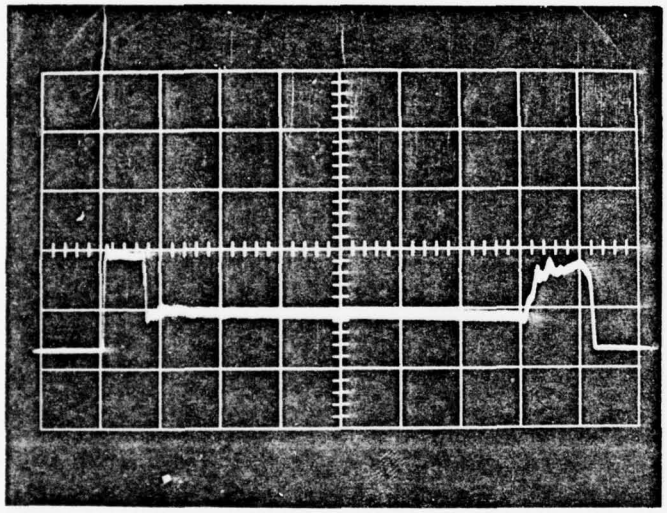

DETECTED RF POWER SAMPLED AT THE FIRST RF PROBE CONNECTED TO THE FOURTH ANODE CIRCUIT ELEMENT. CFA CATHODE PULSE IS 12 MICROSECONDS DURATION AND THE PHOTOGRAPH SHOWS NEGATIVE ELECTRONIC GAIN OF 4 dB. THE MEASUREMENT IS MADE RELATIVE TO THE SAMPLED INPUT DRIVE SIGNAL BEFORE THE CFA CATHODE VOLTAGE PULSE IS APPLIED.

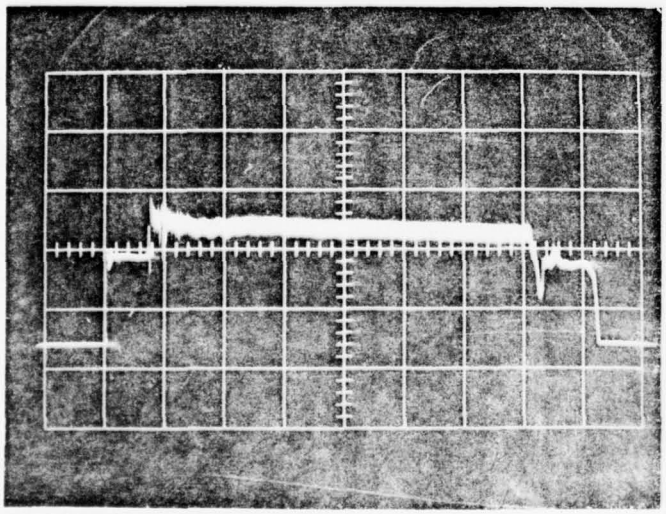

SAMPLED RF SIGNAL AT VANE NUMBER 12. ELECTRONIC GAIN OF 1.3 dB IS MEASURED, BUT THE PULSE LOOKS NOISY.

FIGURE 5

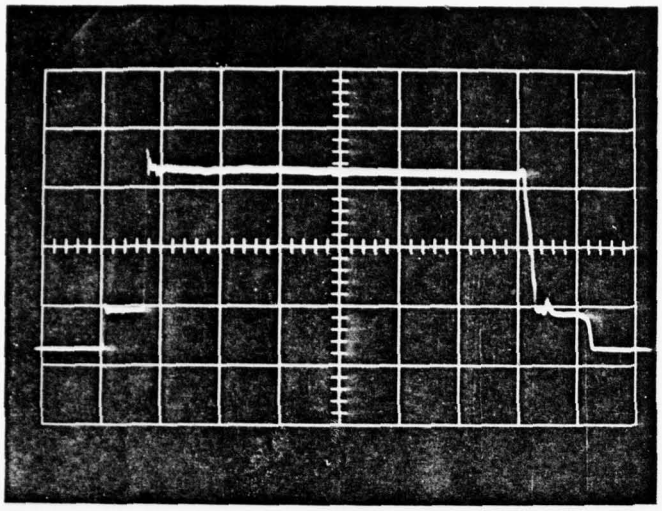

SAMPLED RF SIGNAL AT VANE NUMBER 31. ELECTRONIC GAIN OF 10.6 dB IS SHOWN.

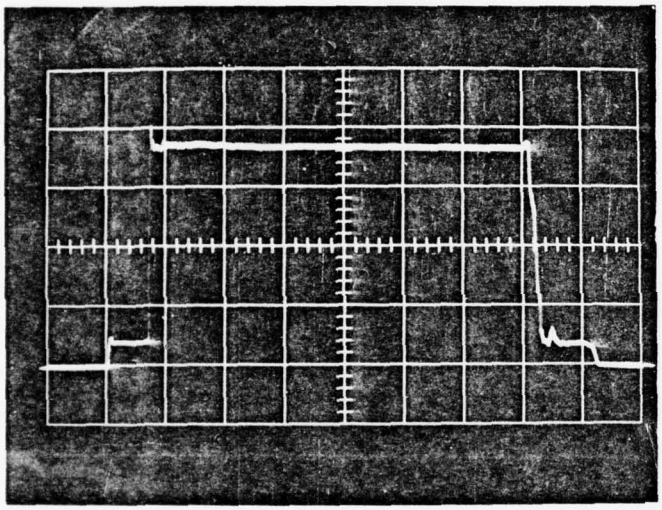

SAMPLED RF SIGNAL AT VANE NUMBER 59. ELECTRONIC GAIN OF 15 dB IS SHOWN.

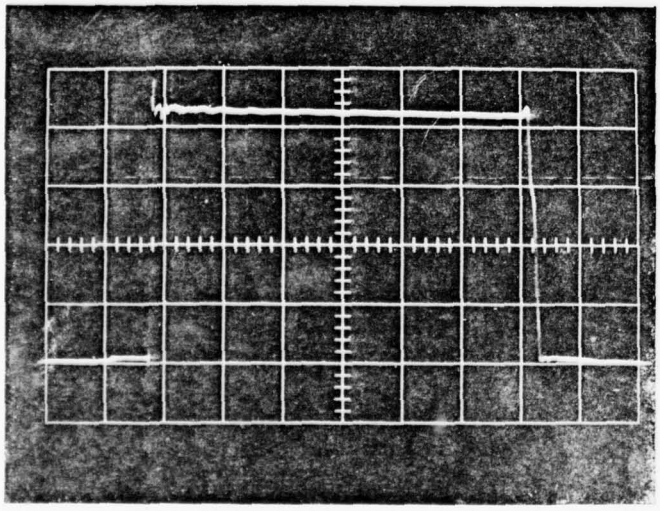

DETECTED RF OUTPUT SIGNAL FROM CFA. ELECTRONIC GAIN OF 15.5 dB IS SHOWN

FIGURE 6

4.1 Description of the Test Set

There were several kinds of measurements that were planned to be made on the instrumented tubes. These included:

(1) RF power level and gain of the input signal as a function of position along the slow wave circuit from input to output.

(2) Noise level as a function of position.

(3) Anode power dissipation along the circuit from which temperature distribution can be measured and/or calculated.

(4) Phase sensitivity to voltage and RF drive level and the cold-to-hot phase change as a function of position along the circuit.

Two kinds of sensors were used to make these measurements. RF coaxial connectors loosely coupled to the slow wave circuit were used to make all RF measurements and thermocouples located at strategic points in the circuit were used to measure temperature at known locations. Both kinds of measurements had been made previously as discussed before in this report. For the new experiments, the test arrangement was altered in some ways with the intent of simplifying data taking and obtaining better results.

The RF probes connected to the anode vanes cannot be made with identical, fixed coupling factors. There will always be differences probe-to-probe and as a function of frequency. Figure 7, for instance, shows a typical coupling response as a function of

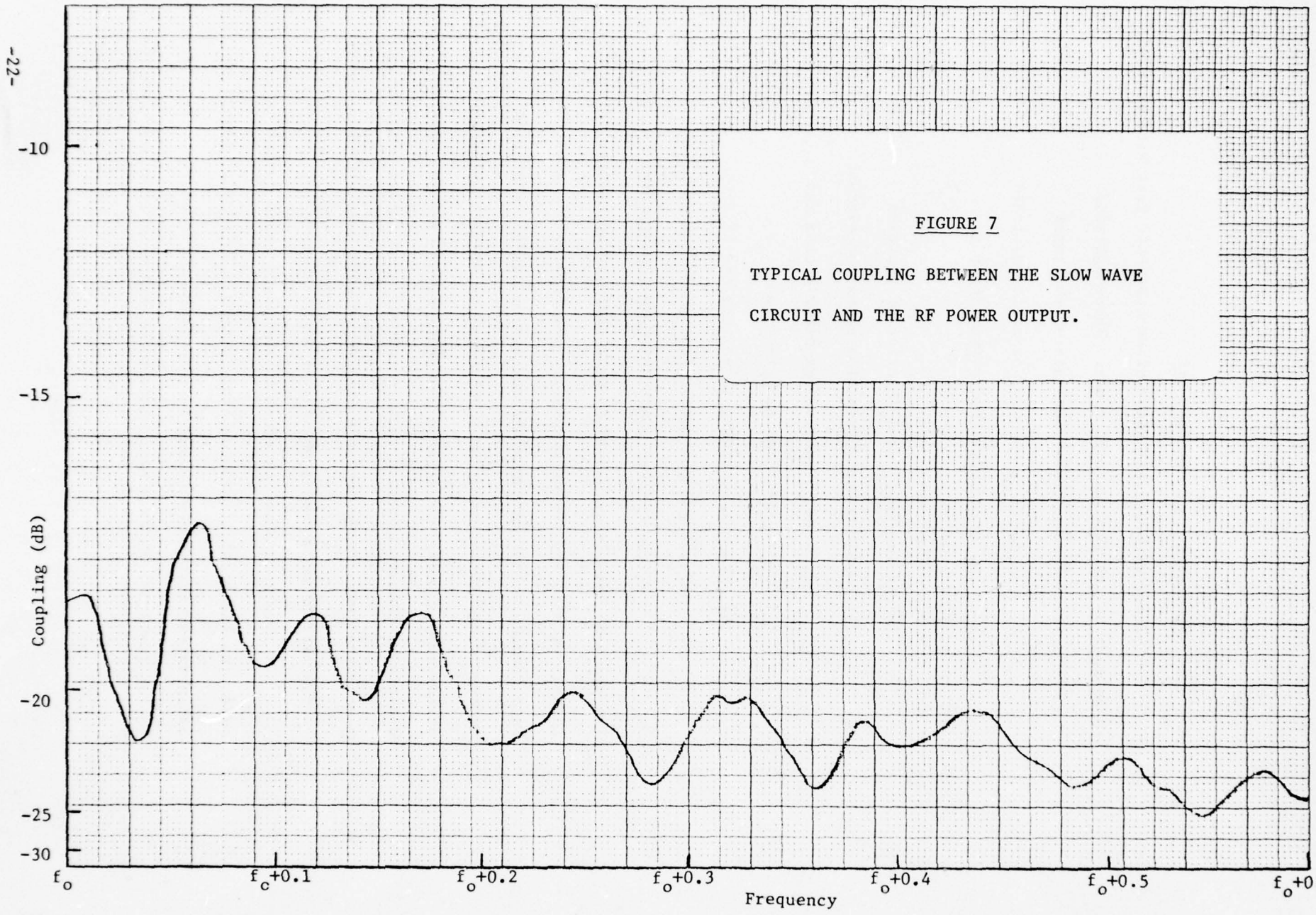

FIGURE 7

TYPICAL COUPLING BETWEEN THE SLOW WAVE CIRCUIT AND THE RF POWER OUTPUT.

frequency obtained from the initial RF probe tube. The coupled signal is down from the input by 20 to 30 dB. It was desirable that this be lower by another 10 to 20 dB, if possible, to minimize any effect on the slow wave circuit propagation characteristics and the waveguide-to-circuit match properties. Each probe could be fully calibrated for absolute coupling magnitude with its own detector, but this leads to unduly complex experimental procedures. The alternative approach that was chosen utilizes a single detector and measurement apparatus that can be switched selectively to each probe output connector. Electronic gain measurements were made by determining the difference in amplitude of the signal at the probe position with and without voltage applied to the amplifier. Net gain and power level at the probe are then calculated from knowledge of the insertion loss through the tube. The procedures for doing this are described in the next section. With this method there is no need to know precise calibration values for the probes. It is only necessary to be sure that the sensor is measuring only the signal power coming from the probe and that it is not, itself, introducing extraneous effects. Several precautions were taken to assure this to be so. The single detector was coupled to the selected probe outputs using an array of three, six-position, rotary coaxial switches. The RF isolation between ports is greater than 70 dB. Connection between the rotary switches and the probe connectors was made using semi-rigid, mini coaxial transmission lines to avoid pick-up of any spurious signals in the vicinity of the tube. The switch terminals

present an open circuit in the disconnect position to the probe connection line. Potential reflections and standing waves in the connecting line were avoided by inserting 10 dB pads between the probe output and the switch. Figure 8 shows a schematic illustration of the RF sensor connection scheme. The RF input and output to the tube and twelve intermediate points along the circuit could be sampled for the initial instrumented tube. Figure 9 shows the tube mounted in the electromagnet with the connecting lines including attenuating pads to the selector panel.

The output of the probe selector panel could be coupled to power meters, oscilloscopes or spectrum analyzers to make whatever measurements were desired.

Temperature measurements were made for the instrumented tubes using thermocouples inserted into radial holes drilled into the tube body and into the vanes of the slow wave circuit. One thermocouple was located at the backwall adjacent to the heat sink, and the other was located far into the vane just behind the helix. Temperature readings using these two thermocouples can be used to calculate a thermal gradient across the vane and an associated heat flow through the vane. From this and additional knowledge of the thermal impedance of the circuit vane element, assuming a uniform heat input to the vane, the temperature at any point in the vane could be calculated. Measurements of this kind were made previously on special experimental models of the SFD-261. Thermocouple outputs were recorded during those experiments using a multichannel strip chart recorder. This permitted showing rather quickly an approximate

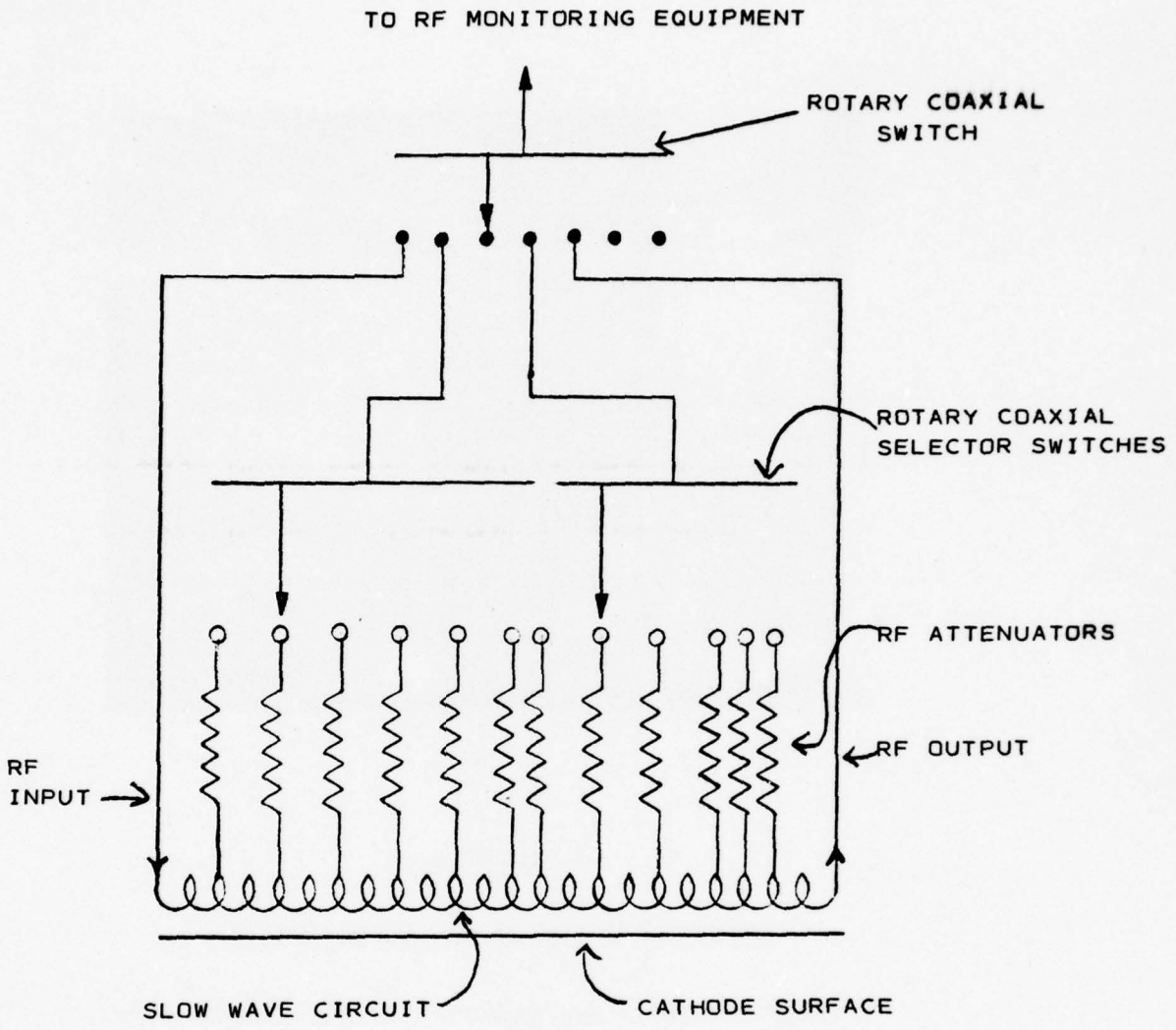

FIGURE 8

SCHEMATIC ILLUSTRATION OF THE RF PROBE SENSOR SELECTOR ARRANGEMENT.

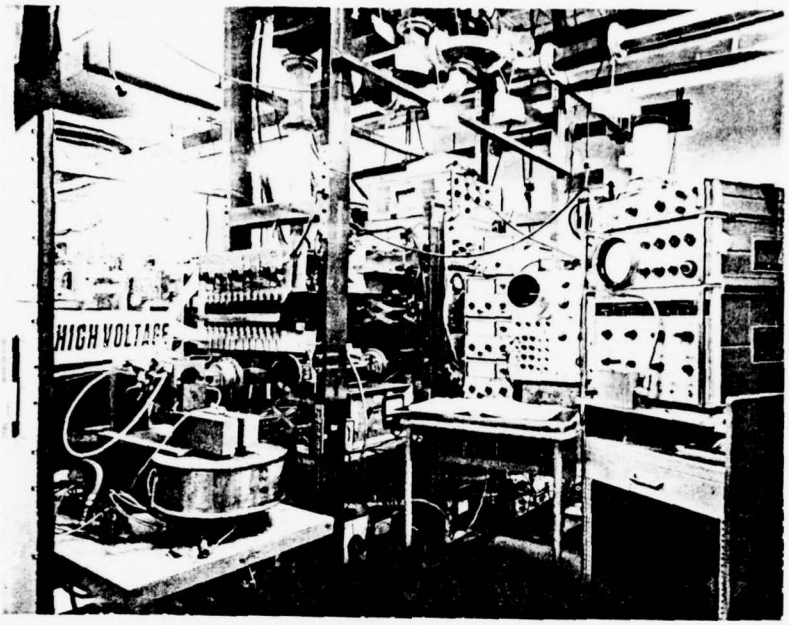

FIGURE 9

INSTRUMENTED TUBE IN THE ELECTROMAGNET

RF PROBE OUTPUTS ARE CONNECTED TO THE SELECTOR PANEL THROUGH SEMI-RIGID COAXIAL CABLE. THE ATTENUATOR PADS AND THE ROTARY SWITCHES ARE MOUNTED ON THE PANEL ABOVE THE TUBE.

display of the thermal profile along the circuit. For an accurate distribution it was still necessary to record and reduce the data further. In addition, the recorder stepped sequentially through all recorder inputs for each cycle, thereby introducing time delays in observations that were sometimes inconvenient. On the present program, an alternate approach was used. The output of the thermocouples was connected by rotary switches to a digital reading millivoltmeter. Identifying numbers for the thermocouples were shown by an LED display. The ease of reading the output and convenience of selecting the desired thermocouple was believed to be beneficial even though this method did not automatically cycle through the thermocouple readouts. It was also much less costly.

Aside from these special measurement arrangements, the amplifier test set was a conventional microwave configuration consisting of a signal source and TWT driver stages together with appropriate waveguides, power supplies, and modulators.

4.2 Measurement Techniques

4.2.1 RF Power Levels on the Slow Wave Circuit

The net RF power gain on the slow wave circuit was determined at each sensor position by measuring the electronic gain (in dB) at that point and correcting it by subtracting the insertion loss (in dB) along the slow wave circuit between the RF input and the vane location of the sensor position. The absolute power level at the sensor position was then equal to the RF input power level multiplied by the net gain at that point. This method required an accurate knowledge of the insertion loss between the input and the vane location of the probe connection.

The insertion loss of the tube at each test frequency was measured in the final test set arrangement. The assumption was made that this insertion loss was uniformly distributed throughout the length of the tube. For this procedure to be valid it was necessary to establish that the insertion loss at input drive power levels was not significantly different from that measured at the milliwatt power levels used for cold test meausrements. For instance, the presence of multipactor along the circuit, if it existed, would completely confound the interpretation of results. The confirmation of this assumption was made by a measurement procedure using recording power meters to sample the input and output power to the tube. The sampled signal to the two meters was adjusted so that both meters read on the same power level scale. The output of one meter

was connected to one input and the output of the other to the second input of an X-Y recorder. The input power to the tube was then adjusted in magnitude. For a constant insertion loss independent of amplitude the recorder trace is a straight line at a 45° slope. Figure 10 shows the result using a cw input signal level varying from zero to 10 watts. The different frequency curves were made by using a deliberate offset in the X-axis of the recorder for each frequency so that the curves do not overlay. The power level was then increased to normal drive power levels of Pi by using the output from the pulsed TWT driver tube. The results are shown in Figure 11. The signal power was varied in amplitude by adjusting the drive power level to the TWT. At low RF drive levels the TWT oscillated at some bandedge frequency outside the pass band of the CFA. As the RF drive level increased, the TWT output divided between the amplified input signal and the bandedge oscillation frequency until some power level was reached. Further increases in RF input signal level to the TWT resulted in increased output power level at the input signal frequency. This phenomena accounts for the behavior shown in Figure 11. The curved portions of the recorder trace at the start caused by power division between the two frequencies. The straight line portion at higher input power levels shows that no untoward effects exist at power levels up to the normal input power levels to the CFA. This was further confirmed by repeating the procedure after deliberately reducing the applied magnetic field

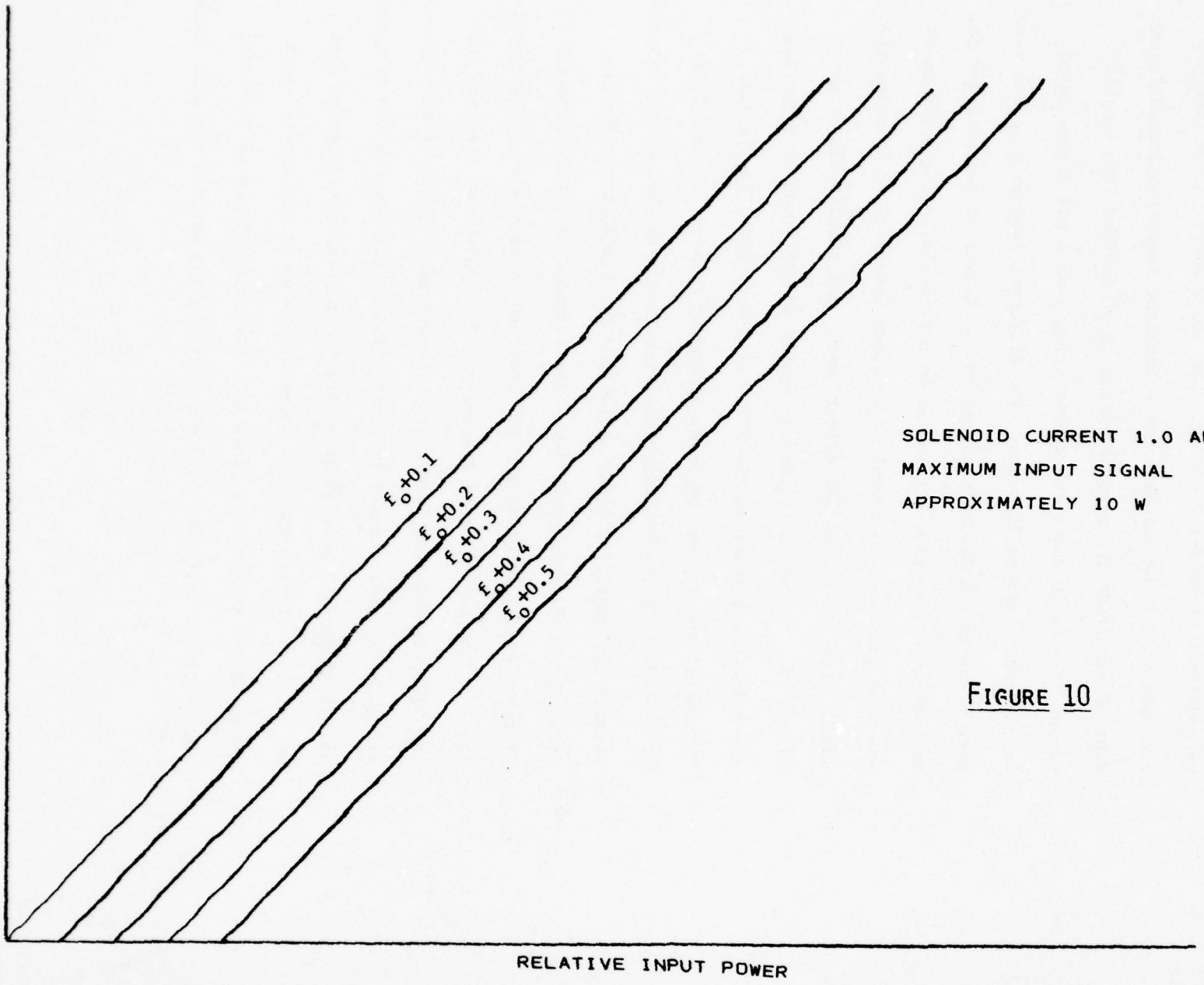

SOLENOID CURRENT 1.0 AMPS
MAXIMUM INPUT SIGNAL
APPROXIMATELY 10 W

FIGURE 10

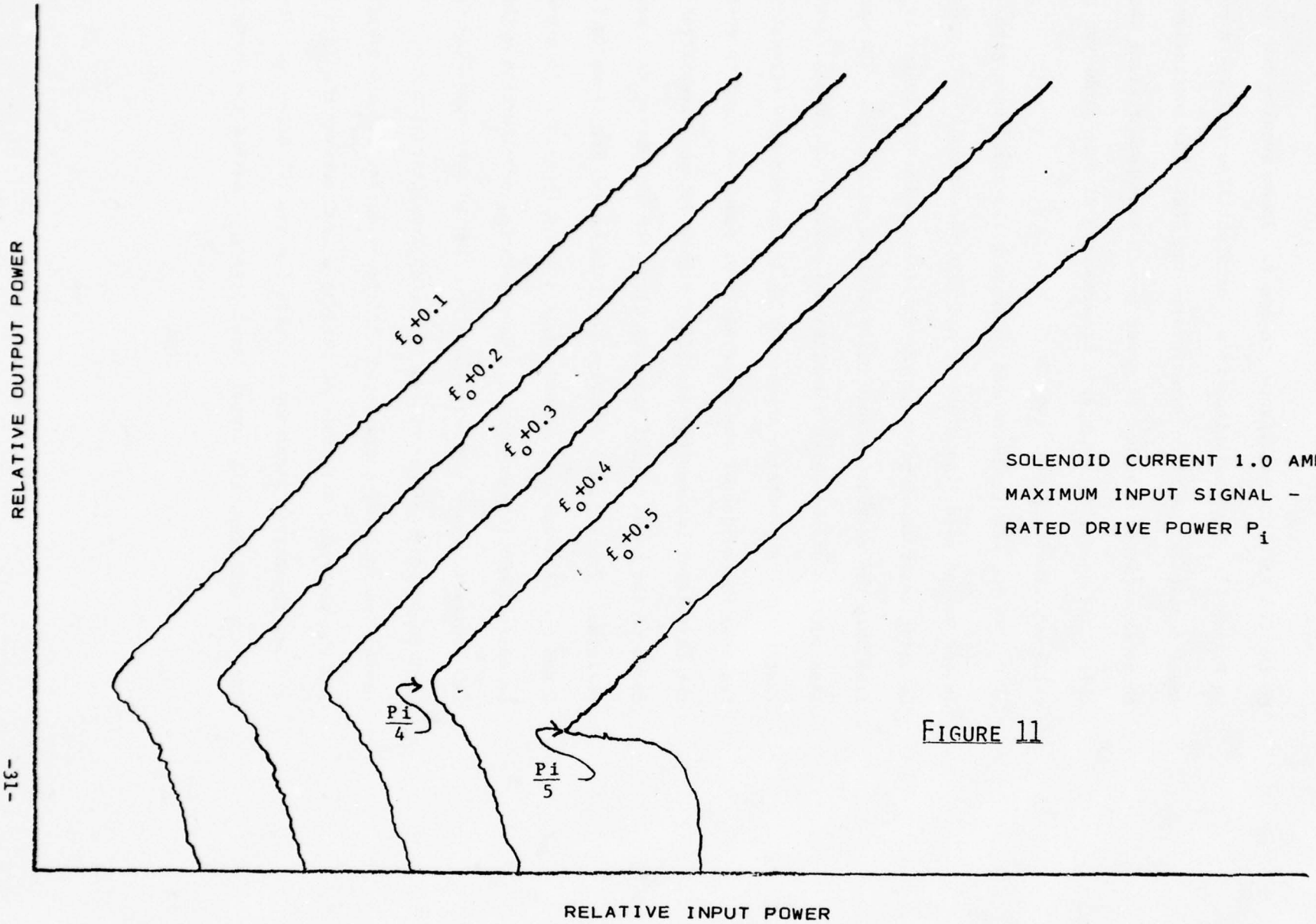

SOLENOID CURRENT 1.0 AMPS
MAXIMUM INPUT SIGNAL -
RATED DRIVE POWER P_i

FIGURE 11

to the CFA to allow multipactor to occur. These results are shown in Figure 12. The deviations from a straight line indicate a power level sensitive insertion loss through the CFA. The conclusion from these experiments was that RF power growth measurement along the circuit based upon electronic gain measurements at each probe was a valid experimental technique.

Two methods were used to measure the electronic gain. In one method used first, electronic gain measurements were made by using an RF input pulse to the amplifier which was longer in time than the cathode voltage pulse applied to the CFA. The unamplified portion of the pulse established a feedthrough signal level to that point. A precision attenuator in the measurement circuitry fed from the output of the probe selector panel was used to establish the gain level between the amplified signal and the unamplified portions of the input signal pedestal along the circuit at each sampling position. Typical data displays for this method are shown in Figures 5 and 6. Although this procedure is a valid technique, it proved to be tedious and time consuming. Consequently, an alternate method was desirable since the multiple probes led to very much data for each measured condition of the CFA. Any simplification was useful and improved operational efficiency during all the experiments for the program. With this in mind, the test set was modified to provide convenient interrupt circuits for the TWT driver and the CFA. In addition, the signal level detection method was changed

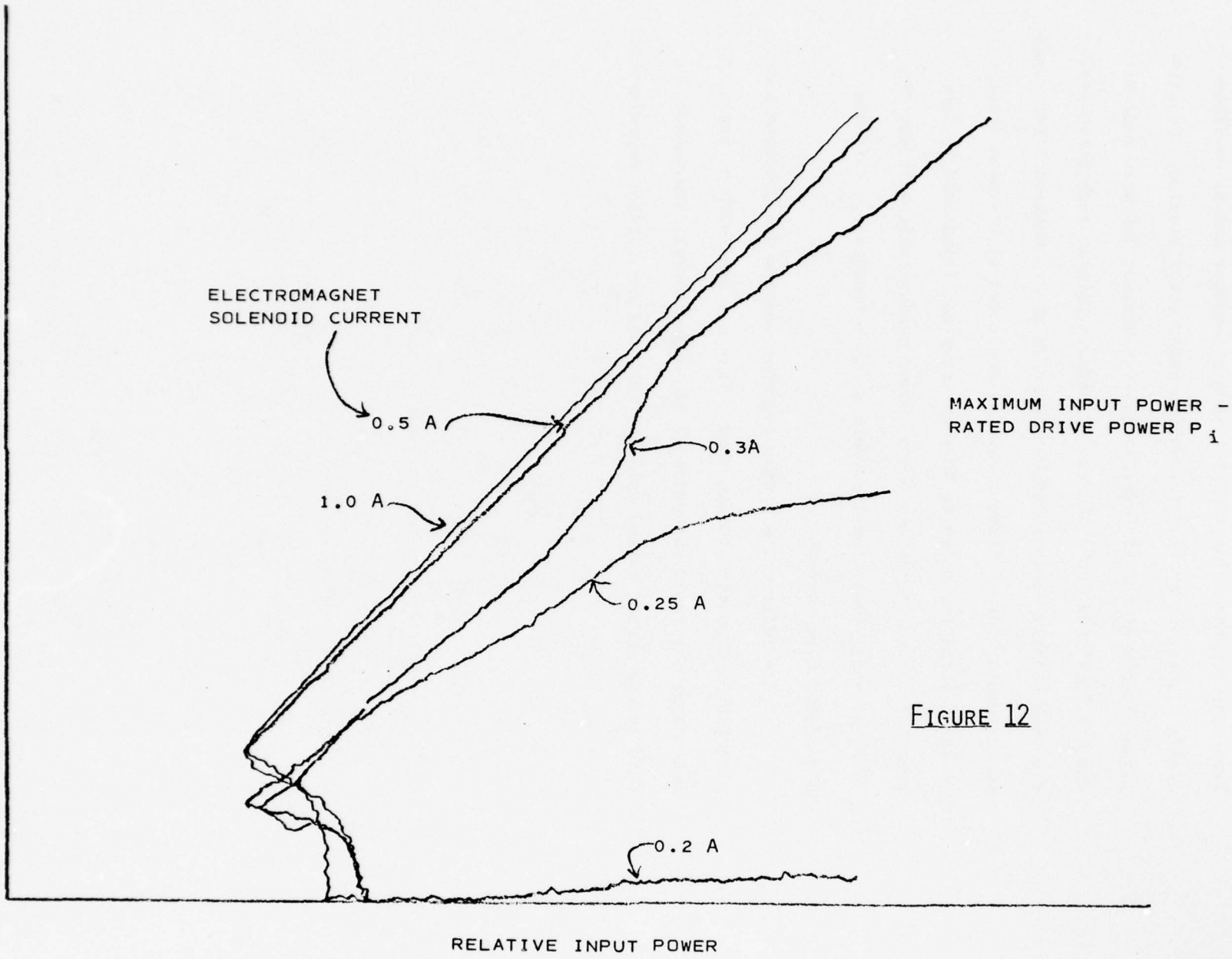
RELATIVE OUTPUT POWER
ELECTROMAGNET
SOLENOID CURRENT
0.5 A
0.3A
1.0 A
0.25 A
0.2 A
MAXIMUM INPUT POWER -
RATED DRIVE POWER P_i
RELATIVE INPUT POWER

FIGURE 12

from measurements using the precision attenuator and an oscilloscopic display to a one using only a power meter reading. Relative signal levels of the RF power at each probe position were made with the CFA "off" and "on". Hence, electronic gain at each probe position was readily established by the ratio of two numbers. For these measurements, the RF drive pulse was shortened to the same length as the CFA cathode pulse so that no error was introduced by the pedestal. Also, input and output power measurements with the CFA "off" provided insertion loss data at each frequency. This was needed for data correction.

In addition, a simple computer program was prepared and placed on a magnetic storage card. This was used with an automatic calculator for rapid reduction of the experimental data outputs. This second method worked well and was used for further experiments.

4.2.2 Thermal Measurements Along the Circuit

The thermal measurements using the thermocouples were used to determine the anode dissipation along the length of the slow wave circuit and to establish the vane tip temperature distribution. This was done by using one thermocouple to measure the temperature of the anode body at the backwall of the vane element. This was essentially the heat sink temperature. A second thermocouple was located at the tip of the support vane element just behind the rectangular helix. Both thermocouples were outside the vacuum wall and were inserted into long holes drilled into the tube body and vane element. The vane support element was a pi-shaped sector for which a thermal impedance can be calculated easily. The two thermocouples were calibrated and used to determine temperature at each end of the vane element when the tube was operating. From the temperature difference and the thermal impedance, the power flow through the vane element could be calculated. In this way, power dissipation along the circuit was determined.

The thermal impedance from the front of the support element around to the front of the helix element was more difficult to calculate. Hence, another kind of calibration method was used that was based upon using an electrical analog for determining thermal impedance experimentally. This is a common place method of evaluating thermal characteristics of vane type, slow wave circuits in crossed-field tubes. For this method, the assumption was made that electron bombardment and heat input was uniform across the vane tip at the

front of the helix. A second pi-shaped anode vane configuration was assumed that had a vane tip geometry of the same dimensions (height and thickness) as the front of the helix exposed to the beam bombardment. It was also assumed to increase the thickness radially in the same manner as the stub-supported, helix vane element so that both were of the same cross-section dimensions throughout and the same thickness at the backwall radius. The thermal impedance of the uniform vane was readily calculated as well as a temperature drop across it for any uniformly distributed heat input at the vane tip. This was simple since heat flow is only radial. Next, experimental electrical analogs for the two vane elements were fabricated for comparison. These were made from resistance paper cut to shape to simulate the changing thermal impedance of the vanes with radial distance; i.e., as the vanes increase in cross-sections the thermal impedance of the vanes decreases. Similarly, the resistance of the electrical analogs must decrease. This was accomplished by increasing the width of the resistance paper analog with distance at a rate proportional to the increase in cross-sectional area of the vane. Figure 13 illustrates two resistance paper analogs for a uniform, pi-shaped vane, and a stub-supported, helix vane. The tips of the resistance paper analogs were seperated into a number of equal pieces, and coated with conductive paint for electrical connections. A low current, multiconnector power supply was used to apply equal amounts of current into each of the sections of the uniform vane analog and

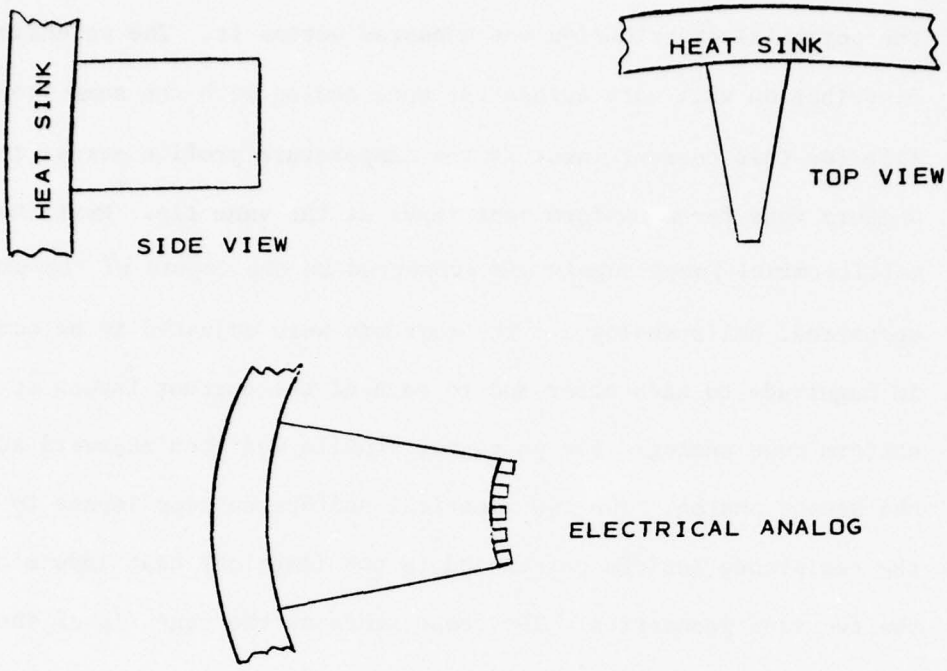

(A) UNIFORM VANE

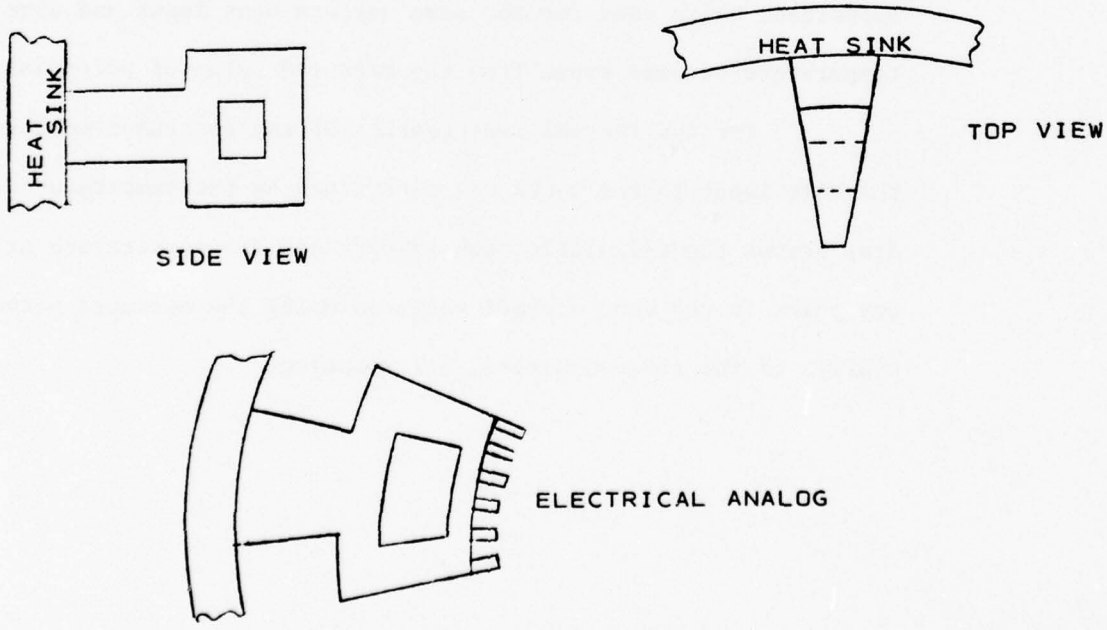

(B) STUB-SUPPORTED HELIX

FIGURE 13 - SCHEMATIC ILLUSTRATION OF ELECTRICAL ANALOG FOR THERMAL IMPEDANCE EVALUATION.

the potential distribution was measured across it. The potential distribution will vary across the vane analog with the same profile for this current input as the temperature profile across the uniform vane for a uniform heat input at the vane tip. Next the multiterminal power supply was connected to the inputs of the stub-supported, helix analog and the currents were adjusted to be equal in magnitude to each other and to each of the current inputs to the uniform vane analog. The potential profile was then measured across the second analog. The two identical uniform current inputs to the resistance analogs correspond to two identical heat inputs to the two vane geometries. The temperature at the vane tip of the uniform vane can be calculated for an assumed heat sink temperature and heat input.

Values for potential become equivalent to values for temperature; therefore, the temperature at any point in the stub-supported, helix vane for the same uniform heat input and sink temperature becomes known from the measured value of potential.

For the thermal measurements of the instrumented tubes, the heat input to the vanes was determined by the temperature drop across the calculable stub support and the temperature at any point in the vane element obtained using the measured potential profile of the stub-supported, helix analog.

4.2.3 Noise Measurements

Two kinds of noise measurements are made on emitting sole CFA's. One of these measures the broadband, extra-spectral line noise and the other measures the intra-spectral noise. The broadband, extra-spectral noise is evaluated using a broadband spectrum analyzer such as the Hewlett-Packard 8551B analyzer. The analyzer is set to sweep across a bandwidth that covers a specified range which is typically equal to the amplifier bandwidth pulse guard bands. This may be equal to the amplifier bandwidth and more.

The oscilloscopic display is set for a logarithmic scale and the extra-spectral spurious output is compared with the amplified signal. The difference between the noise peaks and the amplified signals can be measured in dB's using the calibrated scales. Proper account must be taken of the IF bandwidth of the analyzer over which the noise is integrated.

Intra-spectral line noise is more difficult to measure. The noise levels between the spectrum lines of a pulsed tube must be measured using special equipment to cancel the power contained in the spectrum lines of the amplified signal. Otherwise, this power would obscure the measurement of the noise power. This measurement is complex and involves a considerable amount of test equipment. Because of this, an alternative measurement procedure is used that was developed by Mr. H. Ward of the Raytheon Equipment Division. This procedure assumes that the noise from the tube has a uniform power density across a wide bandwidth. A quantitative

measurement is made of the noise outside of the main spectrum and the intraspectral line noise is calculated from this result. This procedure has been compared with actual interline noise measurement using spectrum cancellation equipment and found to give very nearly the same results. Mr. Ward's method uses equipment more readily available and is much easier to perform. The detailed procedure described in the appendix was taken from the Acceptance Test Procedure for the SFD-261.

It was planned that noise measurements using this procedure would be made at the CFA output and at each probe position along the circuit. This would allow quantitative comparison to be made of the rate of growth of the signal and noise. This would also allow assessment of experiments designed to reduce the noise in the CFA. However, it turned out that internal to the tube the noise spectrum could be very non-uniform as a function of frequency, and sometimes quite different from the noise spectrum measured at the output from the tube. This appears to result from an interference between forward travelling and reflected noise signals from the output matching sections of the tube. Hence the measured result would depend upon whether the noise measurements were made at a frequency corresponding to a peak or minimum in the non-uniform noise spectrum. It was concluded that this method would not be satisfactory.

As an alternative, the broadband spectrum analyzer was connected to each of the RF probe connectors and photographs

were taken of the analyzer oscilloscope display. This procedure has yielded much data but has been very difficult to interpret.

4.2.4 Phase Characteristics

The phase sensitivity of the amplified signal of CFA's to changes of cathode voltage and to changes of the RF drive are measured typically by comparing the input and output signals in a phase bridge. Similar measurements were planned for the instrumented tubes as the interaction space geometries were changed. In addition, it was planned to make similar measurements comparing the input signal with the output of the RF probes so that phase sensitivity could be evaluated along the slow wave circuit. This information would be useful in evaluating various programmed interaction space geometries. Although it would be more difficult, it was also planned to attempt measurement of the change of phase along the slow wave circuit as the tube was switched from the non-operating to operating condition. This information, if it could be obtained reliably, would be useful in comparing the computer predictions with the actual operating tube. However, the instrumented tube measurements proved to be so prolific in yielding data to be interpreted that no phase measurements were made using them.

5.0 EXPERIMENTAL RESULTS

5.1 Early Experiments

5.1.1 The SFD-261 with Tapered Cathode

After the start of the program, a tube-building effort was initiated for fabricating tubes with both thermocouples and RF probes in the same vehicles. It was recognized that several months would be required in order to obtain the first fully instrumented tubes. In the interim, it was planned to perform tests using the existing tube containing only RF probes (S/N C437S) and another tube containing only thermocouples. Both of these tubes were versions of the SFD-261 with the standard tapered cathode geometry. It was planned to adjust the cathode position in each tube to be in similar locations and to use one to obtain RF power growth profiles and the other to obtain vane tip temperature profiles. It was thought that the results could be correlated and some of them used to provide preliminary information for comparison to computer simulation results. It turned out, however, that more effort than anticipated was required to get the instrumented tube and all of the associated test set equipment operating correctly. For instance, it was known that the tube with only the RF probes (S/N C437S) had an inferior waveguide-to-slow wave circuit match. This caused reflected waves from the output back toward the input inside the tube. The RF probes sense only the magnitude of the localized RF voltage on the slow wave circuit. Therefore, any form of reflected power on

the circuit causes the voltage at a probe location to be the result of the vector summation of two voltages. One is the voltage associated with the forward travelling wave which is growing with distance from the RF input, and one is the reflected wave which is attenuated as it travels away from the RF output. The resultant RF voltage pattern on the slow wave circuit can be a complicated standing wave pattern. Furthermore, since the RF probes were located only on a relatively few circuit elements, it was difficult to determine the location of the sensor on the standing wave pattern. The resultant measured power growth profiles were very erratic with peaks and valleys which could not possibly indicate the true characteristics of the growing wave in the tube.

Some attempts were made to improve the situation by using an adjustable mismatch tuner on the output of the CFA to alter the match. This was not very satisfactory because arcing occurred at high peak power levels. Nevertheless, it was possible to demonstrate that the irregularities could be made smoother and a more nearly monotonically increasing power growth curve could be obtained. This was adequate to develop the measurement techniques that were described previously.

A standard technique used on reentrant stream, emitting sole, crossed-field amplifiers is to adjust the position of the cathode relative to the slow wave circuit while the tube is operating to tailor the tube performance. The criteria normally

used for adjustment is to obtain the best broadband compromise toward optimizing power output, gain, and efficiency with the lowest output noise level. The gross effect of these changes was understood from consideration of programmed interaction; i.e., the crossed-field interaction parameters were changed along the length of the slow wave circuit as the power level grows. However, the details of what really happens in the tube were not known. One of the prime objectives of this effort was to learn this information.

To obtain more insight to the tube operation, other cathode positions were studied as well. Initially, three cathode positions were studied with this first vehicle. These corresponded to: (1) mechanical center, (2) electrical center, and (3) best or optimum position to meet tube specification performance. Mechanical center is that position for which the axis of rotation for the cathode stem coincides with axis for rotation for the anode. The cathode in this first tube had a programmed cathode radius around its surface, hence the mechanical center position did not correspond to a uniform spacing between the cathode and the anode in the interaction space. The electrical center position corresponds to that location of the cathode that leads to the highest electrical impedance; i.e., maximum voltage and minimum current. In magnetrons this position is the same as mechanical center, but this is not so in a CFA with a growing wave and/or a programmed interaction space. This position was located by observing the anode-cathode

voltage as the cathode position was changed. The optimum position is that location that leads to rated power output and gain across the operating band consistent with the best overall signal-to-noise performance. In each case, the position was readily determined and definable within a tolerance of a few thousandths of an inch on location.

These three positions were selected for examination because they were quite reproducible. Even with the difficulties encountered with this tube because of the circuit match, it was possible to demonstrate that the cathode position had marked influence on the rate of power growth along the circuit length. This was true even though the variation in peak power output did not change much at constant RF input signal. These experiments represent the first to demonstrate this effect. Experimental curves showing these effects were presented in the first semi-annual report. They will not be repeated here since more meaningful data were obtained later with the fully instrumented tubes with improved circuit match.

5.1.2 The SFD-261 with Circular Cathode

The first RF probe tube (S/N C437S) was assembled using a standard circuit and cathode for the SFD-261 CFA. This cathode was not circular, but had a tapered radius profile along the circumference. This was intended to program the d.c. electric field generally in an increasing fashion from input toward output as the RF power level on the circuit increased. On the other hand, the initial attempts to simulate by computer model the internal functions of a reentrant CFA were directed toward a tube with a completely symmetrical cathode located on mechanical center of the tube. In an attempt to get some experimental results which could be compared with the computer calculations, the first tube was rebuilt with a circular cathode (S/N C437S-1). The new cathode radius was the approximate mean radius of the tapered cathode. This corresponded to a nominal cathode/anode spacing of 0.090 inches. This tube was assembled for evaluation in spite of the fact the poor circuit match caused standing waves that produced results difficult to interpret fully. It was reasoned that some information might be obtained while awaiting completion of the new tubes, that would impact upon the selection of the cathode geometry to be used in them.

Measurements were made with this rebuilt tube similar to those made on S/N C437S. The cathode position was ajdusted for mechanical center, electrical center, and optimum performance. At each frequency the mismatch at the output was adjusted to improve the circuit match. Even so, the presence of the standing wave was

still evident for some measurements. This complicated the interpretation of the results. Nevertheless, it was possible to determine differences in the rate of power growth in the different configurations. Several power growth profiles for this tube were presented in the second semi-annual report. These will not be repeated here since more meaningful data for similar configurations were obtained later with the fully instrumented tubes having improved circuit matches.

All of these initial results with this RF probe tube (S/N C437S) for both cathode shapes showed clearly that variation of cathode position or cathode anode space can produce significant changes in the power growth profile along the circuit length. It was not clear at all what the optimum profile should be. That has still not been fully established at the conclusion of this phase of the effort. It was one of the goals of this program to try to determine this using experimental results of this kind and computer simulations. It will be seen, however, that much insight to the inner workings of the CFA has been obtained.

By the time these initial experiments were completed, new fully instrumented tubes containing both RF probes and thermocouples were available for experimentation. It is, of course, advantageous to have both sensor types in one vehicle. Therefore, no further experiments were performed using these partially instrumented tubes. All further experiments were performed using the new tubes.

5.2 Fully Instrumented CFA's

5.2.1 The Fully Instrumented CFA with Circular Cathode

The first fully instrumented CFA that was fabricated specifically for this program was S/N B193T. It contained both RF probe sensors and thermocouples located at critical points in the circuit vane elements as described previously. It was assembled with a circular cathode and a symmetrical cathode-anode space of 0.090 inches. The RF probes and thermocouples were not attached to the same circuit element, but were displaced to avoid mechanical interference with each other. There were twelve RF sampling probes along the circuit together with a measurement of the input and output power providing a total of fourteen measurements of the RF power growth profile. There were thirteen pairs of thermocouples located along the slow wave circuit. The locations of the sensors were not uniformly spaced, but were dictated by mechanical considerations. Figure 14 shows the first fully instrumented tube mounted in the electromagnet at the test set.

In the initial instrumented tube the center conductor of the RF sampling connector was attached to the stub support of the circuit 0.100 inches away from the tube body. The coupling was further decreased for subsequent tubes by moving the connection point to a location 0.060 inches from the tube body. This was intended to further reduce any potential effect of the RF coupler on the slow wave circuit properties and match. The resulting match

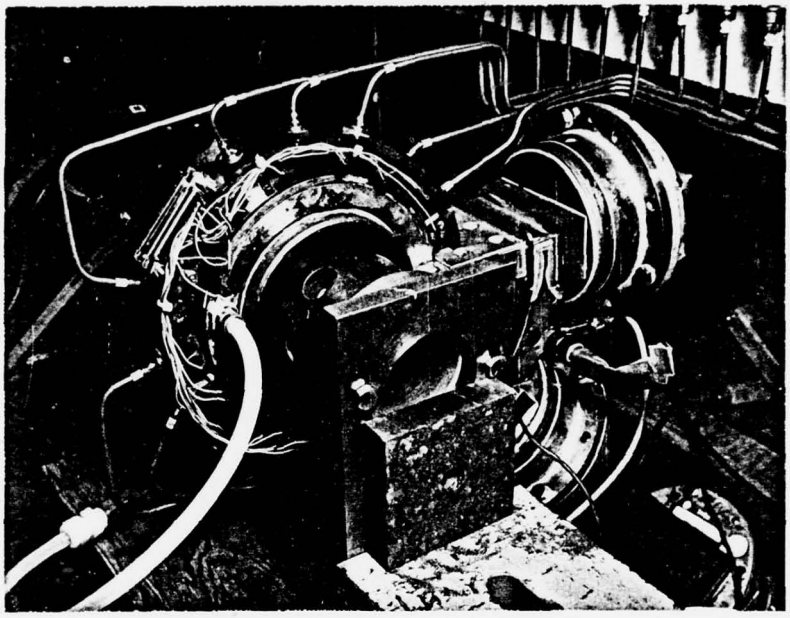

FIGURE 14

INSTRUMENTED CFA WITH RF PROBES AND THERMOCOUPLES MOUNTED IN THE ELECTROMAGNET FOR OPERATION.

characteristics are shown in Figure 15. The operating band for the tube is identified arbitrarily as the linear frequency reqion between fo+.1 to fo+.5. The match for this tube was considerably better than for the initial instrumented tube, but it still degraded toward the lower end of the operating band. It will be seen that this was enough to cause the presence of standing waves on the circuit. However, in the middle of the operating band near fo+.03, the circuit match was very good.

As mentioned previously, several attempts were made to arrive at a quantitative method of assessing the noise performance of the tube that would be meaningful. However, noise is a broad-band phenomenon and it is difficult to give a meaningful characterization that is summarized by a single number unless the distribution is uniform.

It was decided finally to take the data for the tube in a way that preserved as much information as possible. The power growth and temperature profiles through the tube were measured in the normal way as described previously, but noise performance was recorded by photographing the oscilloscopic display of a broad-band spectrum analyzer output when connected to each of the RF sensors. Later it was also recognized that in some cases it was of interest to photograph the video output pulse from the sensors as well. The data output from the experiments were then assembled in a coordinated fashion by mounting all of the photographs, together with graphs showing power growth and vane tip temperature

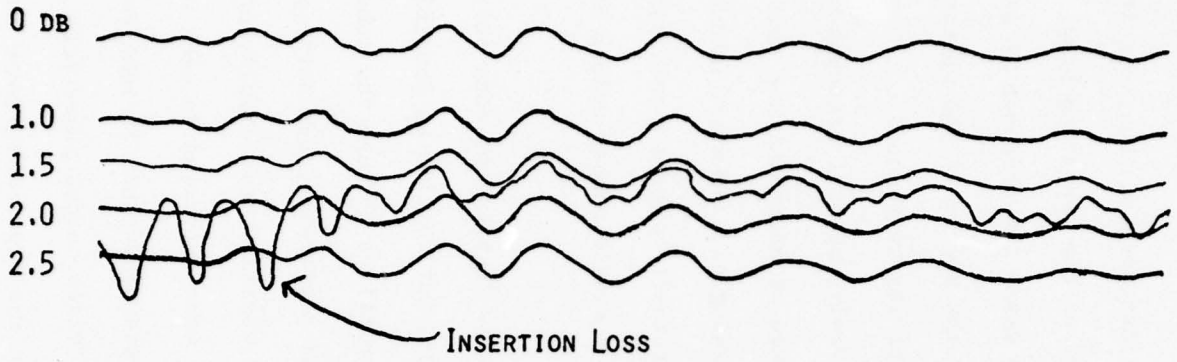

WAVEGUIDE MATCHING CHARACTERISTICS OF INSTRUMENTED CFA S/N B193T

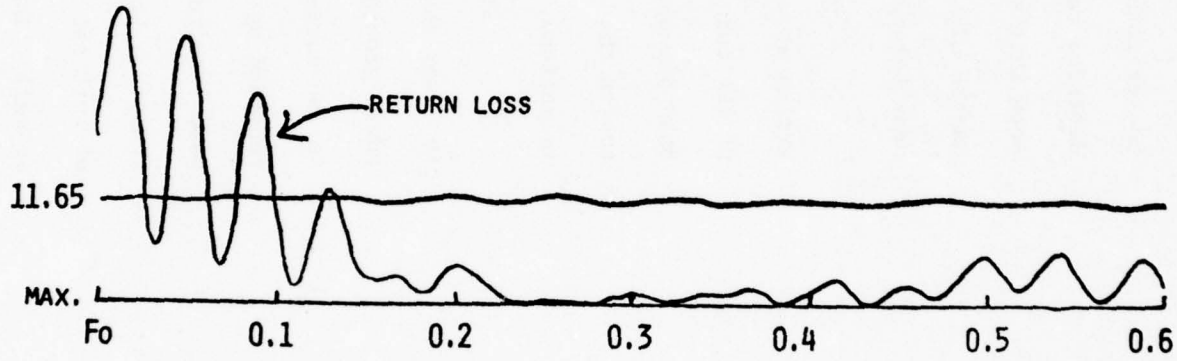

FIGURE 15

profiles, on a single display. In addition, the variation in cathode-anode spacing around the tubes was also shown. Provision was also made to show the variation of the ratio of the applied voltage to the Hartree voltage around the interaction space. This was to be used to evaluate the effects of programmed interaction around the tube. This would also be useful in comparing the experimentally measured profiles with computer simulations. However, this conputation requires an accurate knowledge of the magnetic field in the interaction space. Initially, the electromagnet was not calibrated so the computations could not be made. Later when the calibration was made it was done incorrectly for unknown reasons. Attempts were made later to recalibrate in a way that would allow a correction to be applied, but it was not possible to duplicate the initial calibration meausrements. Hence the calculated Hartree voltages were not reliable for these early experiments.

A series of experiments were performed with this tube. The results are discussed in grouped form, although this is not necessarily the order in which they were obtained. The tube performance characteristics are reported for several conditions as follows:

1. Power and temperature profiles together with spectrum photographs were taken for the tube with the circular cathode on mechanical center at frequencies fo+0.1, fo+0.2, and fo+0.3.

2. Performance data were taken at fo+0.3 at reduced cathode current, but at rated drive power.

3. Performance data were taken at fo+0.3 at reduced drive power.

4. Performance data were taken at fo+0.3 with cathode position adjusted for best signal-to-noise at different points along the slow wave circuit.

6. Performance data were taken with the cathode symmetrically adjusted for a specific offset in the interaction space.

7. Spectrum photographs were taken to assess harmonic power.

8. Experiments were performed to detect the presence or absence of feedback caused by electronic regeneration or circuit reflections.

5.2.1.1 Cathode on Mechanical Center

Figures 16, 17, and 18 show the results from the first series of experiments. The power growth and temperature profiles are shown to the left of the figure. The RF probe connectors and thermocouple pairs are numbered consecutively from the tube input to output. By reference to the abscissa showing the circuit section number, the particular circuit element to which the RF probes and thermocouples are attached can be determined. The peak power is shown in normalized form to avoid classification problems. The measured temperatures of the tips of the circuit elements are shown in °C. These temperatures reflect the fact that the experiments were made at one-third of normal duty operation. The variation in cathode-anode spacing is shown as a function of position along the slow wave circuit. For these experiments with the circular cathode on mechanical center the spacing was a constant 0.090 inches. The format provides for displaying the photographs of the spectrum and detected RF pulse from the TWT output before the circulator at the input to the CFA. It also provides for showing the reverse directed power from the CFA, and for each RF probe psoition as well as the CFA output. These are appropriately designated in the figure. The spectrum photographs show a 2 GHz bandwidth (200 MHz per cm) across the abscissa and a relative amplitude sensitivity on the ordinate of 10 dB/cm. The frequency scale reads from left to right. The time scale for the detected RF pulses is 2 μsec/cm. Vacancies for

Figure 16

RF Power and Vane Temperature Profiles
in Instrumented Tube S/N B193T

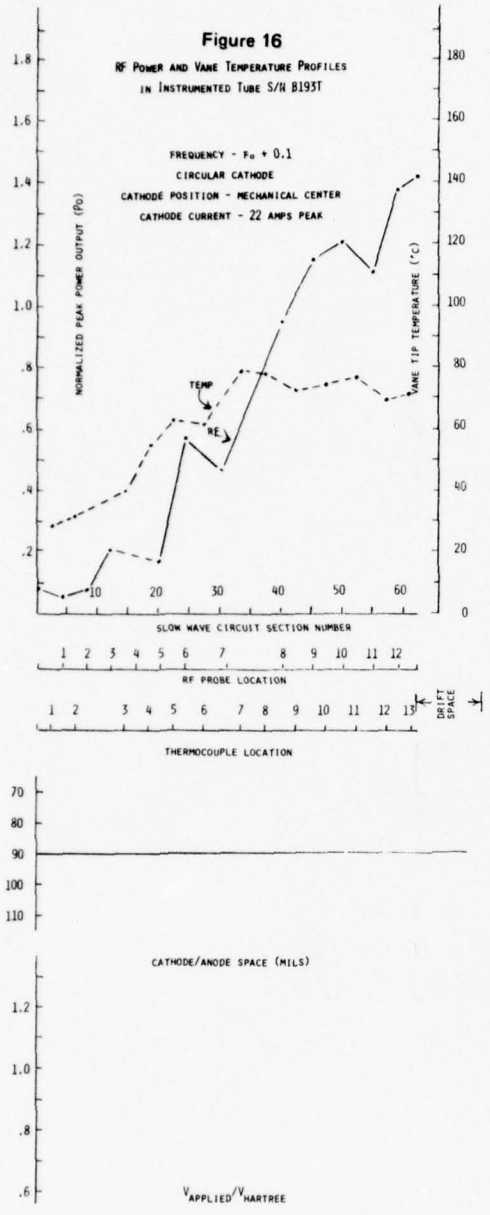

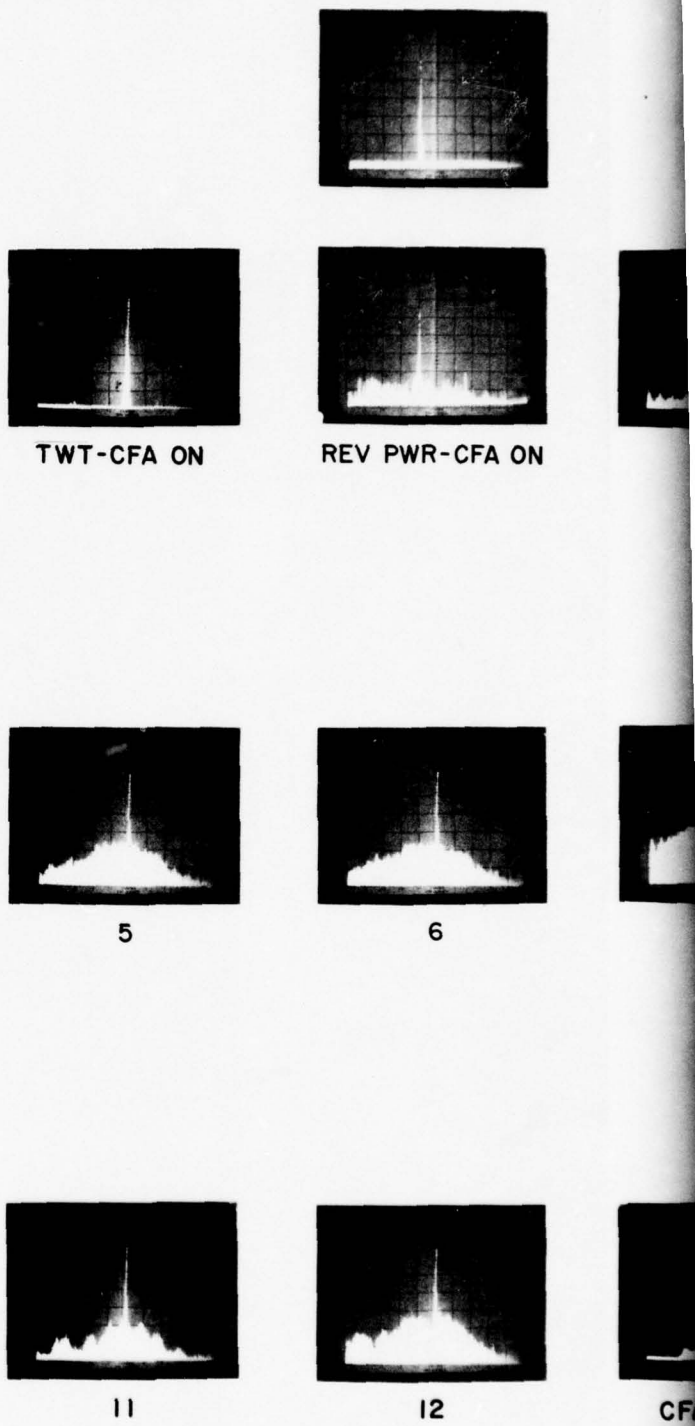

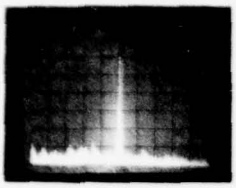

1

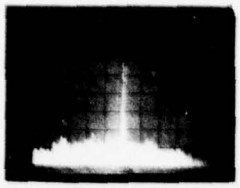

2

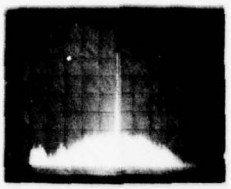

3

4

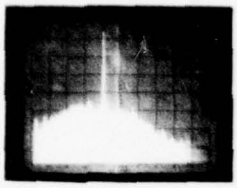

7

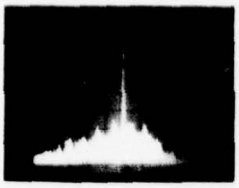

8

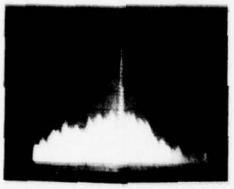

9

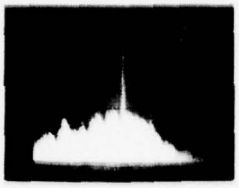

10

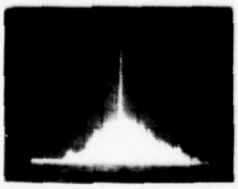

CFA OUTPUT

Figure 17

RF Power and Vane Temperature Profiles in Instrumented Tube S/N B193T

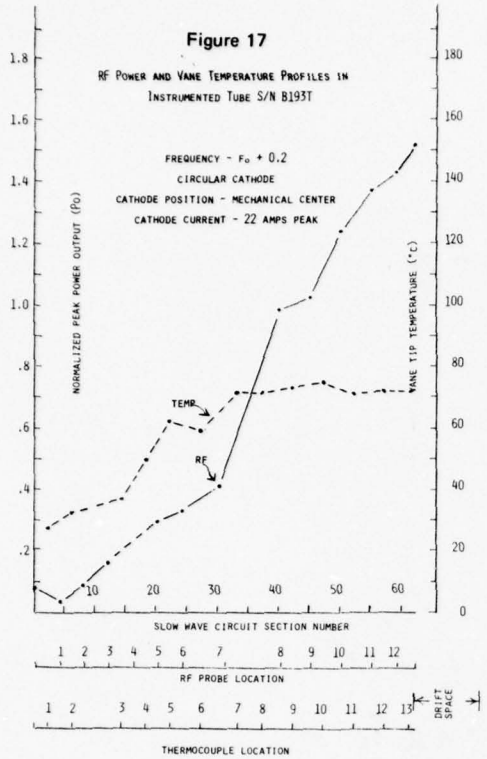

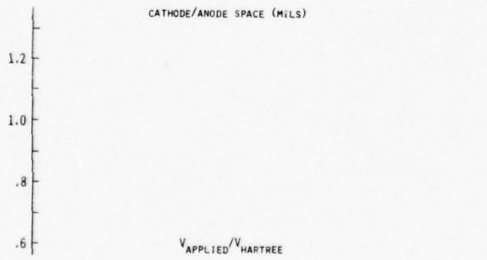

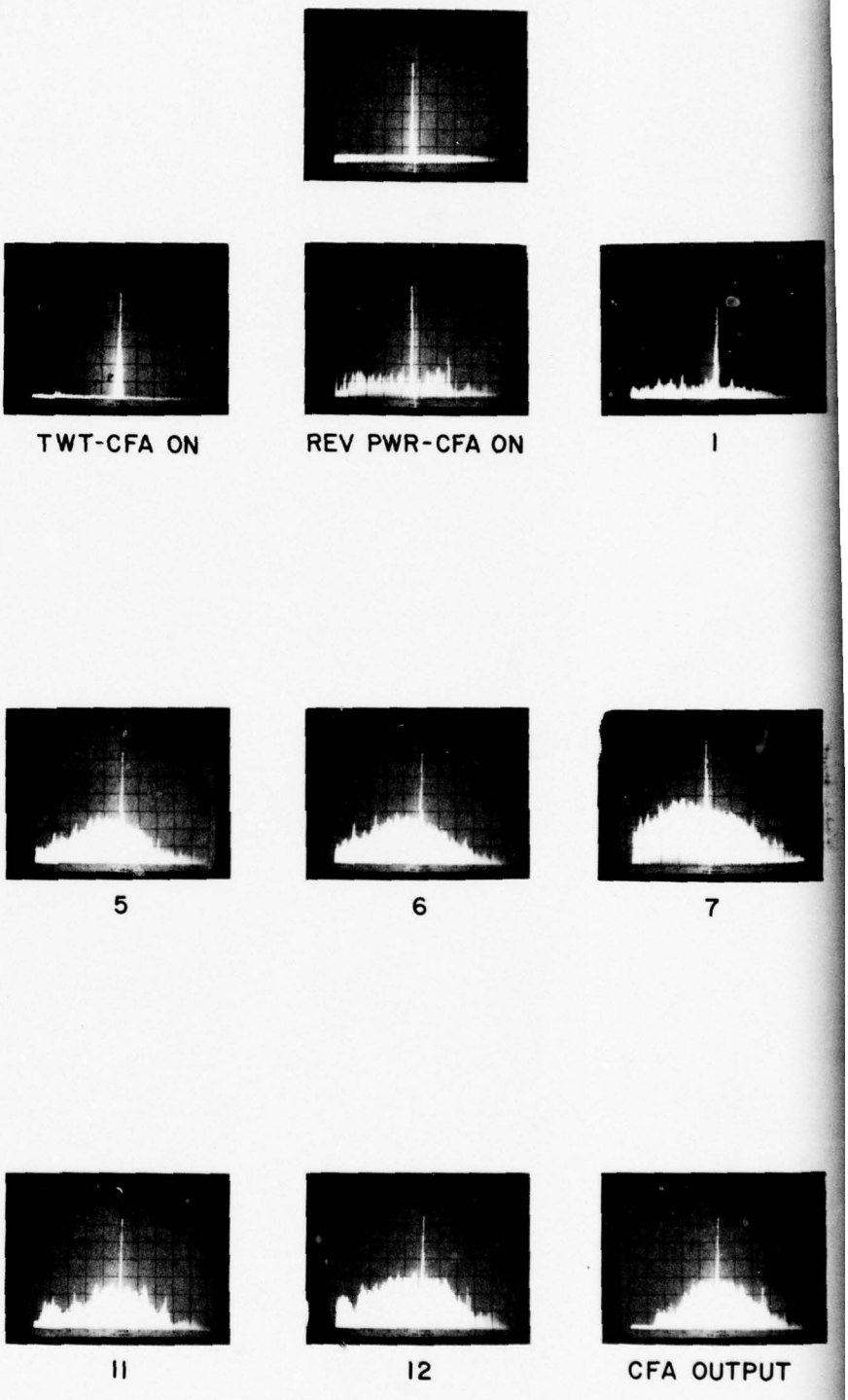

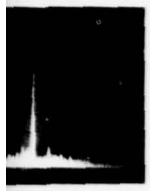

1

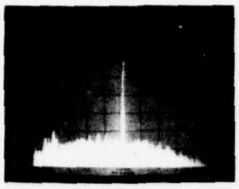

2

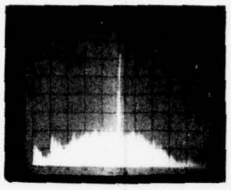

3

4

7

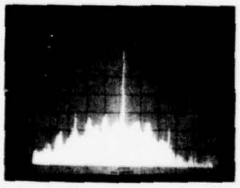

8

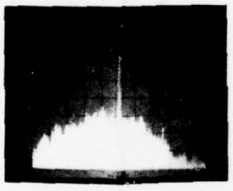

9

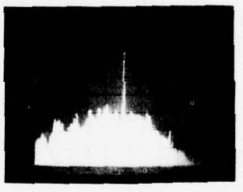

10

UTPUT

Figure 18

RF Power and Vane Temperature Profiles in Instrumented Tube S/N B193T

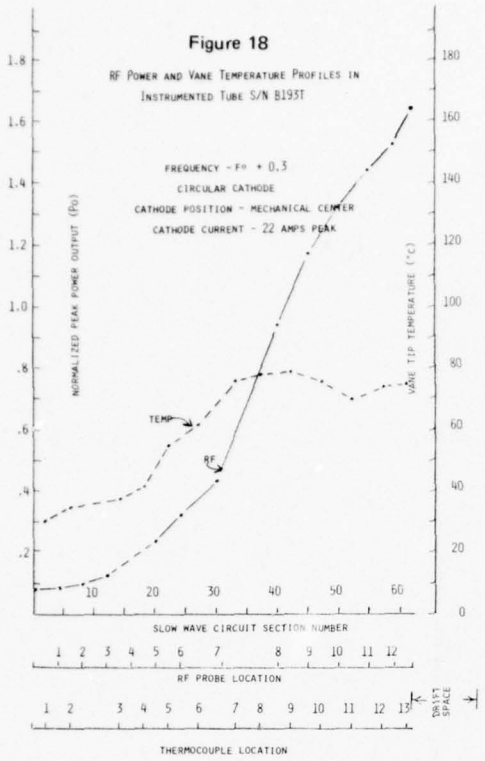

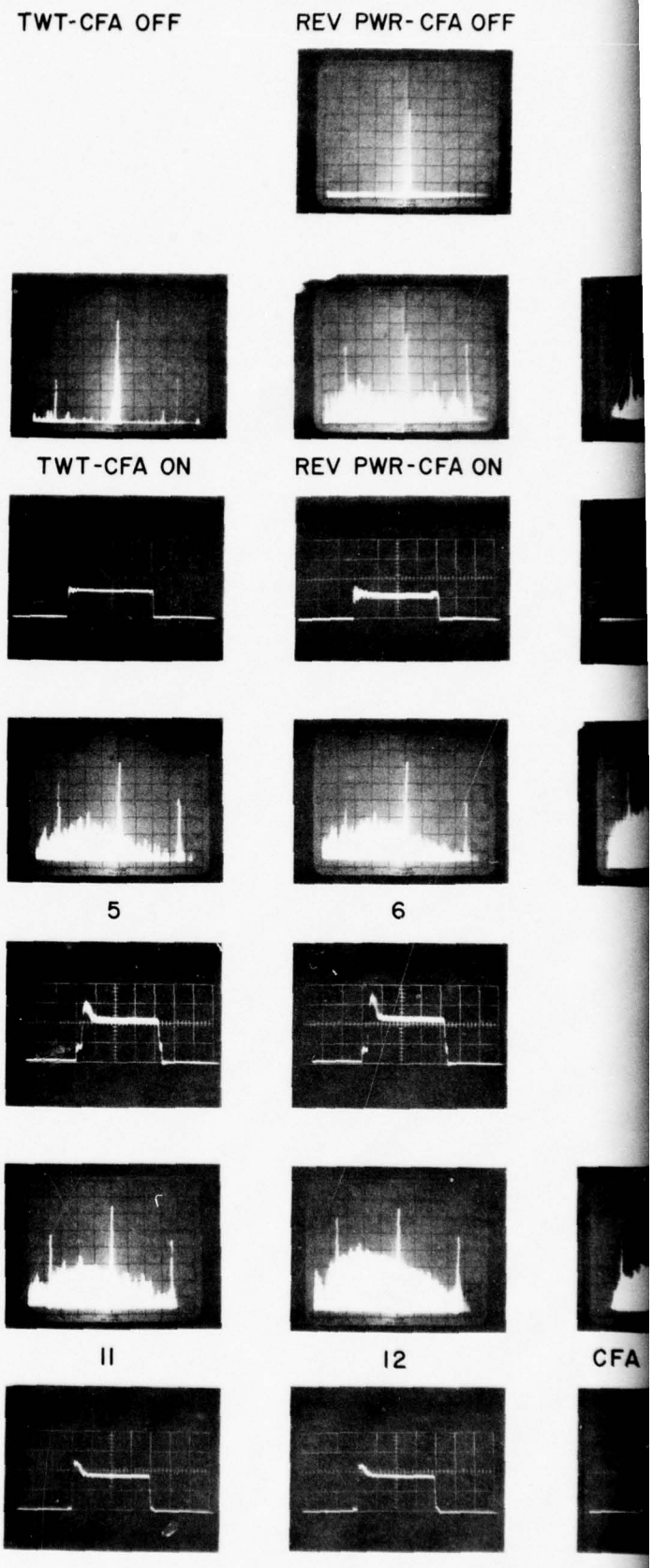

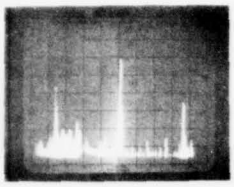

1

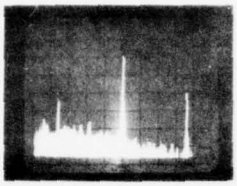

2

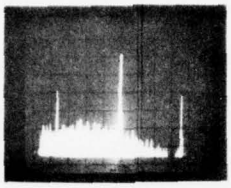

3

4

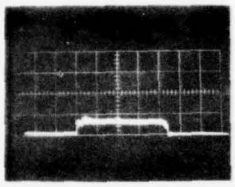

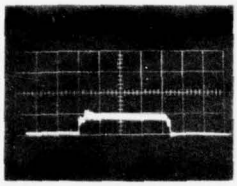

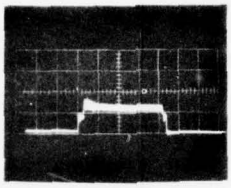

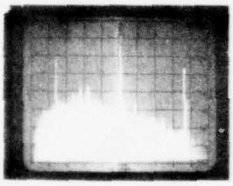

7

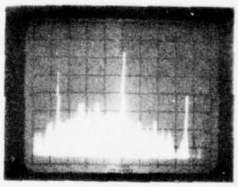

8

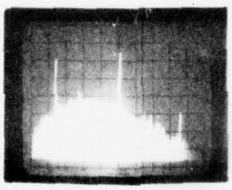

9

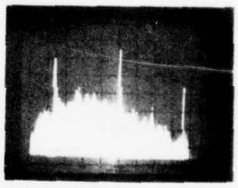

10

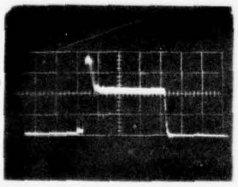

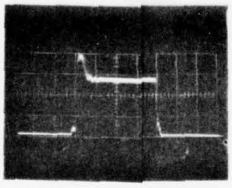

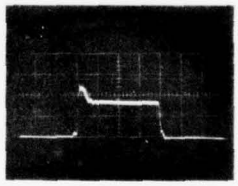

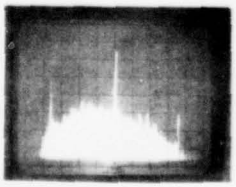

CFA OUTPUT

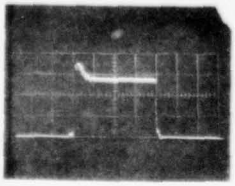

photographs occur when no photographs were taken for one reason or another. For instance, RF probe number four was open circuited for these first experiments and no data could be obtained from that probe. No photographs are shown and the power profile was arbitrarily connected between probe No. 3 and 5 by a dashed straight line.

Several things can be noted from these experimental results. First, the tube would not operate at a frequency above fo+0.3 at rated RF drive signal and rated d.c. input power. In fact, poor operation was obtained at fo+0.3 for rated d.c. input conditions. Next, the effect of the circuit match (causing standing waves) on the sampled RF signal level at the probes is still evident at the low frequency end of the operating band at fo+0.1. This effect becomes less severe at fo+0.2 and is not evident at fo+0.3.

The power profile at this frequency is a reasonably smooth curve and is believed to depict quite closely what is actually occurring within the tube.

The spectrum photographs show the change in signal-to-noise ratio along the length of the circuit. The pictures cannot be compared to each other directly in a quantitative fashion since the absolute value of the coupling coefficients for the RF probes differs between probes and was not measured. In addition, the frequency dependence of the coupling factors were not all the same. The local noise power must be estimated from the signal-to-noise ratio shown in the photographs and from the peak signal power shown

in the power growth profile. The detected noise signals were also affected by the circuit match. Notice that the noise distribution at RF probe No. 12 is different from that coupled out of the tube when the CFA is driven at fo+0.1. The circuit match degrades below fo+0.1, hence the noise coupled from the tube is clipped due to reflections. When driven at high frequencies, the noise output from the tube is not so different from that at RF probe No. 12.

The spectrum photograph of reverse directed power with the CFA operating shows significantly more noise than with the CFA non-operating. Also, the spectrum photographs at the RF probes show the noise growing through the tube with a significant amount of noise at probe No. 1. This probe was located at the fourth circuit section, hence noise on the circuit appeared very quickly. This can occur for one or both of two reasons. First, the reentrant electron steam from the drift space of the tube could be very noisy and noise signals close to the anode could couple to the circuit very quickly. Or noise signals could be reflected from the tube output because the circuit match was not perfect. The reflected noise power would travel backwards through the tube and be detected at the reverse directed power sensors. In some photographs some noise could be detected at the output of the TWT with the CFA operating. This was limited by the frequency attenuation characteristics of the circulator located between the two tubes. It will be seen that both

effects have been detected in the instrumented tubes. It will also be seen that different approaches should be used to minimize or alter each effect.

The spectrum photographs do not show a uniform distribution in noise power with frequency at the different RF probes. Noise signals are always correlated to some degree for a period of time dependent upon the bandwidth and characteristics of the noise. Therefore, noise signals on the slow wave circuit near the output of the tube that are reflected can set up interference patterns for some distance along the circuit similar to coherent signals. The randomness of the noise would control when the effect was present, but the slow sweep rate of the spectrum analyzer integrates over this limitation. The result is that for probes near the output of the tube it was possible to see in some of the photographs a periodic variation in the noise power with frequency. For probe positions more remote from the CFA output, the transmission line length of the structure is sufficiently great that the correlation between the incident and reflected wave deteriorates due to the greater elapsed time. Hence, the periodic fluctuations with frequency of the noise power level shown in the photographs generally disappear toward the input of the tube.

The circuit matching configuration used on the SFD-261 is a multistep, quarter wave matching transformer. This approach was selected to minimize the physical size of the matching arrangement. However, such transformers have band pass characteristics

that rely upon interference patterns between reflections from the transformer discontinuities to obtain the proper matching characteristics. These do not function in the same manner for noise signals. Hence better matching and loading for broadband noise signals would be obtained by using more broadband matching circuits, such as tapered transitions, provided the larger physical size can be tolerated.

The operating current for the CFA for the experimental results of Figures 16, 17, and 18 was the rated current for the tube corresponding to 22 peak amperes. The results of Figure 18 show that the tube at fo+0.3 is experiencing difficulty at this current level. The spectral photographs show two sharp signal peaks symmetrically disposed about the drive signal frequency, but significantly lower in amplitude. The detected RF pulse shows operation at two different levels. The cold cathode CFA appears to start amplification at the signal frequency and then to change operating conditions so that amplification of the signal frequency is occurring simultaneously with an oscillation. The oscillation frequency is indicated by one of the signal peaks and the other is an intermodulation product resulting from interaction between the oscillation and the desired signal. The drive signal frequency accounts for the other frequency peak. It is not completely clear from this data which peak is the oscillation and which is the intermodulation product.

The cathode pulse voltage was reduced a small amount to lower the peak power from the tube and the tube performance stabilized. The detected output pulse for the case when the output power was reduced to approximately equal to Po is shown below the performance graphs in Figure 18. Note that the detected RF pulse shows only one power level. More will be said about operation at reduced voltage later when noise reduction techniques are discussed.

The temperature at the vane tips along the circuit is shown in Figures 16, 17, and 18. The operating temperaures are lower than normal because the tube was operated at approximately one-third of normal duty for these experiments. With the cathode on mechanical center it is seen that the vane tip temperatures increases approximately linearly over the first half of the tube and is approximately constant over the last half. This will be seen to change radically as the tube cathode position was moved in other experiments.

The power profiles for these experiments show that power grew very slowly over the first 20% of the circuit and then increased approximately linear over the remainder. This too will be seen to change markedly with cathode position. The significance of the change in power growth rate with distance along the slow wave circuit was not fully recognized initially. This was especially true for a tube with a symmetrical interaction space and uniform slow wave circuit. It will be seen, however, that two different amplification mechanisms are effective in a reentrant stream amplifier.

Near the input to the tube, interaction occurs primarily with reentering electron current near the anode somewhat like an injected beam tube. Further along the slow wave circuit amplification occurs using space charge extracted from the circulating electron hub. These effects had been suggested before, but never demonstrated. It will be seen that this effect is also indicated by the computer simulation. This will have important implications regarding the best method of utilizing programmed interaction.

Some other experiments were performed with this tube at frequency fo+0.3 where a good match exists. Figure 19 shows the performance results when the cathode current was reduced from 22 to 20 amperes peak. The power output from the tube is reduced somewhat, but the profile for power growth and vane tip temperature remain essentially the same in shape. The bandedge oscillations are not present.

Next the tube was operated at reduced RF drive. The RF drive level was lowered to 75% and 50% of rated RF drive power. The cathode pulse voltage was increased only to a value for which the RF output pulse shape did not deteriorate. This corresponds to lower peak power output in each case. The purpose of the experiment was to determine if significant changes in the power growth and temperature profiles occurred. The results are shown in Figures 20 and 21. It was observed that for drive power equal to one-half of rated value the cathode voltage and current could only be raised to a point where the power output from the

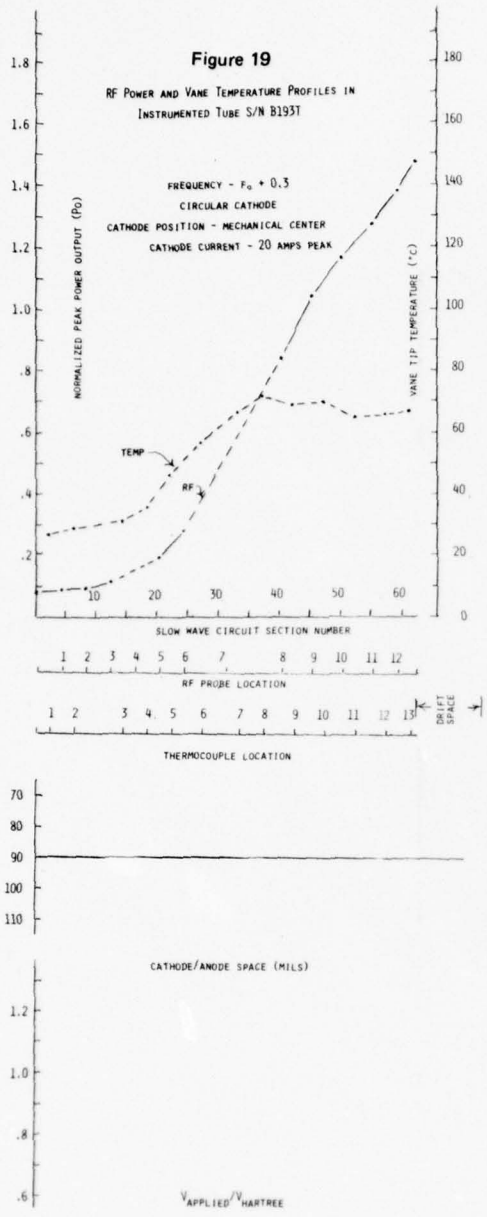

TWT-CFA OFF

REV PWR-CFA OFF

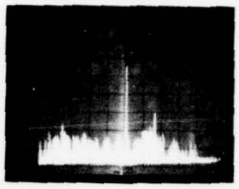

TWT-CFA ON

REV PWR-CFA ON

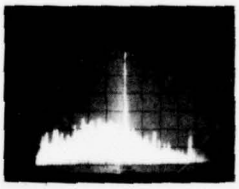

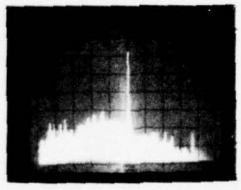

5

6

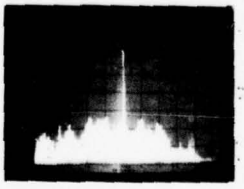

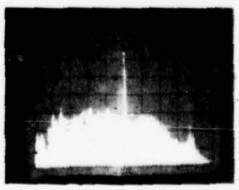

11

12

CFA OU

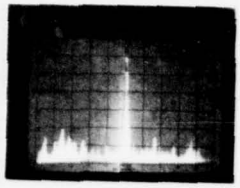

1

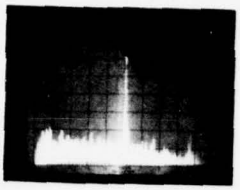

2

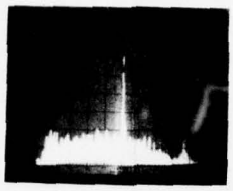

3

4

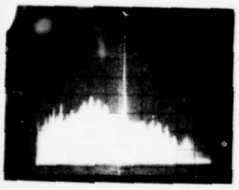

7

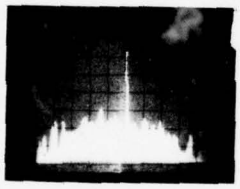

8

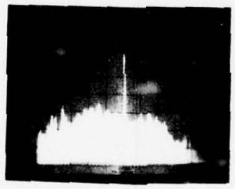

9

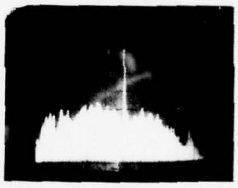

10

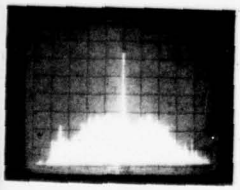

CFA OUTPUT

2

FIGURE 20

RF POWER AND VANE TEMPERATURE PROFILES IN
INSTRUMENTED TUBE S/N B193T

FREQUENCY - F_o + 0.3
CIRCURLAR CATHODE
CATHODE POSITION - MECHANCIAL CENTER
RF DRIVE POWER - 0.5 P_I
CATHODE CURRENT - 11.7 AMPS PEAK

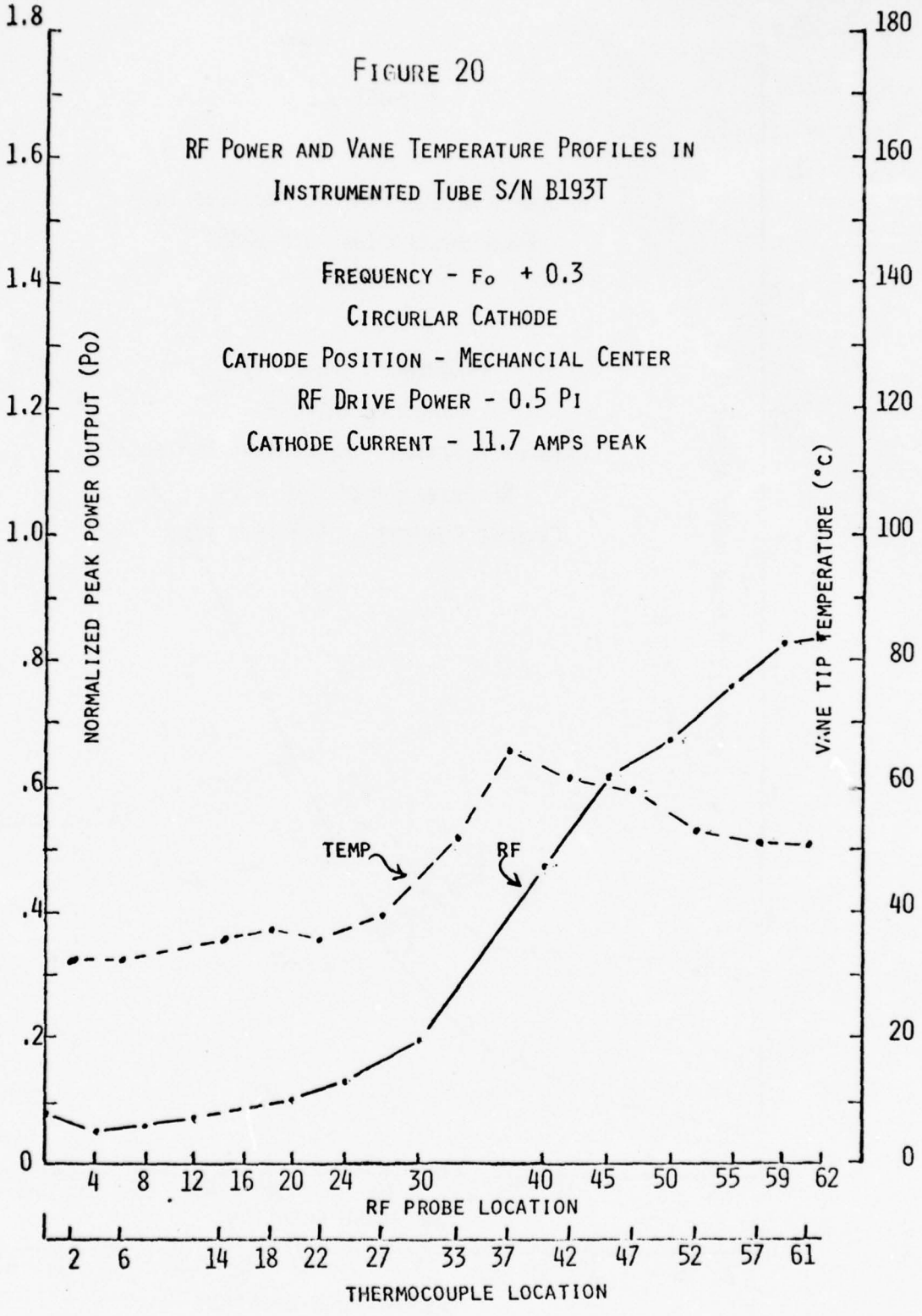

FIGURE 21

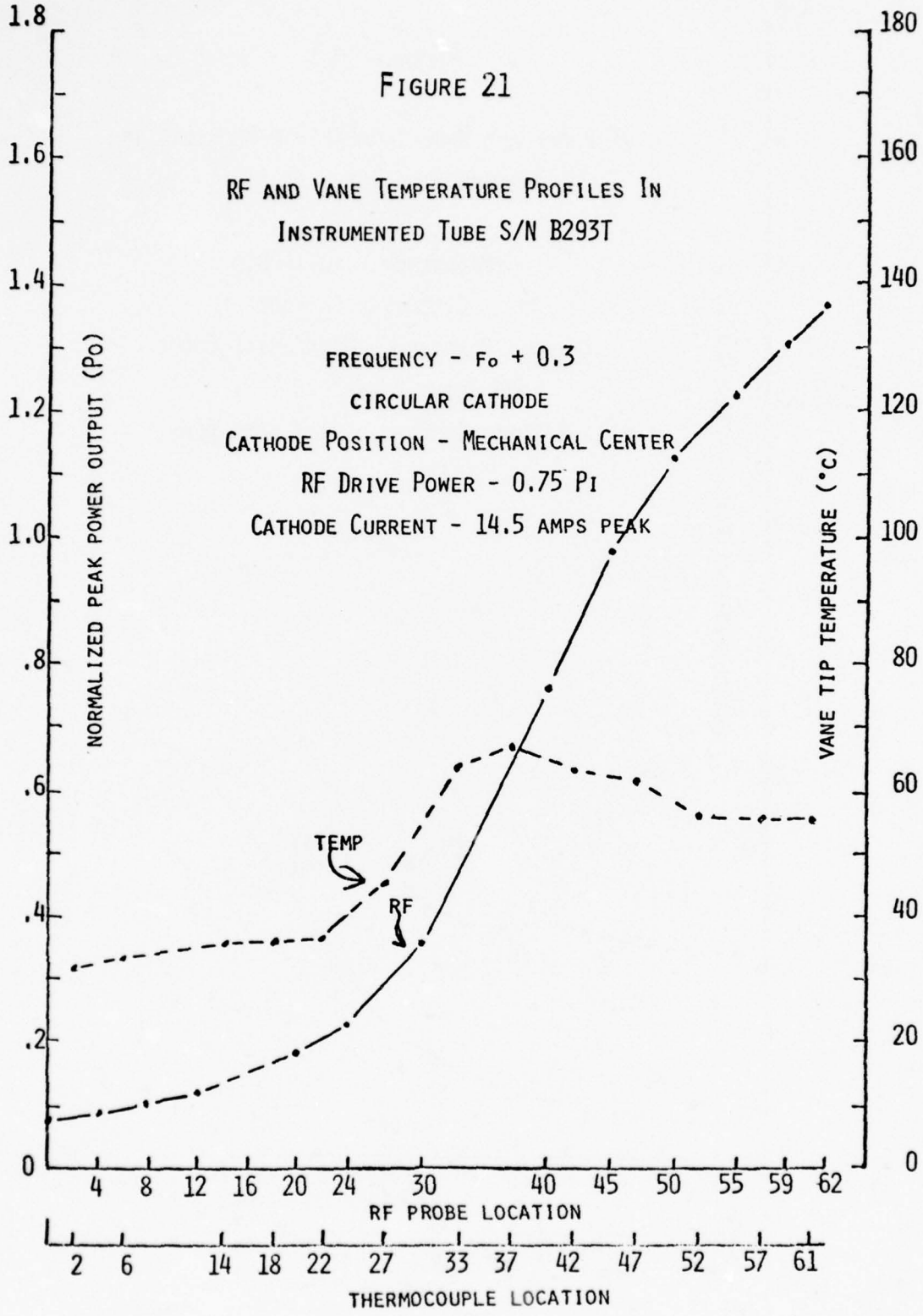
RF AND VANE TEMPERATURE PROFILES IN
INSTRUMENTED TUBE S/N B293T
FREQUENCY - Fo + 0.3
CIRCULAR CATHODE
CATHODE POSITION - MECHANICAL CENTER
RF DRIVE POWER - 0.75 PI
CATHODE CURRENT - 14.5 AMPS PEAK
NORMALIZED PEAK POWER OUTPUT (Po)
VANE TIP TEMPERATURE (°C)
TEMP
RF
1.8
1.6
1.4
1.2
1.0
.8
.6
.4
.2
0
180
160
140
120
100
80
60
40
20
0
4 8 12 16 20 24 30 40 45 50 55 59 62
RF PROBE LOCATION
2 6 14 18 22 27 33 37 42 47 52 57 61
THERMOCOUPLE LOCATION

tube was half the value obtained at rated drive. For drive power equal to three-quarters of rated drive the cathode voltage and current could be increased a little more and power output could be increased to about 85% of the value obtained at rated drive power. In all cases, the power growth and vane tip temperature profiles had the same general shape, but differ in peak values obtained.

Photographs of the broadband spectrum and of the detected RF pulses were taken for all subsequent experiments as shown in Figures 16-19. However, these have not been as useful in adding insight to the CFA operation at this point as the measured power and temperature profiles as a function of cathode position. The data has been preserved for future review, but for the remainder of this report the photographs generally will not be reproduced.

5.2.1.2 Cathode on Electrical Center

Since the experimental results with this new fully instrumented tube showed little effect due to circuit reflections at midband and since this is the frequency at which all the computer simulation calculations were being made, it was decided to perform most of the additional experiments at only this frequency. The first experiment was made by adjusting the cathode position for the highest d.c. impedance; i.e., electrical center. The results are shown in Figure 22. For this condition, the cathode was deflected toward the drift space and the RF input section. The cathode-anode spacing varied from 0.080 to 0.100 inches along the interaction space. The power profile showed negative electronic gain near the RF input with a near linear power growth over the last eighty percent of the circuit. Less peak power output was obtainable before serious degradation of the output signal occurred. The vane tip temperature distribution changed significantly. A region of high anode dissipation occurred near the first third of the circuit where the peak power level was only about one-third of the final power output. Vane tip temperatures were actually higher than near the output sections of the circuit and were nearly equal to those obtained near the output of the tube with the cathode on mechanical center where the circuit power level was three times as high. The reasons for this thermal peak were not fully understood at the time that these data were taken. Similar effects had been observed earlier with SFD-261 CFA's employing standard circuits and cathodes. More insight to this

was obtained as more experiments were performed and as the computer simulation was improved. It will be shown that this is related to electron reentrancy condition and to electronic interaction changes in a reverse taper region. This will be discussed more later in this report.

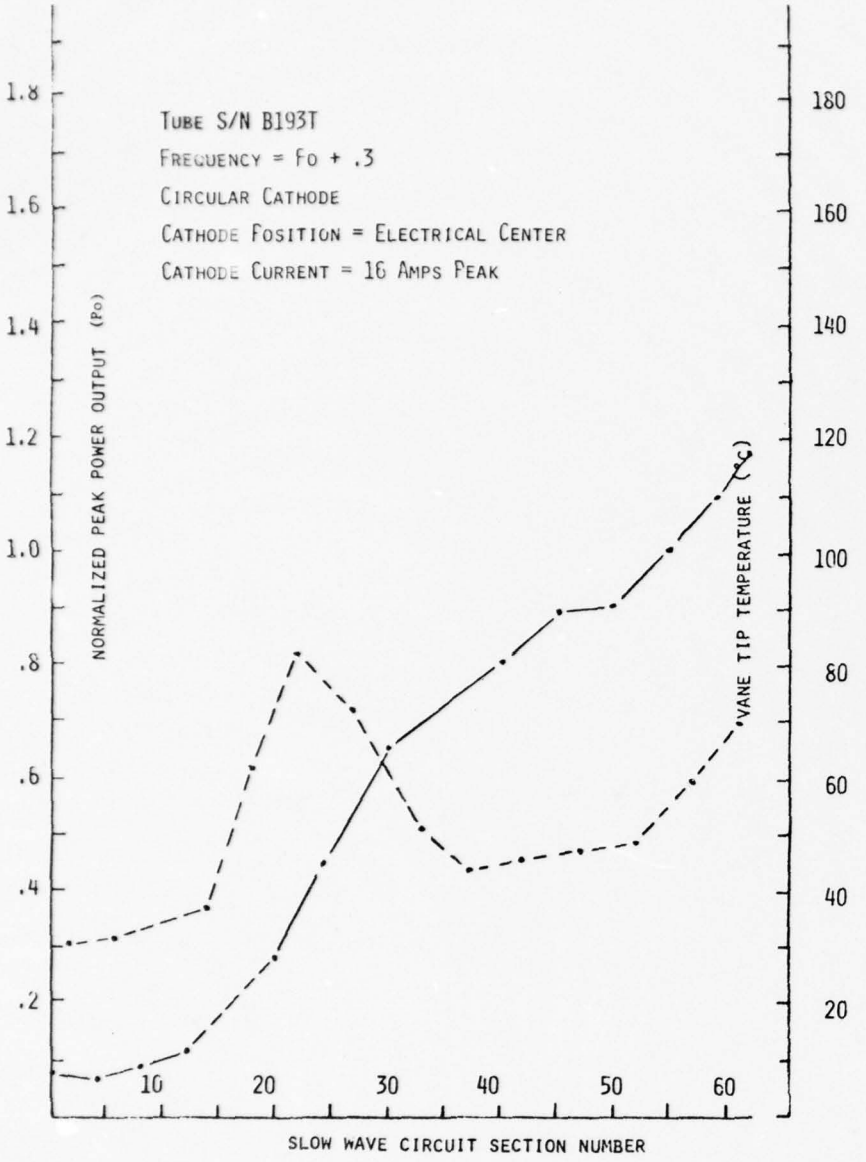

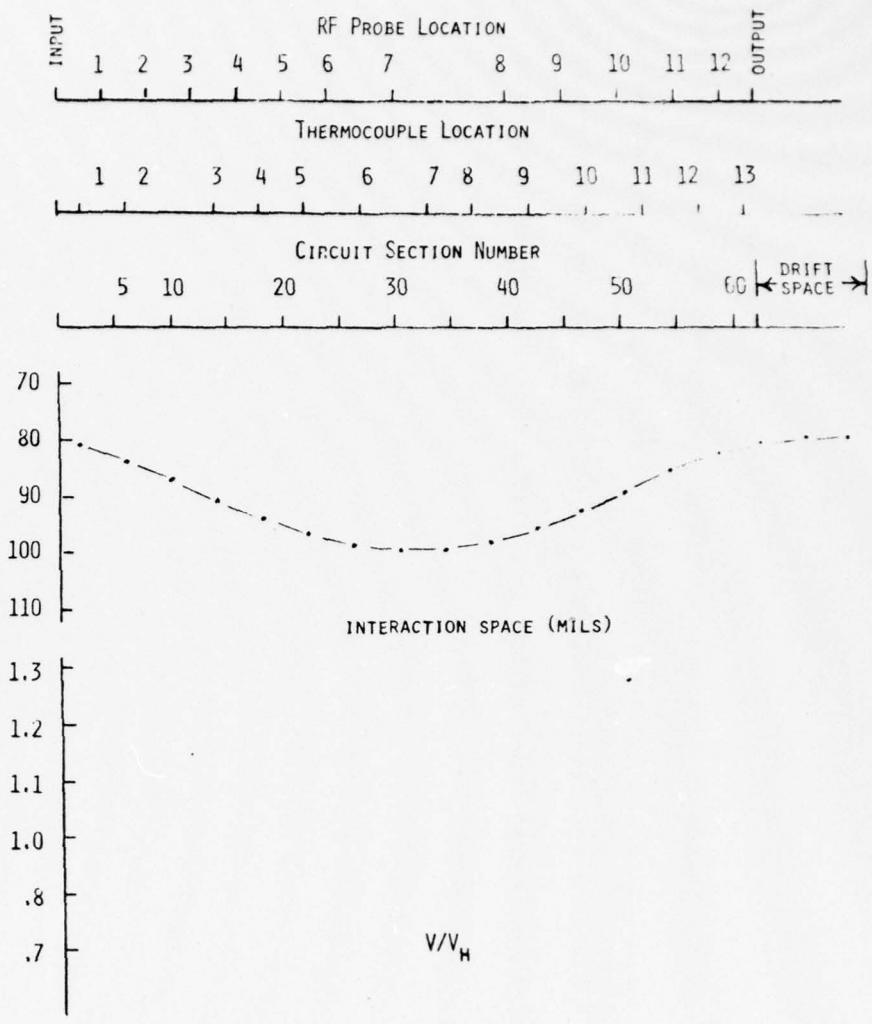

FIGURE 22--RF POWER AND VANE TEMPERATURE PROFILES IN INSTRUMENTED TUBE (S/N B193T)

5.2.1.3 Cathode Adjusted for Best Signal-to-Noise Ratio

It is common practice to move about the cathode position of reentrant CFA's to alter the performance characteristics of the tube. Typically, as the cathode position is changed, the signal-to-noise ratio at the tube output changes as well as the peak power output. Sometimes, the tube efficiency also changes. Generally, the cathode position is adjusted to give the best overall compromise in performance across the operating bandwdith of the tube. The adjustment procedure is subject to individual interpretation of results, but experience has shown that the final position for the cathode is nearly always very close to the same position for any particular tube type regardless of who does the adjustment. The changes in internal operation produced by variation in cathode-anode spacing are only partially understood. The theory of programmed interaction as originally conceived shows that the d.c. electric field caused by a change of anode-cathode spacing should generally increase along the interaction space from input to output as the RF signal on the circuit grows. There is no theory that predicts what geometry is best for minimizing the noise output. Indeed, there had been no firm reason to believe that the interaction space geometry has any significant effect on the noise output from the tube. In the interest of trying to gain insight to this subject, a series of experiments were performed in which the RF probes were used to observe the changes in noise levels. It was decided arbitrarily to adjust the cathode positions for best measured signal-to-noise performance using several RF probes as a group for monitors for

what was occurring locally on the slow wave circuit. Measurements were made using probes, 1 2 and 3: 4, 5 and 6; 7, 8 and 9; 10, 11 and 12; and using only the output signal. The output of only one probe could be observed at one time, hence the adjustment was made by switching between them and averaging the results. The result was subject to interpretation and could vary with the individual experimenter. The results are shown in the second semi-annual report. It is not particularly useful to reproduce all of them here since alternative views have been developed since then. However, the results for best signal-to-noise ratio at the output are shown in Figure 23.

Several observations could be made from these results. First, the cathode position for best localized performance did change. However, in general, the cathode was pushed for each condition toward the anode at a point about 75% of the way along the interaction region. The magnitude of the cathode offset from center position and the point of closest separation between cathode and anode varied somewhat. No conclusions could be drawn at the time. More information was needed. By comparison of the spectral photograph, however, it was observed that changes in the local noise power could be obtained. These suggested that the interaction space profile can be used in a reentrant CFA to alter the noise characteristics. Just how this should be done for optimum results was not clear because moving the cathode position changes conditions all along the circuit length instead of producing only a local change.

Other factors also are clearly involved. For one anode-cathode space geometry the cathode voltage was lowered to reduce the

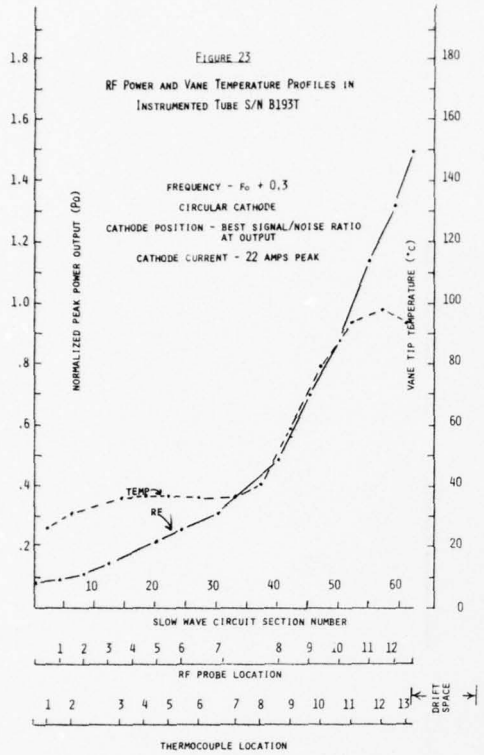

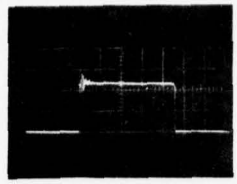

TWT-CFA OFF

REV PWR-CFA OFF

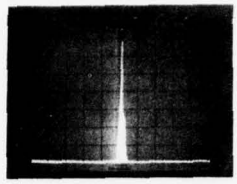

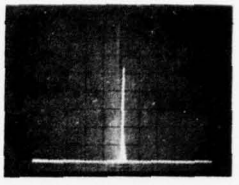

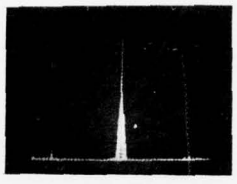

TWT-CFA ON

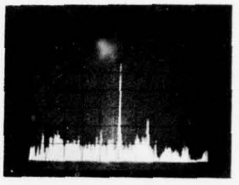

REV PWR-CFA ON

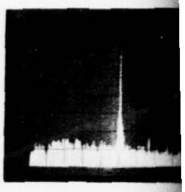

1

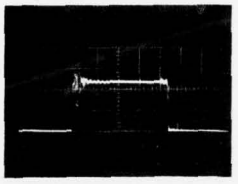

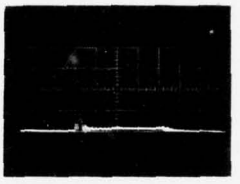

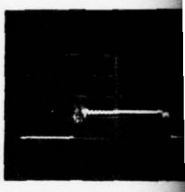

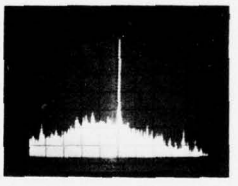

5

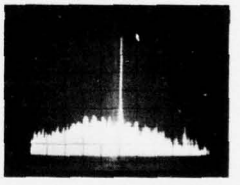

6

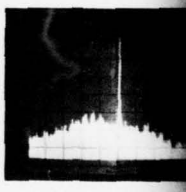

7

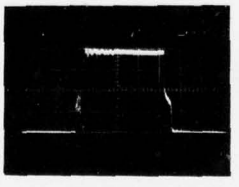

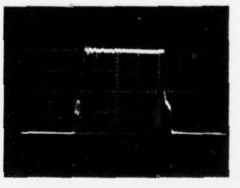

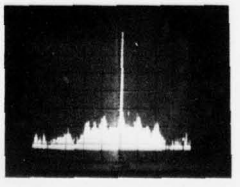

11

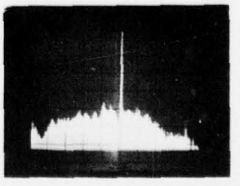

12

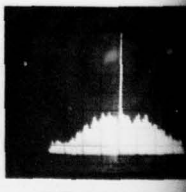

CFA OUTPU

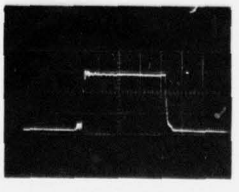

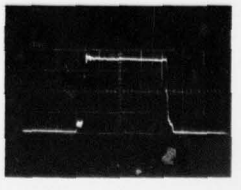

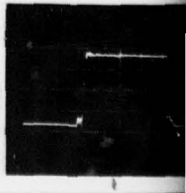

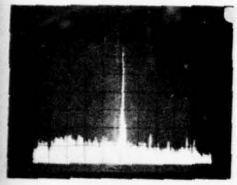

1

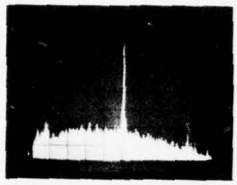

2

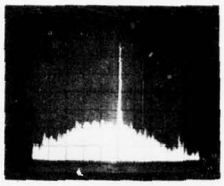

3

4

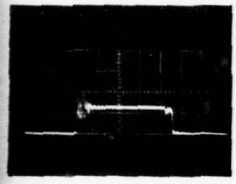

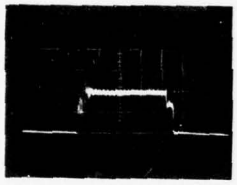

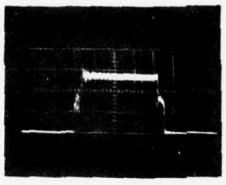

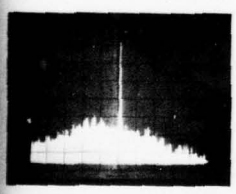

7

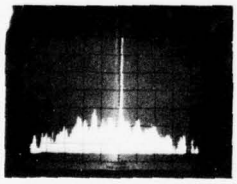

8

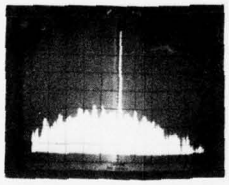

9

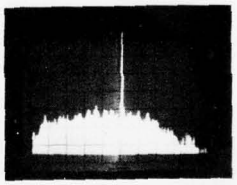

10

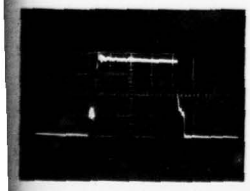

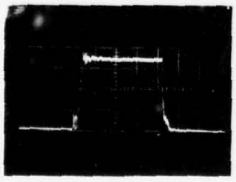

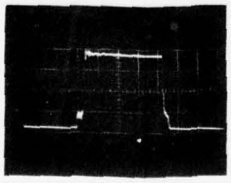

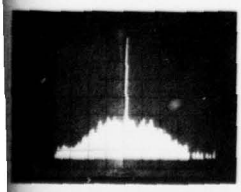

CFA OUTPUT

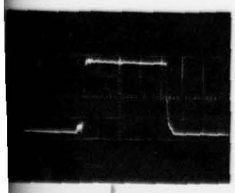

power output by about 2 dB. The power output for this case is about equal to the normalized reference power, Po. In this case, the signal-to-noise ratio improved by 8-10 dB although the power output dropped by 2 dB. This effect will be discussed later.

The power growth and temperature distribution profiles were quite different for these conditions compared to those with the same cathode on mechanical center. The peak power output is about a half dB lower than that obtained with the cathode on center and was about the same for all of the test conditions that were tried. Very little power growth occurs over the first half of the circuit and a very rapid power build up occurs over the last half. The vane tip temperature distribution shows little anode dissipation over the first half of the tube and shows a marked peak in anode temperature distribution near to the region of close separation between anode and cathode. However, the data shows that the maximum temperature point does not always occur exactly at the point of minimum separation. This will be more evident in the results from. the next group of experiments described in the next section.

The other set of measurements were made with the cathode adjusted for best signal-to-noise performance at the RF output. It has been noted previously that the cathode position is generally very close to the same first position regardless of who performs the adjustment. However, it has also been observed that the peak power output does not vary rapidly with cathode radial position once the cathode offset is in the proper radial direction. Therefore,

the question was raised about the sensitivity of the internal vane tip temperature to the cathode radial offset. The tube was operated at one-third normal duty and the RF power growth and vane temperature profiles measured. The RF power growth profiles did not change markedly, but the peak vane tip temperature changed significantly. Figure 24 shows the results. The peak power output and the maximum vane tip temperature are shown as a function of cathode-anode spacing. The vane tip temperature increases rapidly even though the power output did not change much.

This result led to changes in cathode adjustment procedures. A lower limit was placed upon the interaction space gap for production models of the SFD-261 regardless of tube performance. This was intended to provide protection for the circuit against overheating.

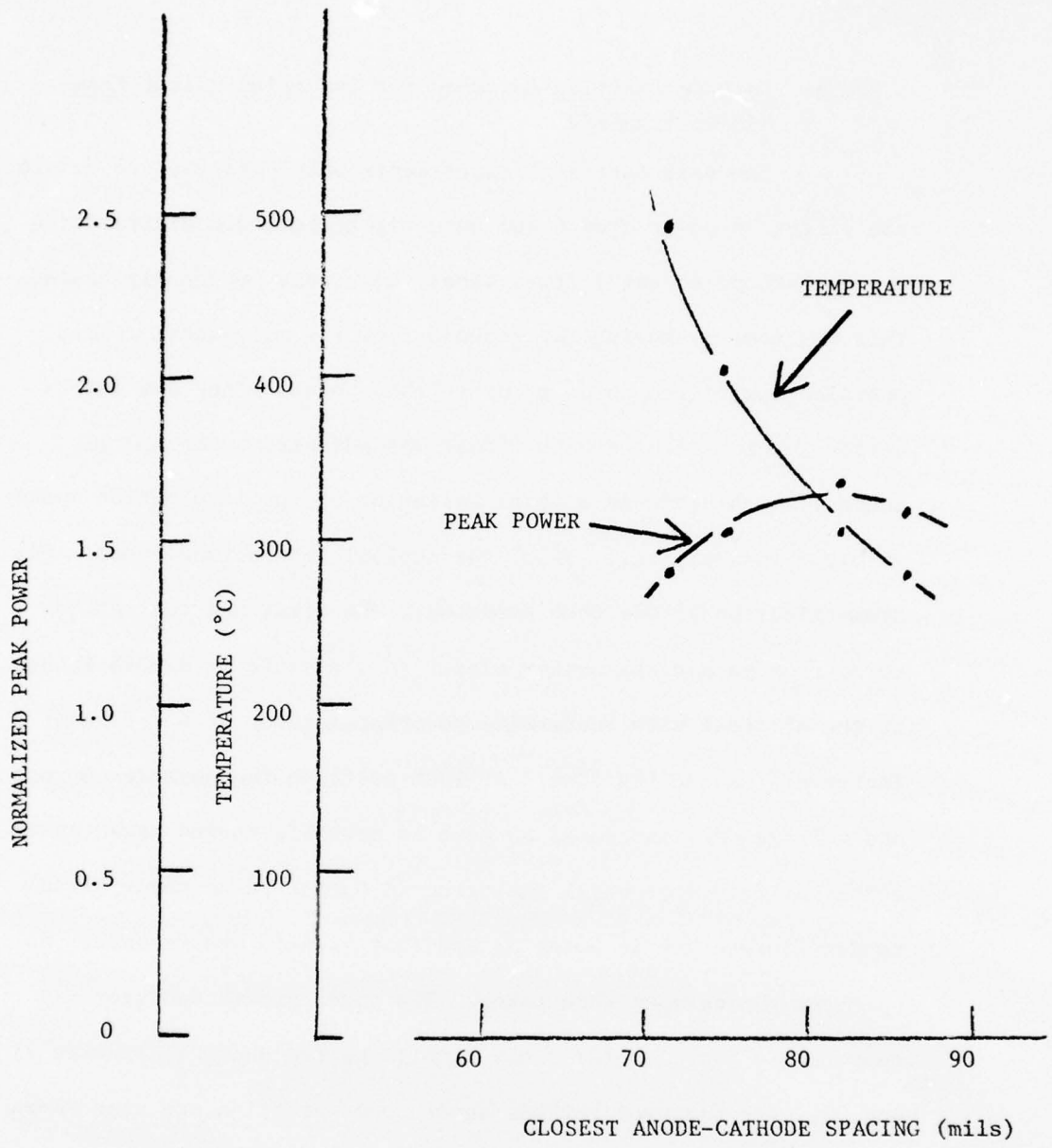

FIGURE 24

MAXIMUM VANE TIP TEMPERATURE ASSUMING FULL DUTY AND 140°C HEAT SINK TEMPERATURE AND PEAK OUTPUT POWER AS A FUNCTION OF MINIMUM ANODE-CATHODE SPACING. TAPERED CATHODE CFA, S/N F376T.

5.2.1.4 Cathode Position Adjusted for Specified Offset from Center Position

The next series of experiments were performed to determine the effect on power growth and vane tip temperature distribution due to cathode eccentricities other than those previously tested. This was done by moving the cathode from the mechanical center position toward the anode at prescribed points along the interaction length. The cathode offset was adjusted to be 0.0045 inches, which produces a total variation of the interaction space of 0.009 inches; i.e., 10% of the nominal interaction space. Six symmetrical positions were selected. The first had the cathode moved from mechanical center closer to the anode by 0.0045 inches at the RF input with successive position located at 60° angular increments around the tube. At each position the cathode current and voltage were increased as much as possible toward rated power output at fo+0.3 or until the detected output pulse shape began to deteriorate due to noise or spurious signal interference. No spectrum photographs were taken. The power growth and vane tip temperature profiles for these conditions are shown in Figures 25 and 26. The measured cathode-anode space profiles are also shown. At the first position with the cathode moved toward the first vane, the peak current was limited by stability to 13 peak amperes and the maximum power output obtained was 0.95 Po. Notice that the peak in the temperature profile occurs near the middle of the circuit and not near the position of closest cathode-anode spacing. Similarly for the second position with the cathode located closest to the

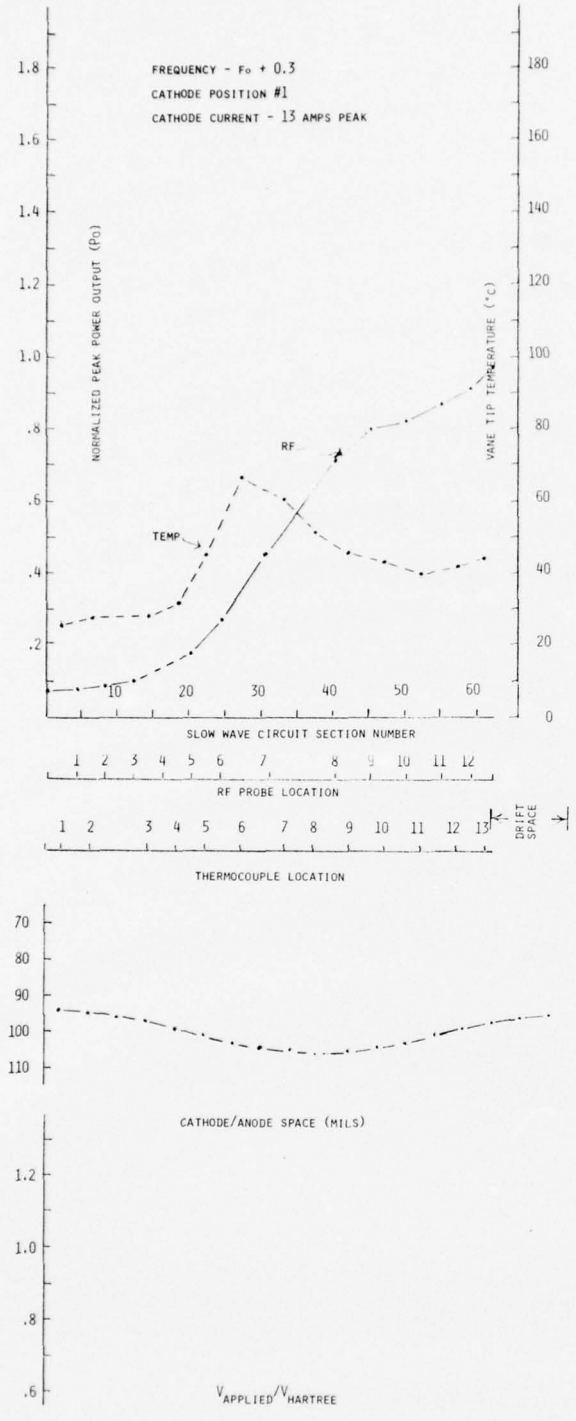

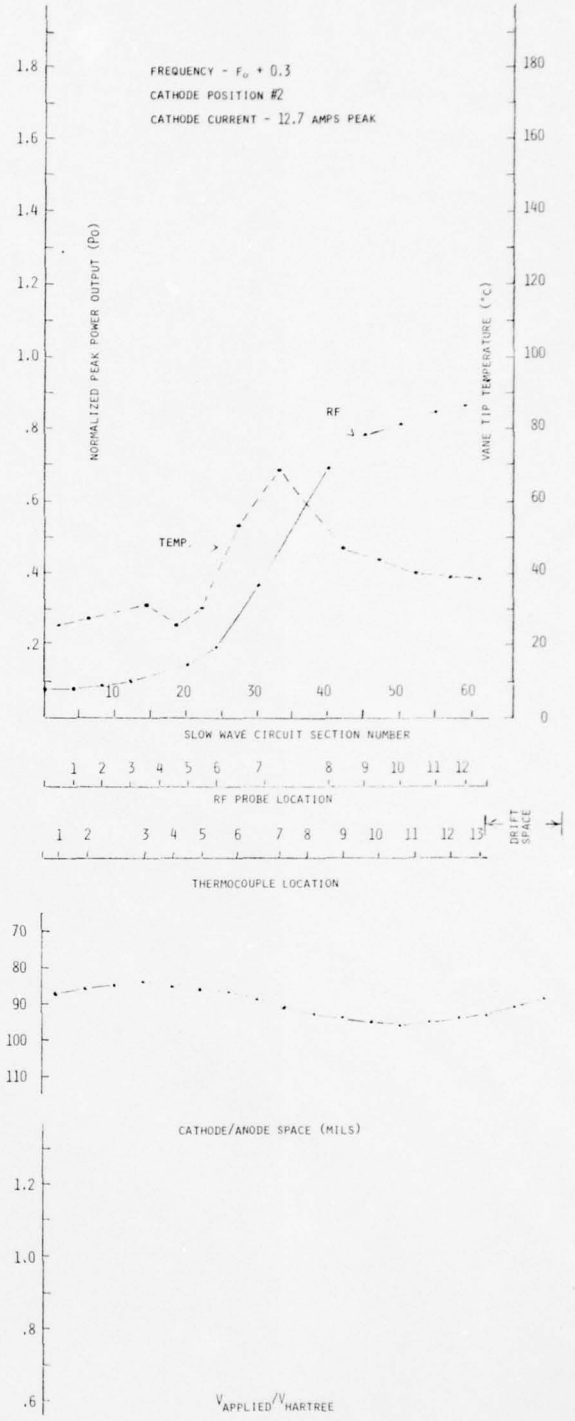

Figure 25 - RF POWER AND VANE TEMPERATURE PROFILES FOR INSTRUMENTED CFA
CATHODE POSITION ADJUSTED FOR SPECIFIED OFFSET.

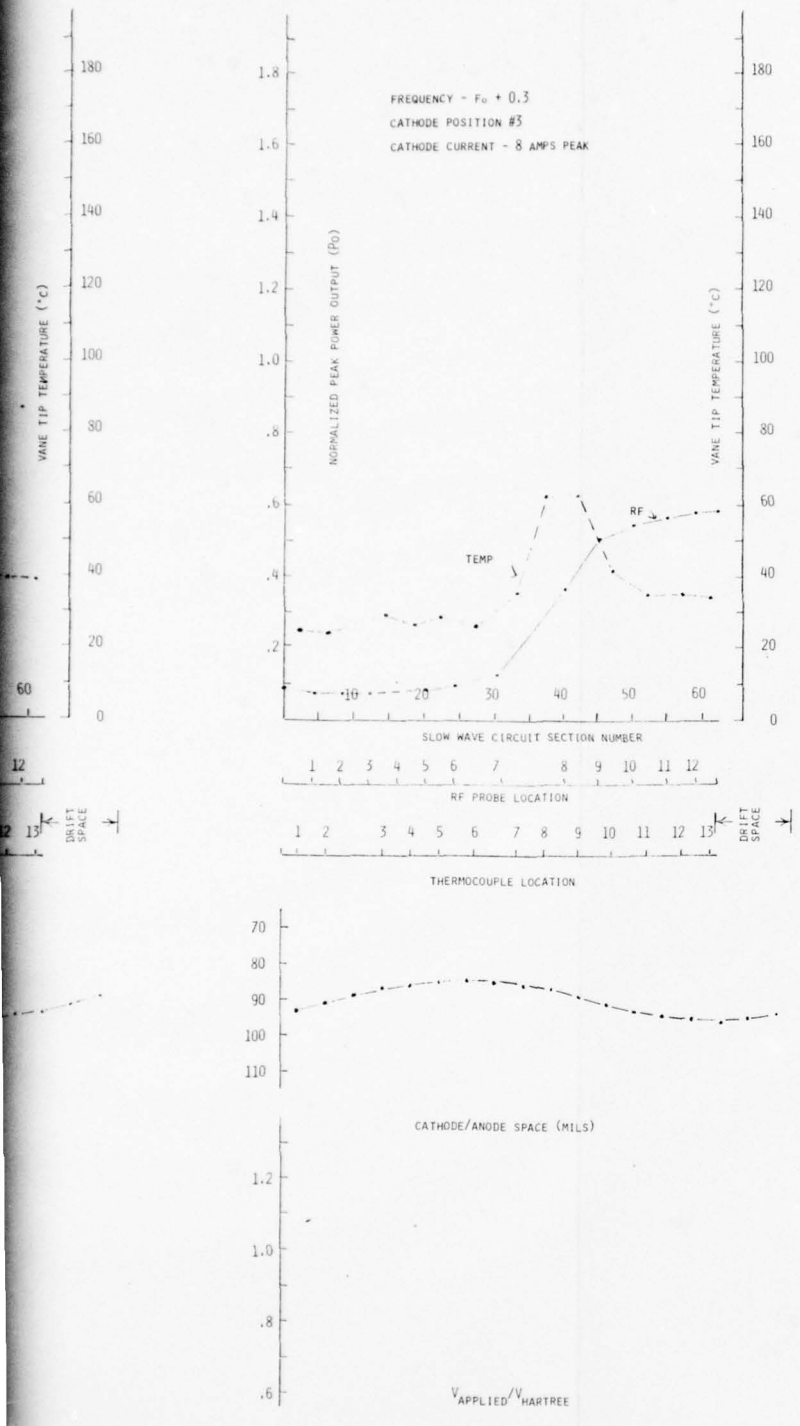

NSTRUMENTED CFA (S/N B193T) WITH
F.

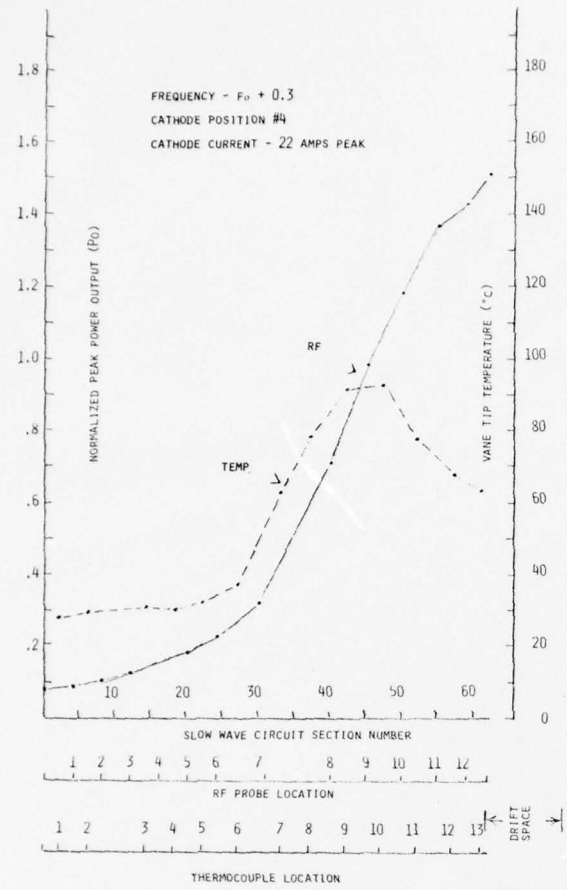

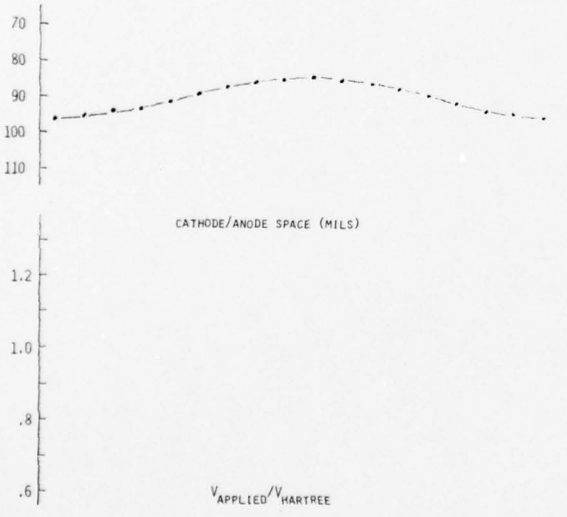

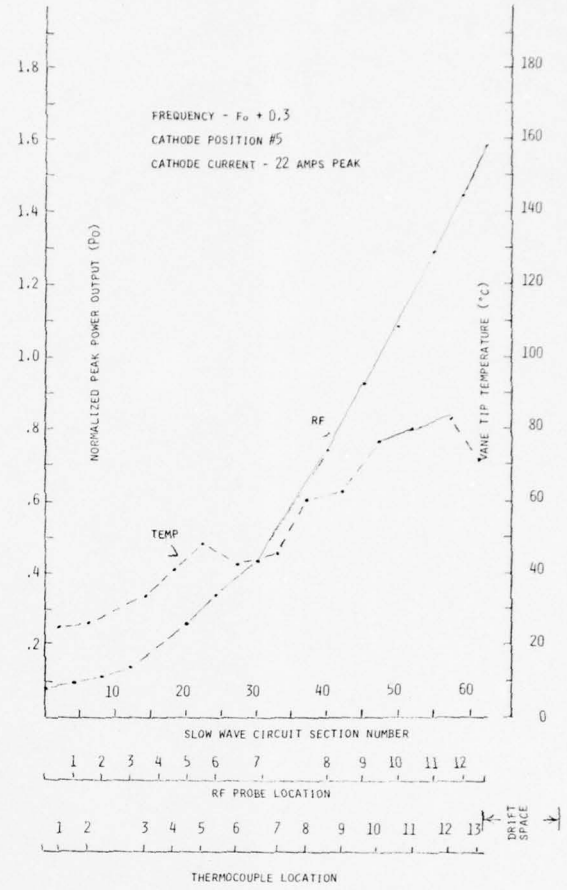

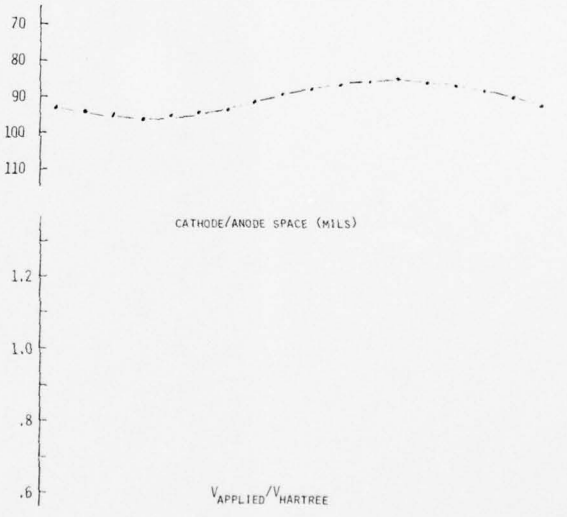

Figure 26 - RF POWER AND VANE TEMPERATURE PROFILES FOR INSTRUMENTED CFA (S/N B193T) WITH CATHODE POSITION ADJUSTED FOR SPECIFIED OFFSET.

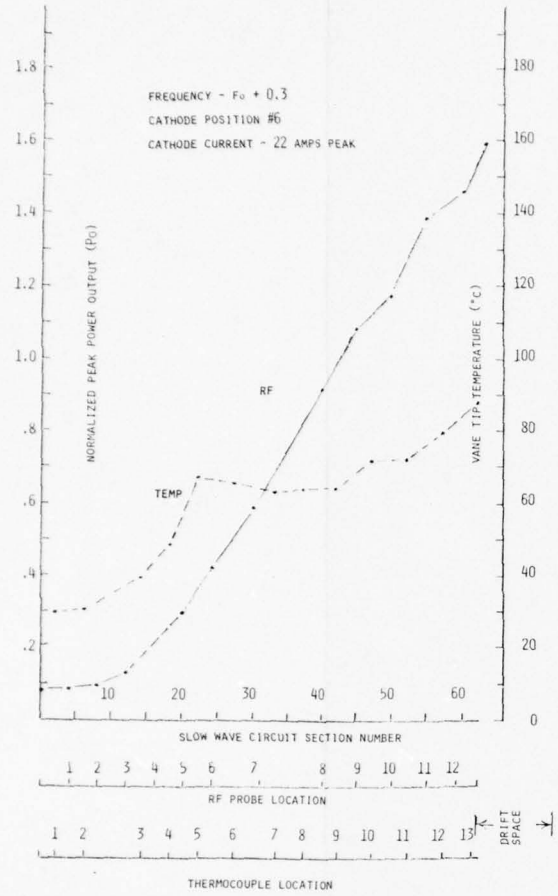
FREQUENCY - Fo + 0.3
CATHODE POSITION #6
CATHODE CURRENT - 22 AMPS PEAK
NORMALIZED PEAK POWER OUTPUT (Po)
VANE TIP TEMPERATURE (°C)
RF
TEMP
1.8
1.6
1.4
1.2
1.0
.8
.6
.4
.2
180
160
140
120
100
80
60
40
20
0
10 20 30 40 50 60
SLOW WAVE CIRCUIT SECTION NUMBER
1 2 3 4 5 6 7 8 9 10 11 12
RF PROBE LOCATION
1 2 3 4 5 6 7 8 9 10 11 12 13
DRIFT SPACE
THERMOCOUPLE LOCATION

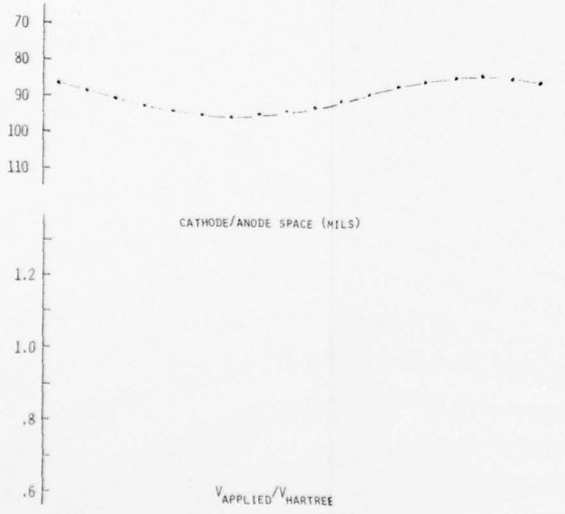
70
80
90
100
110
CATHODE/ANODE SPACE (MILS)
1.2
1.0
.8
.6
VAPPLIED/VHARTREE

B193T) WITH

2

andoe in the vicinity of circuit section number 12, the peak current was limited to 12.7 peak amperes and the peak power output to about 0.95 Po. Again, the peak in the thermal distribution did not occur near the point of closest anode-cathode spacing, but was located a little further along the slow wave circuit from where it was in position number 1. In position number 3 with the cathode closest to the anode in the vicinity of circuit element numbers 24-26, the cathode current was limited to 8 peak amperes and the obtainable peak power output was only 0.55 Po. The peak in the thermal distribution was located, as before, at a position further along the circuit from the point of closest cathode-anode spacing. However, notice that the separation between the position of closest spacing and location of the peak temperature was progressively decreasing as the position of closest spacing moves along the slow wave circuit toward the output. At position number 4 the cathode-anode spacing is closest in the vicinity of circuit element number 36-38. For this position, the cathode voltage and current could be increased to the rated current of 22 peak amperes. The peak power output increased to 1.5 Po. A peaked thermal distribution is still evident with the peak located along the circuit a few sections beyond the closest cathode-anode spacing. The power growth curve shows a build up over the first half of the circuit and a near linear growth over the last half. For positions 5 and 6 the cathode is closest to the circuit near elements numbers 50 and 62, respectively. In both cases, the cathode voltage and current could be increased to rated peak current of 22 peak amperes and a peak output power of about 1.55 Po

was obtained. The thermal distributions for these positions began to lose the peaked nature shown in the others and looked more like those obtained with the cathode on mechanical center. In position 6 the power growth is very nearly linear over the last 80% of the circuit length. The profile for this position approximates a linearly tapered cathode-anode interaction space and the results gave support to the concept of programmed interaction. However, later experiments and computer simulation have suggested alternate reasons for programming the cathode/anode space.

The fact that the peak in the temperature distribution did not occur at the closest cathode-anode spacing was unexpected. It led to speculation that a reverse taper in the cathode-anode spacing might lead to a rapid removal of space charge from the spoke. Since the voltage above Hartree is reduced by a reverse taper, less space charge would be fed into the base of the spoke. Meanwhile, RF interaction would continue to cause the remaining space charge in the spoke to be transported toward the anode. The net result would be a reduction of space charge within the spoke boundary.

An attempt was made to simulate this effect using the computer. At the time the programs for tapered interaction were still being refined. A space charge reduction in the spoke was indicated, but the amount of reverse taper needed in the simulation to produce the effect was greater than the reverse taper in the actual tube. This concept needs to be explored further.

The concept of using a reverse taper to produce space charge depletion in a spoke may prove to be important in reducing noise in a reentrant CFA. It has long been speculated that the reentrant space charge may be a significant factor in contributing noise to the RF output. Experimental results to be presented later will support this argument. Some experiments will be described which partially reduced the reentrant space charge and led to a reduction in noise output from the tube. This was done by collecting space charge recirculating close to the anode. Space charge depletion by a reverse taper geometry may also prove to be beneficial in noise reduction. In fact, it may be that this is the reason that cathode adjustment yielding the best compromise in power output, gain and signal-to-noise ratio in a forward wave CFA always has the cathode pushed closest to the anode at some point before the end of the interaction region. This results, of course, in a reverse taper near the output. This effect needs further investigation.

AD-A065 735 VARIAN ASSOCIATES BEVERLY MASS F/G 9/1
CFA DESIGN IMPROVEMENT PROGRAM. VOLUME I. INSTRUMENTED CFA STUD--ETC(U)
JUN 78 G K FARNEY N00123-75-C-1294
NL

UNCLASSIFIED

2 OF 2
AD
A065735

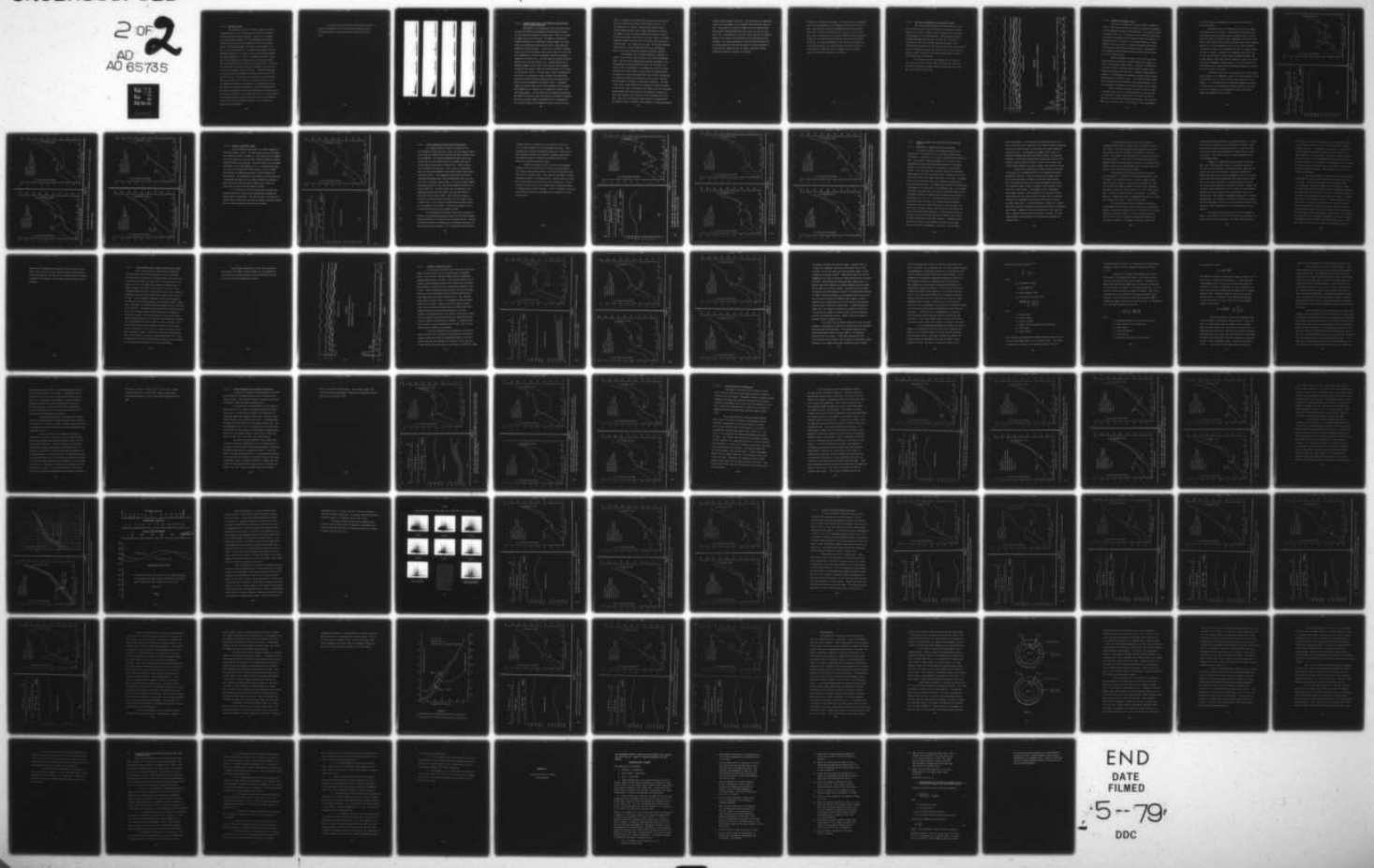

END
DATE
FILMED
5-79
DDC

5.2.1.5 Harmonic Signals

The presence or absence of harmonic signals in the CFA interaction region and at the CFA output could also be observed using the broadband spectrum analyzer. Figure 27 is an example of the experimental results. For this experiment, the cathode position was adjusted for best signal-to-noise ratio at the CFA output. Spectrum photographs were taken at probes numbers 1, 7, and 12, and at the CFA output. The spectrum photographs cover the frequency range from fo to fo+8.0 in four equal bandwidth segments. The signal frequency is at fo+0.3. Broadband noise power is seen with a high frequency cut-off that occurs at the upper frequency end of the passband where a relatively sharp peak occurs. This peak is caused either by low level pi mode oscillations or by an oscillation due to bandedge circuit reflections. Signals corresponding to the second and third harmonics are also visible on the circuit and in the output. The reason for the absence of a third harmonic peak at probe number 12 is not clear, but may be due to a null in a standing wave pattern at that position. No significance should be attached to the relative amplitudes of the signal peaks because the coupling coefficients of the sampling loops are not the same and they vary with frequency. The output match effects the signal coupled to the output waveguide, and the waveguide also becomes multimodal for the second and third harmonic signals. This can effect the detected signal amplitude.

It was observed that varying the cathode position could affect the amplitudes of the second and third harmonic signals. No attempt was made to obtain quantitative comparisons at this time.

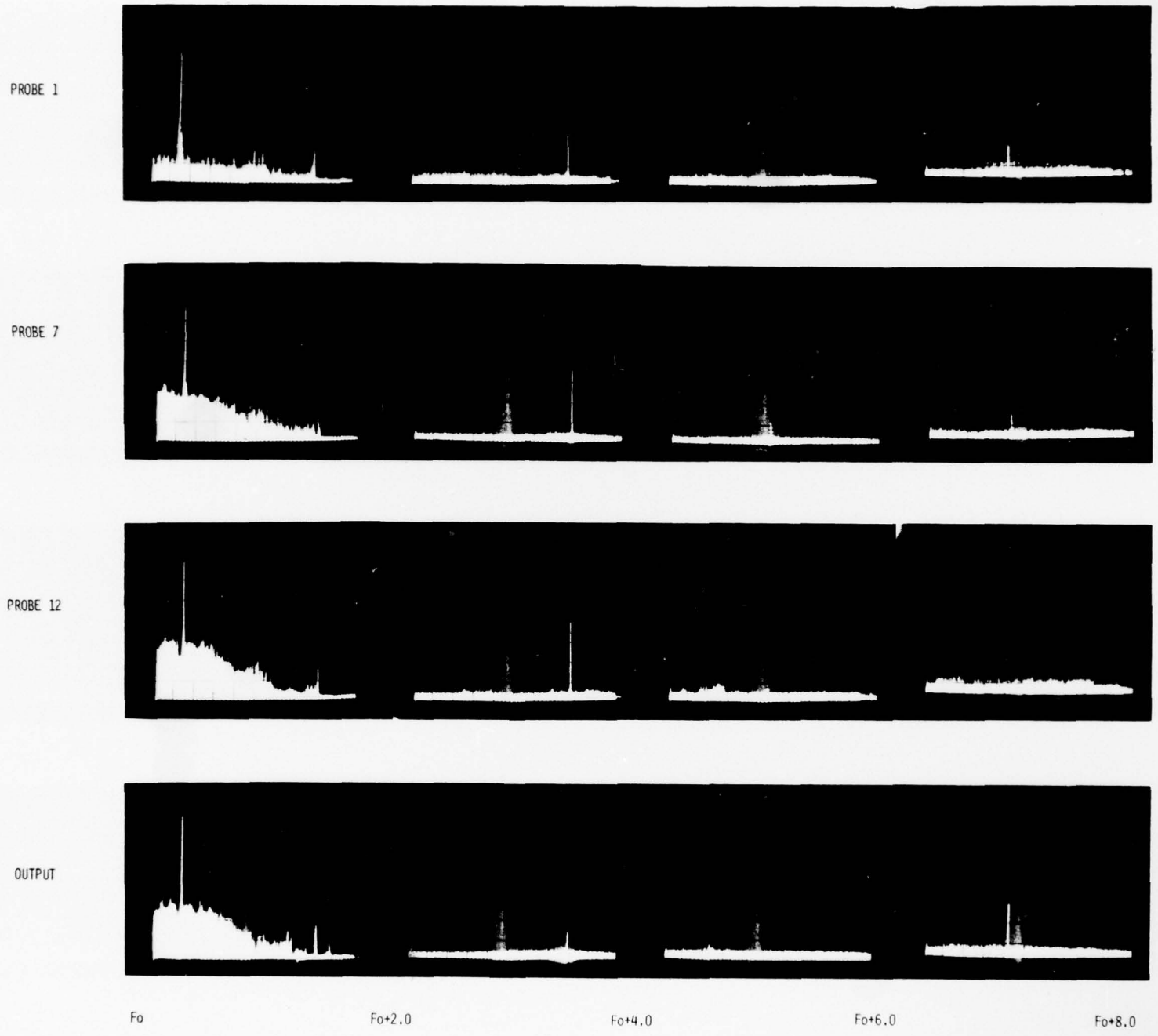

Figure 27 - SPECTRUM PHOTOGRAPHS SHOWING AMPLIFIED SIGNAL AND HARMONICS

5.2.1.6 Feedback Effects Due to the Reentrant Electron Stream and/or Circuit Reflections

Measurements of the signal gain along the slow wave near the input for different experiments has shown apparent evidence of both positive and negative electronic gain. This can be caused by either or both of two sources. For instance, one source is residual modulation of the reentrant electron stream if the space charge in the phase-sorted spoke pattern has not been completely dispersed in the drift space. In this case, a positive or negative effect on the actual electronic gain near the input to the tube can occur depending on the phase relationship between the electronic signal and the circuit wave. A second source is multiple reflected signals on the slow wave circuit; i.e., a signal reflected by an impedance mismatch at the output of the tube can travel backward through the tube and may or may not be reflected again at the input to the slow wave circuit. In either case, a kind of standing wave will exist on the slow wave circuit resulting from interference between the forward traveling, growing wave and the back-directed signal which is attenuated by the circuit losses. An apparent change in electronic gain occurs as the amplitude of the standing wave changes due to a variation in the magnitude or phase of the interfering signals. The two effects can be separately identified. The change in electronic gain due variations in electronic reentrancy will have a periodic change with frequency that is determined by the electrical length of the combined slow wave circuit and drift

space. In addition, the effect will be lost as the circuit wave grows and controls the current in the interaction space. On the other hand, the periodic variation with frequency due to circuit reflections will have a period determined by an electrical length of twice the distance between the location of the RF probe and the output of the slow wave circuit. Hence, a frequency-dependent periodic variation due to this effect will change with probe location. For a probe near the input, the periodic amplitude variation due to circuit reflection would occur approximately twice as often as one caused by reentrant electronic feedback.

An experiment was performed attempting to determine if either or both of these effects existed in the fully-instrumented tube. This was done by examining the frequency dependence of the RF amplitude at different probe positions. An X-Y recorder was used to record the amplitude of the sampled RF voltage at a probe position as the input signal was swept across the operating band. The signal at a probe was recorded first with the CFA non-operating, but with drive signal passing through the tube to get a reference trace showing the variation of coupling with frequency. The shape of this trace is also affected by the presence of reflected signals on the circuit. Next, the amplifier was turned on and the attenuation between the RF probe and the detector was adjusted to provide the same input voltage to the recorder at the low frequency end of the band. Next, the input signal was swept across the operating band. Any departure from the reference trace signifies a frequency dependent

variation in RF voltage at the probe. The results were not completely clear in this experiment, but it appeared that both effects were present. The presence of electronic feedback could be detected along the circuit at several probes until the circuit wave had increased about 3 dB. The presence of the circuit reflection could be detected because of the change in the periodicity of the pattern with probe positions. No further experiments of this kind were performed, but it was speculated that this approach might be a useful technique to obtain data for comparison with the computer simulation results insofar as electronic reentrancy is concerned.

variation in RF voltage at the probe. The results were not completely clear in this experiment, but it appeared that both effects were present. The presence of electronic feedback could be detected along the circuit at several probes until the circuit wave had increased about 3 dB. The presence of the circuit reflection could be detected because of the change in the periodicity of the pattern with probe positions. No further experiments of this kind were performed, but it was speculated that this approach might be a useful technique to obtain data for comparison with the computer simulation results insofar as electronic reentrancy is concerned.

5.2.2 The Fully-Instrumented CFA with Tapered Cathode

The second fully-instrumented CFA (S/N F376T) had a slow wave circuit that had a uniform pitch and an isolated drift space similar to the first. However, it had a cathode with a non-uniform radius similar to the standard SFD-261. The waveguide-to-circuit matching characgeristics are shown in Figure 28. The match is excellent at fo+0.3, but degrades toward the bandedges. The deterioration is greatest at the lower end of the band. The deterioration is not enough to prevent tube operation, but will be seen to be enough to cause fluctuation in the power growth profile caused by the standing wave on the circuit.

The calibration of the electromagnet was not correct at the time this tube was studied. Hence, the calculated values for the ratio of operating voltage to Hartree voltage were not correct. They are not shown for this tube.

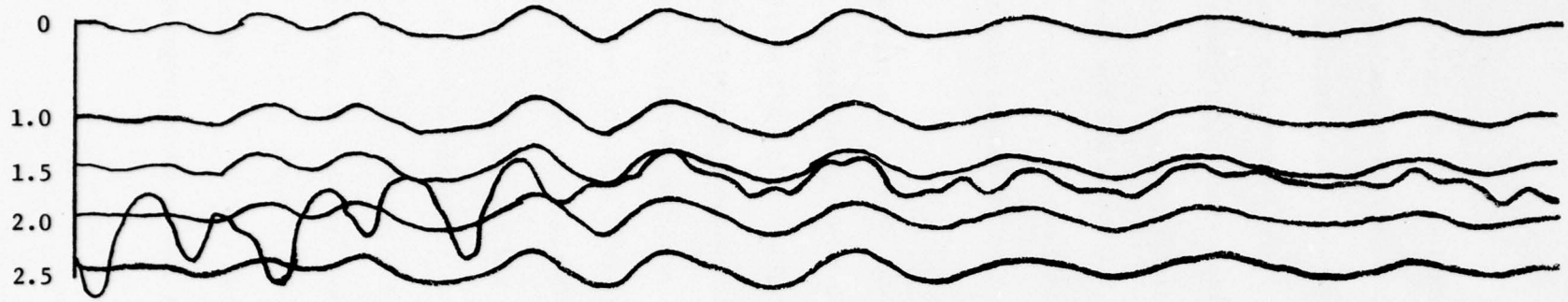

FIGURE 28

WAVEGUIDE MATCHING CHARACTERISTICS OF INSTRUMENTED CFA, S/N F376T.

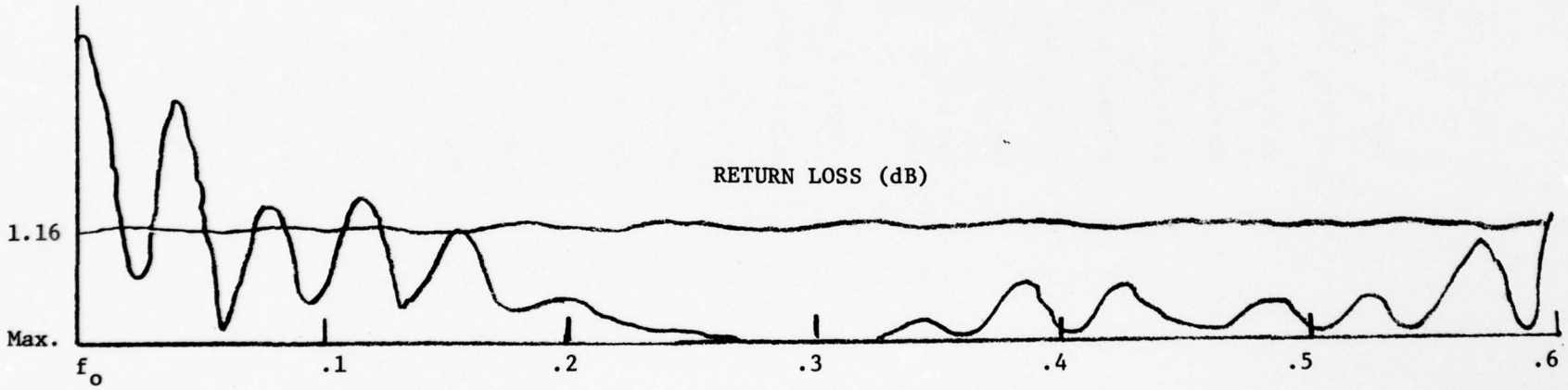

5.2.2.1 Cathode on Mechanical Center

The tube was tested first with the cathode on mechanical center. Power growth and vane tip temperature profiles were measured at five frequencies across the operating band. The results are shown in Figures 29 thru 31. The variation in the interaction space dimension defines the cathode profile variation since the cathode was on mechanical center. The effect of the circuit mismatch is clearly evidnet at fo+0.1 and fo+0.2. At higher frequencies the smoother power growth profiles reflect the improved match. Photographs of the broadband spectrum displays and detected RF pulses were taken but are not reproduced here.

Several differences were noted. First, this tube would operate across the full band at rated RF input drive signal, but only at 20 peak amperes above midband. Contrarily, S/N B193T with a circular cathode on mechanical center would not operate above midband and operated poorly at fo+0.3. Bandedge oscillations were present at 22 peak amperes and disappear only when the peak current was decreased to 20 amperes or less. The cathode profile improved the tube operation across the band, but was not sufficient to meet full performance requirements at the high frequency end of the band.

Next by comparing the power profiles for these two tubes at mid band where there is no interference from the circuit match it is seen that the power growth rate is more rapid near the RF input end of the S/N 376T with the tapered cathode. The final peak power output from each tube is about the same. Hence programming

of the interaction space parameters near the input does improve the RF interaction.

In addition, there are differences in the vane tip temperature profiles for the two tubes. Tube B193T with the uniform interaction space shows an increasing vane tip temperature over the first half of the tube and a nearly constant temperature over the last half. However, tube F376T with the tapered interaction space shows a definite peak in the vane tip temperature profile near the input followed by a progressive increase in the temperature profile to a higher temperature near the output. The peak in the temperature profile near the RF input was seen before in other tubes with tapered cathodes, and in some cases for tubes with circular cathodes but that are off center to produce a programmed interaction space. It is now believed that this results from the manner that reentering space charge is utilized. More will be said of this later.

The decrease in the vane tip temperature at the last thermocouple position is not understood. There is no obvious reason why this should actually occur in a tube, and it has not been seen in other vehicles. It is possible that the thermocouple embedded in the vane at this position was not making proper thermal contact to the vane. If true, it is likely that the temperature profile should show a higher peak temperature at the output.

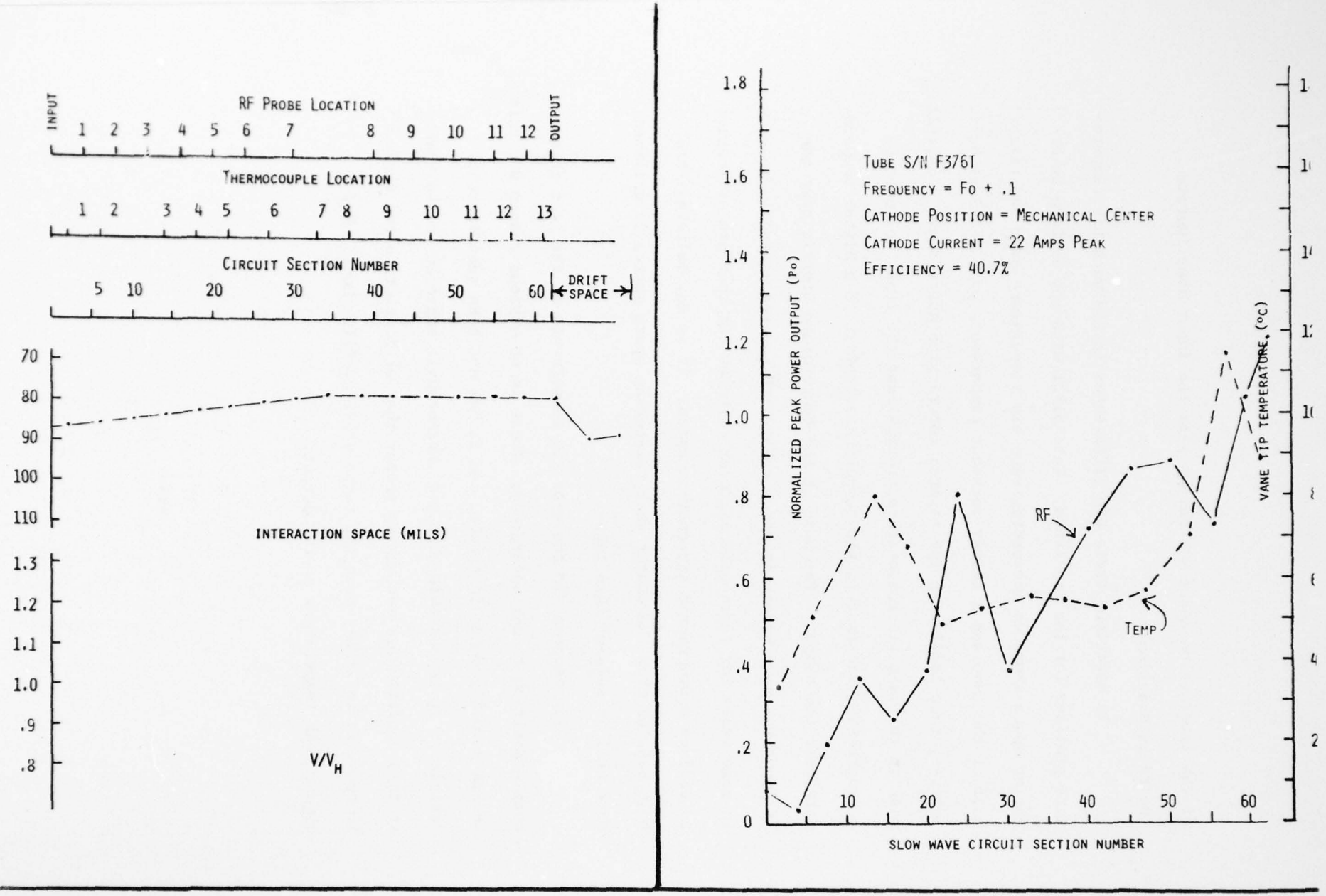

FIGURE 29

RF POWER AND VANE TIP TEMPERATURE PROFILES IN INSTRUMENTED CFA (S/N F376T) WITH TAPERED CATHODE ON MECHANICAL CENTER.

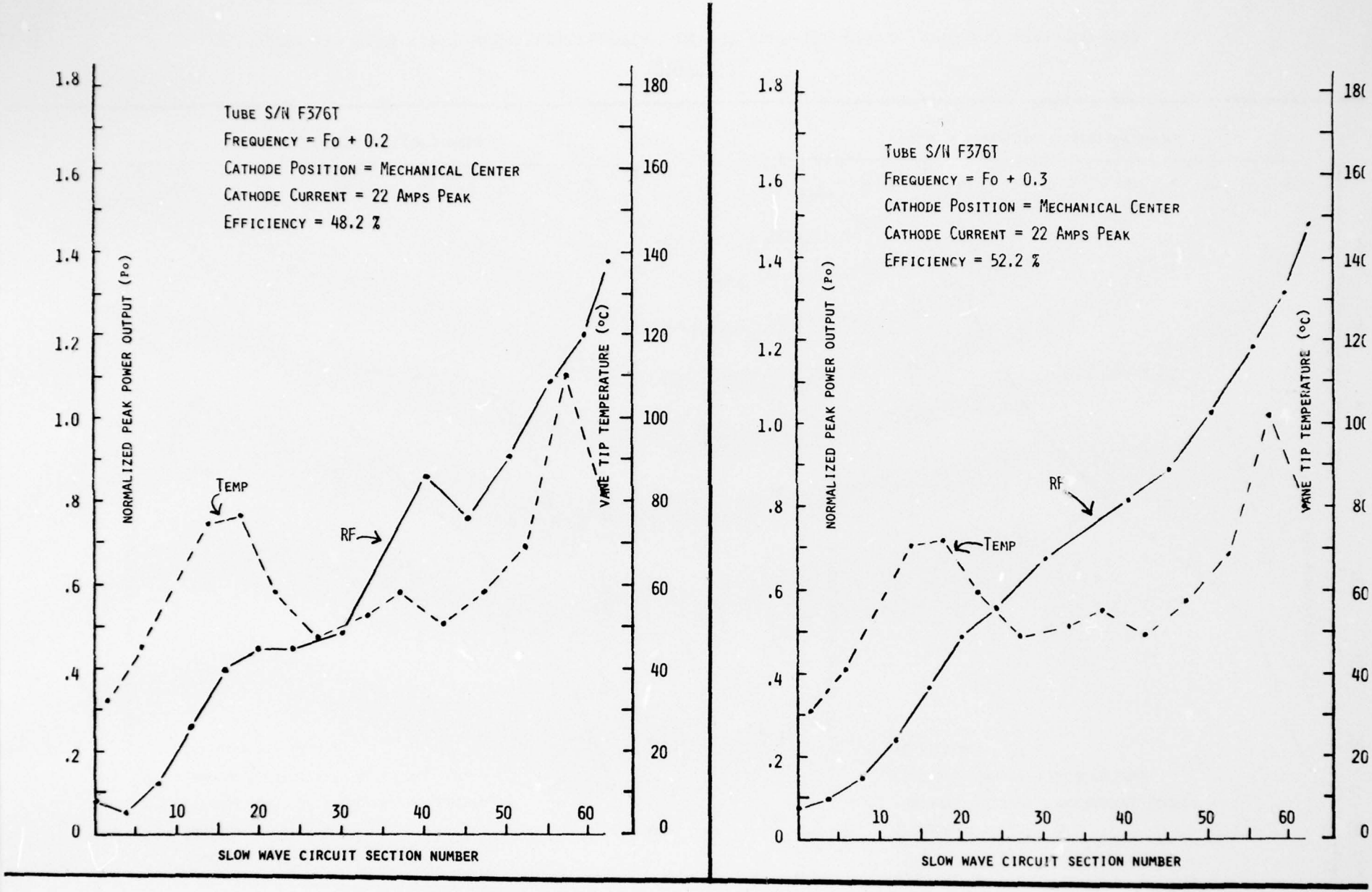

FIGURE 30

RF POWER AND VANE TIP TEMPERATURE PROFILES IN INSTRUMENTED CFA (S/N F376T) WITH TAPERED CATHODE ON MECHANICAL CENTER.

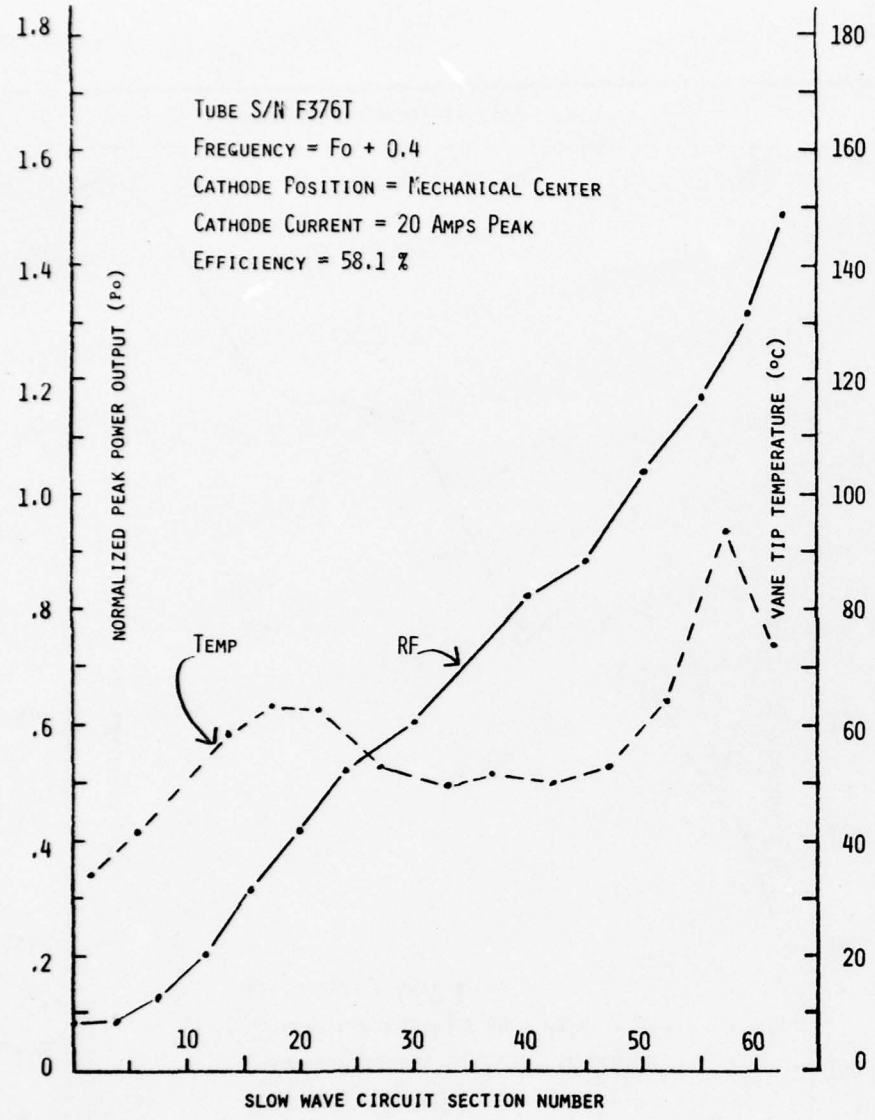

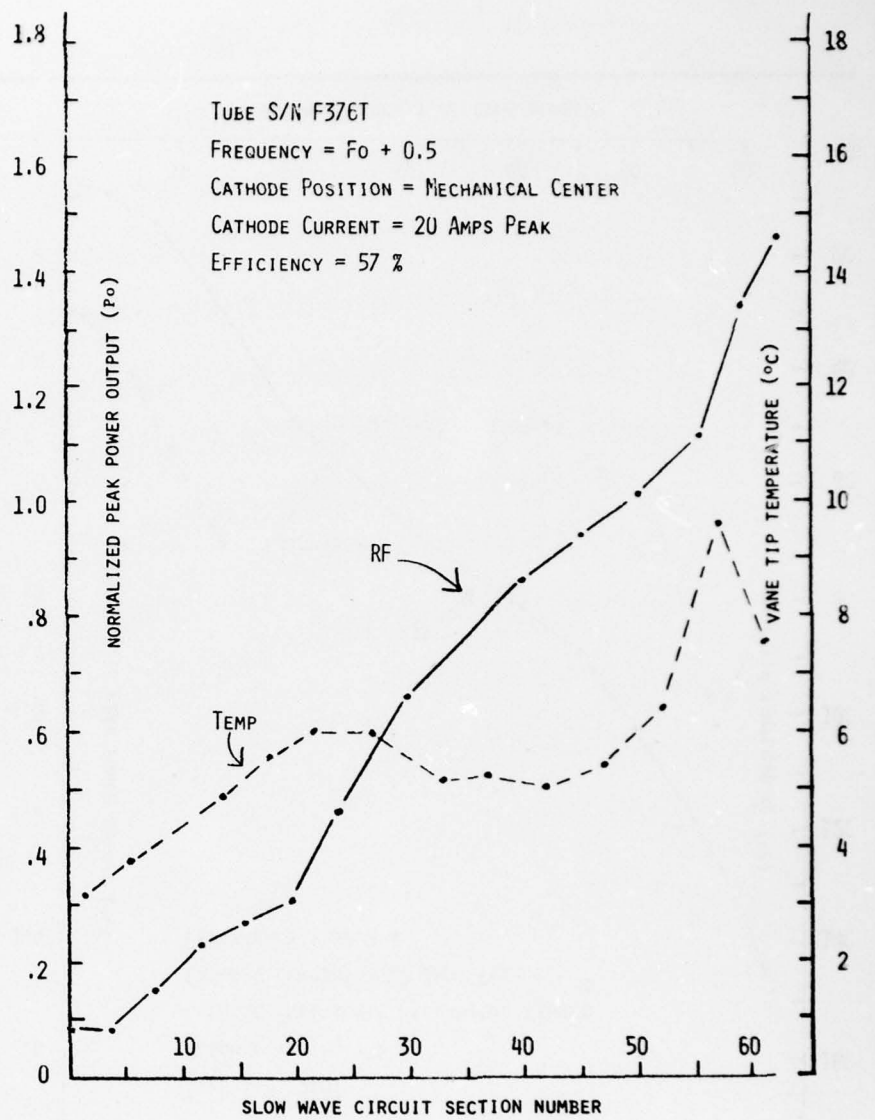

FIGURE 31

RF POWER AND VANE TIP TEMPERATURE PROFILES IN INSTRUMENTED CFA (S/N F376T) WITH TAPERED CATHODE ON MECHANICAL CENTER.

5.2.2.2 Cathode on Electrical Center

The tube F376T was studied with the cathode adjusted for electrical center at fo+0.3. The power growth and vane tip temperature profiles are shown in Figure 32. These results can be compared to those in Figure 22 for the circular cathode on electrical center. Several differences are apparent. More peak current can be obtained from F376T; e.g., 22 amps compared to 16. A normalized peak power of 1.5Po can be obtained with F376T compared to 1.2Po for B193T. Also the vane tip temperature profiles are quite different for the two tubes. The cathode-anode space profile for B193T shows that a significant perturbation of the cathode position was required to obtain electrical center for B193T, whereas only a slight off center shift of about 2 mils was needed for F376T.

It is difficult to draw any conclusions from these data. As stated previously, these cathode positions were examined only because they are reproducible. The data may prove to be useful for further study at some future time when the computer simulation techniques for tapered interaction spaces are more refined.

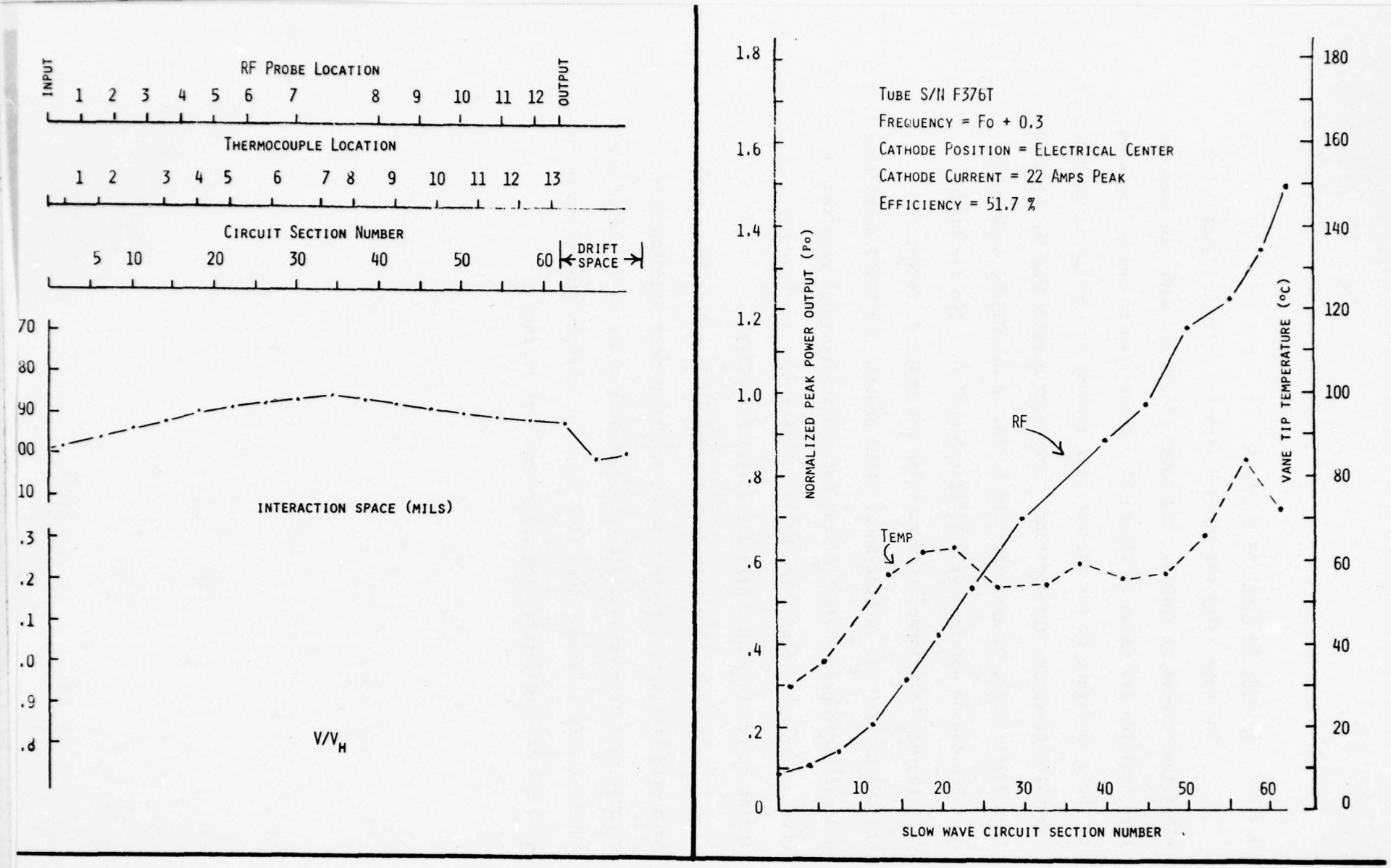

FIGURE 32

RF POWER AND VANE TIP TEMPERATURE PROFILES IN INSTRUMENTED CFA (S/N F376T) WITH TAPERED CATHODE POSITION ADJUSTED TO ELECTRICAL CENTER.

5.2.2.3 Cathode Adjusted for Best Signal-to-Noise Ratio

The cathode position of F376T was adjusted for the best compromise between peak power output, gain and signal-to-noise ratio across the operating band following the usual procedures used for the SFD-261. The resulting cathode-anode space profile and the profiles for power growth and vane tip temperatures across the operating band are shown in Figures 33-35. Several things can be observed from these data. First, there is a significant amount of cathode displacement from mechanical center that results from this procedure. This exaggerates even further the kind of programmed interaction space that was deliberately built into the tube by the non-uniform cathode radius. In fact, the final cathode-anode space profile for this tube was not markedly different from that in B193T with a circular cathode that was adjusted for best compromise between peak power output, gain and best signal-to-noise ratio for the output signal. The cathode was closest to the anode at a position near vane number 50 in both tubes so that a reverse taper, or an increase in cathode-anode spacing, existed for the remainder of the circuit. This was not expected in view of the built-in profile for the cathode in F376T.

A second observation is that in both tubes the amount of change in the cathode-anode spacing around the tube was much greater than was believed to be desirable for an emitting sole CFA. However, the general approach for decreasing the cathode-anode spacing as the power level grows was preserved. It is now believed that the final

cathode position is dictated more by the effect on noise than it is by the requirements for the programmed interaction. This suggested that a properly designed CFA might have a double adjustment procedure involving one procedure to optimize power growth and another procedure to minimize noise output from the tube. More will be presented about this later.

Another observation is that the effect of the degraded mismatch at the low frequency end of the band is quite apparent. The irregular power growth profile is the result of the interfering waves on the slow wave circuit. This effect is diminished at higher frequencies because of the improved match. However, there is a power dip at vane number 55 at mid band that is not understood. The circuit match is very good at this frequency and no significant amount of reflected power should be present. It may be, therefore, that this point reflects some kind of experimental error instead of an interference effect.

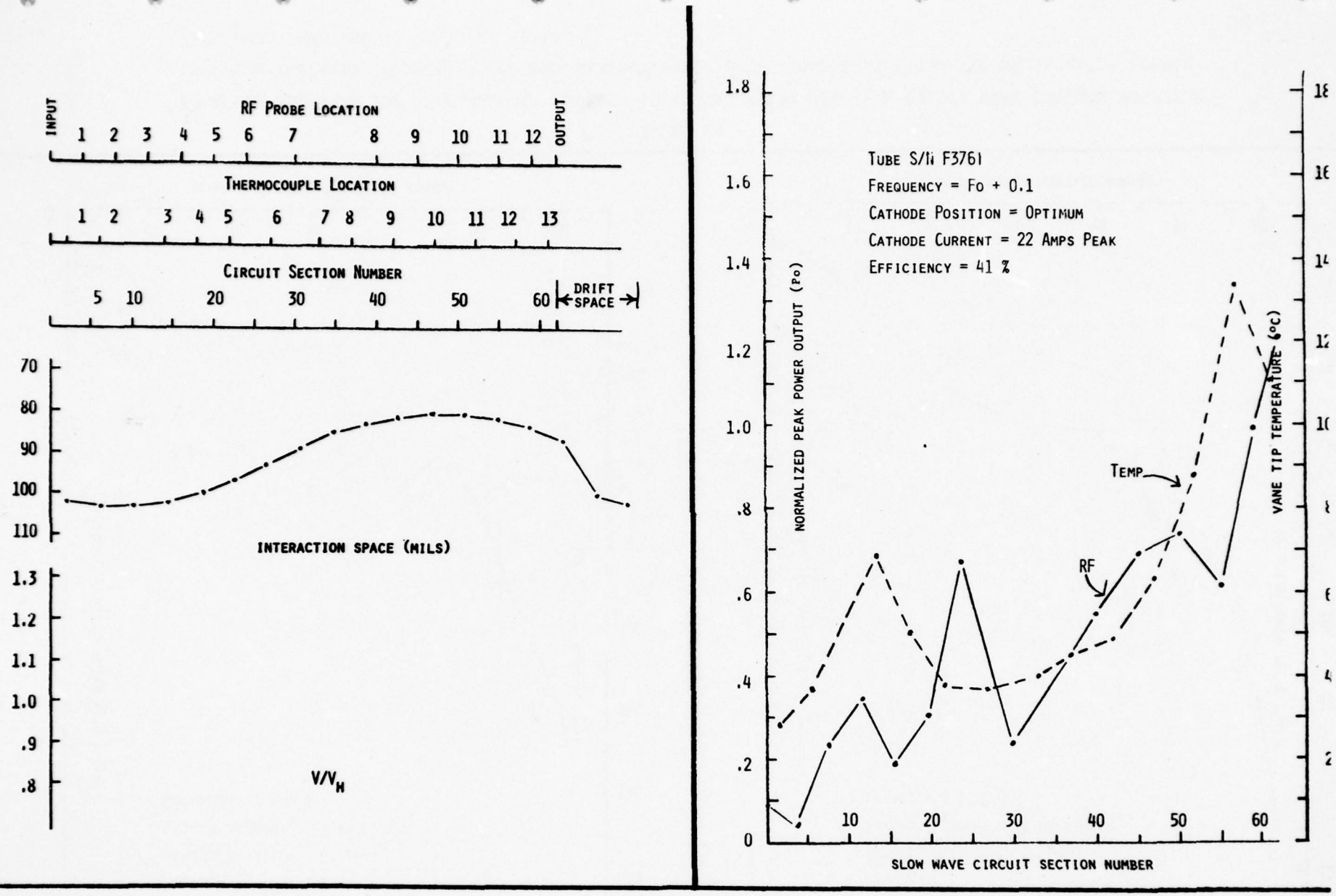

FIGURE 33

RF POWER AND VANE TIP TEMPERATURE PROFILES IN INSTRUMENTED CFA (S/N F376T) WITH CATHODE POSITION ADJUSTED FOR BEST COMPROMISE BETWEEN MAXIMUM POWER OUTPUT AND BEST SIGNAL-TO-NOISE RATIO ACROSS THE OPERATING BAND AT RATED RF INPUT.

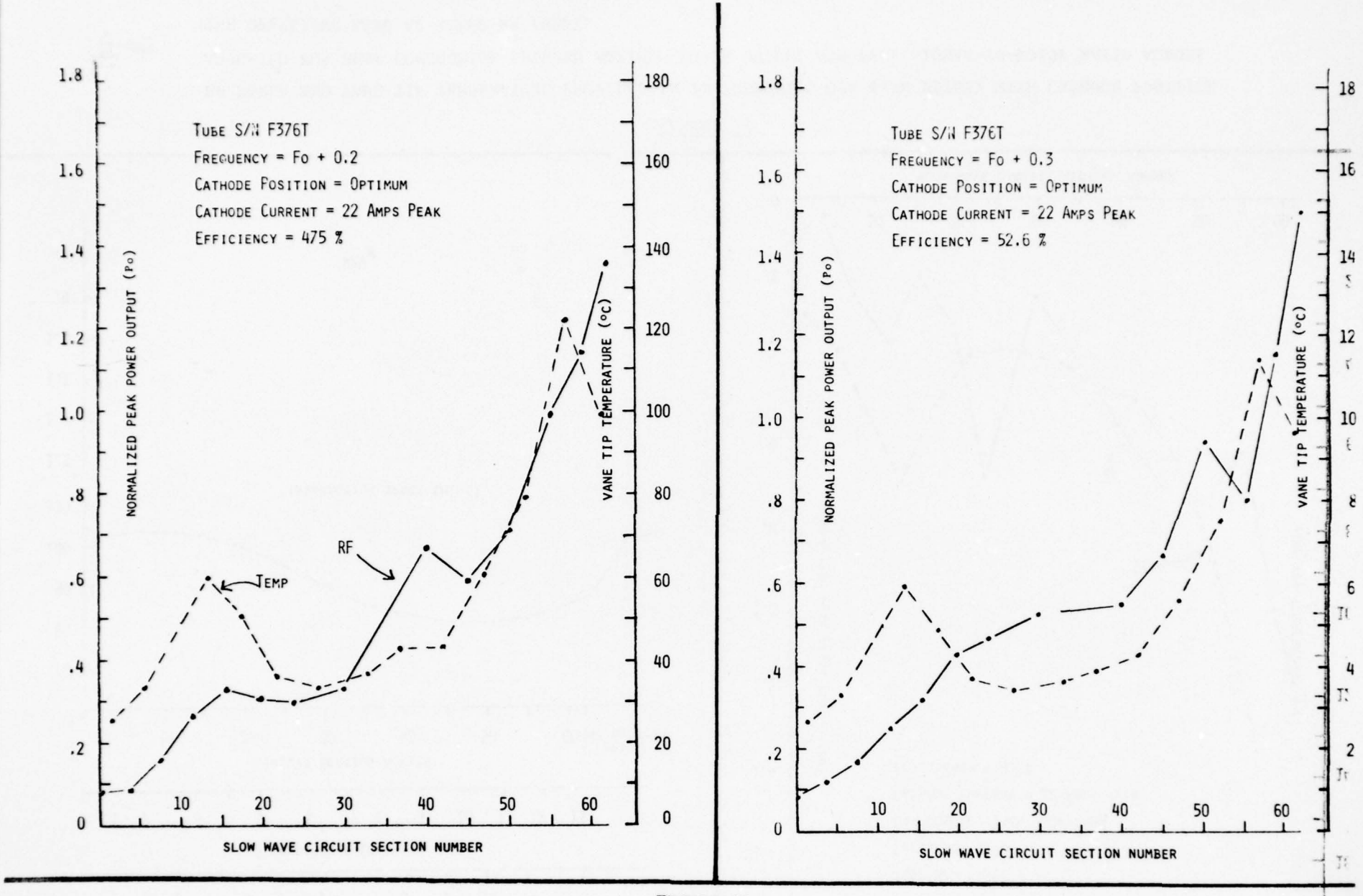

FIGURE 34

RF POWER AND VANE TIP TEMPERATURE PROFILES IN INSTRUMENTED CFA (S/N F376T) WITH CATHODE POSITION ADJUSTED FOR BEST COMPROMISE BETWEEN MAXIMUM POWER OUTPUT AND BEST SIGNAL-TO-NOISE RATIO ACROSS THE OPERATING BAND AT RATED RF INPUT.

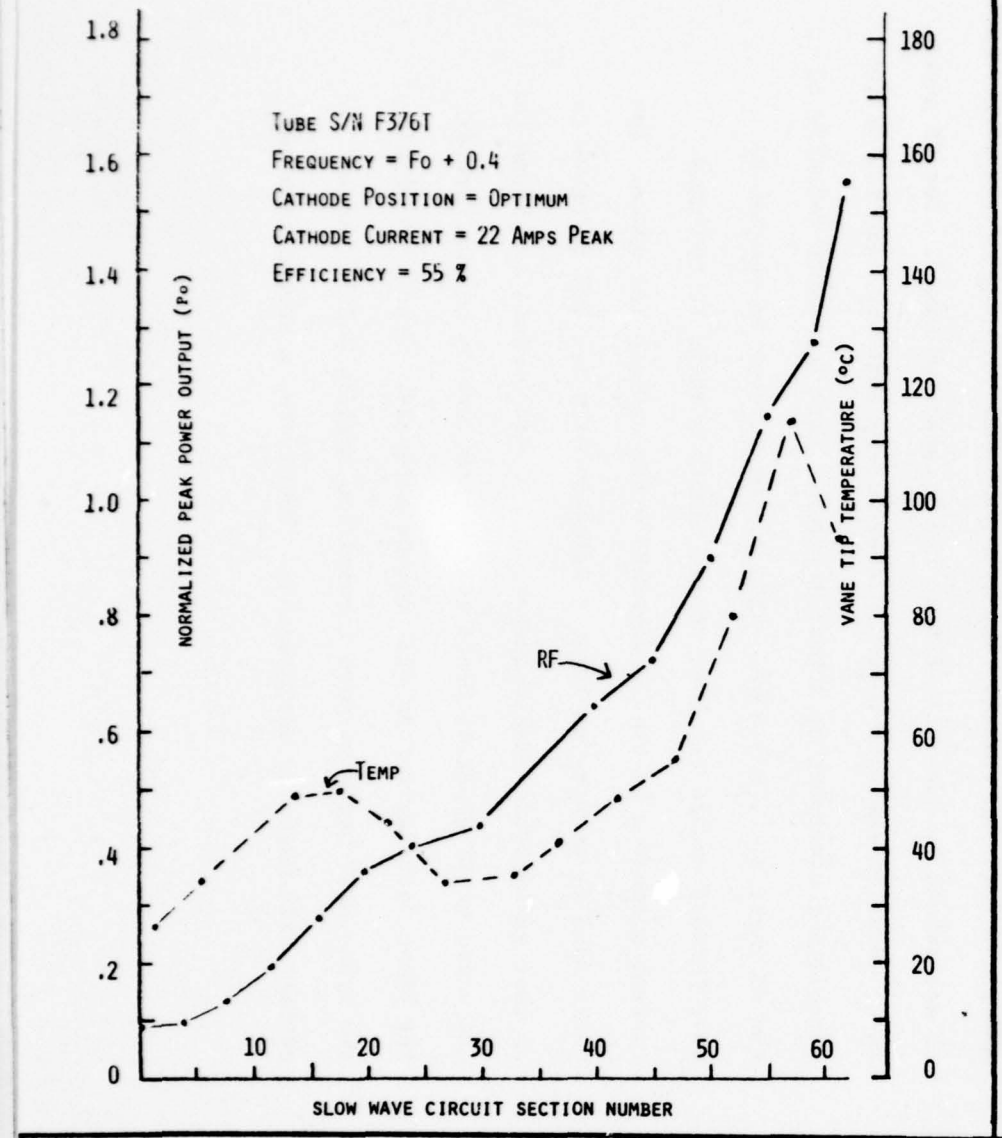

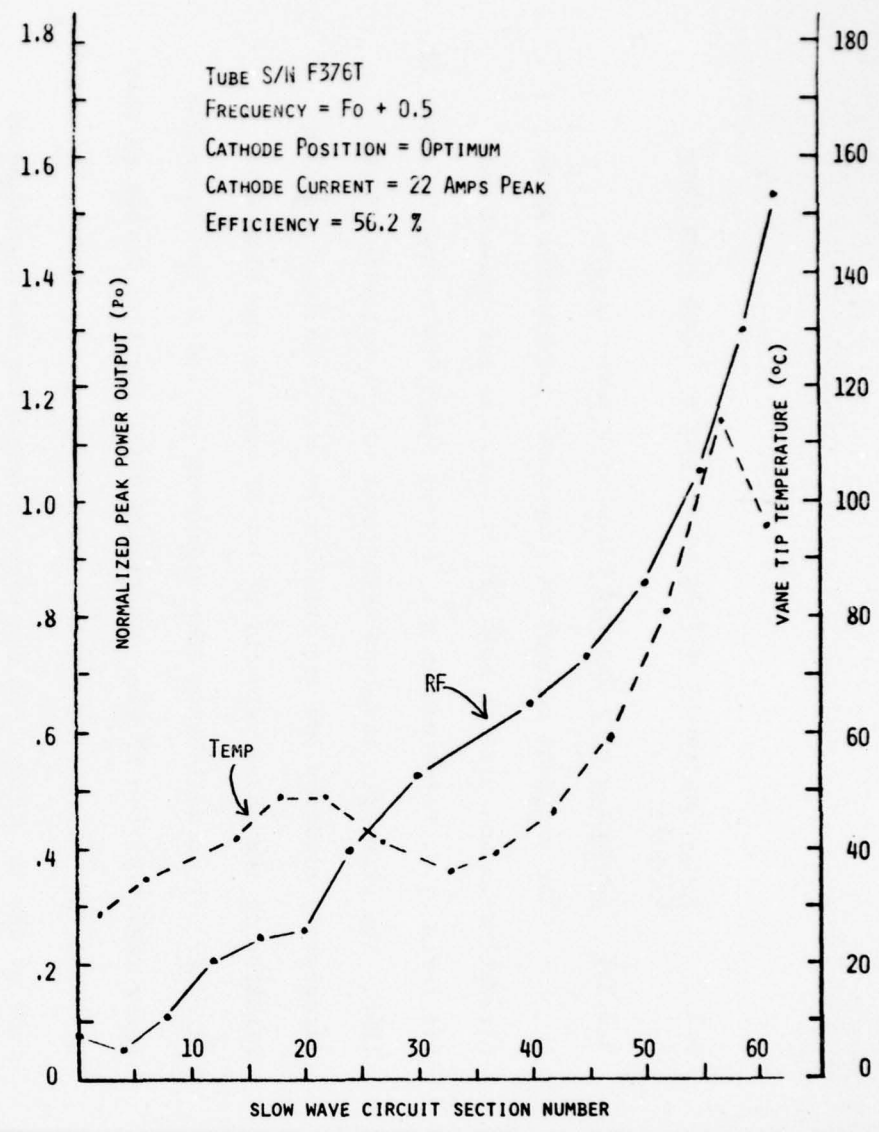

FIGURE 35

RF POWER AND VANE TIP TEMPERATURE PROFILES IN INSTRUMENTED CFA (S/N F376T) WITH CATHODE POSITION ADJUSTED FOR BEST COMPROMISE BETWEEN MAXIMUM POWER OUTPUT AND BEST SIGNAL-TO-NOISE RATIO ACROSS THE OPERATING BAND AT RATED RF INPUT.

5.2.3 Fully-Instrumented Tube with Tapered Pitch Slow Wave Circuit

5.2.3.1 Advantage of a Tapered Pitch Slow Wave Circuit

The original concept of programmed interaction space parameters in an emitting sole CFA to optimize performance was set forth by J. Feinstein in U.S. Patent 3,069,594 issued December 18, 1962. The principle involves adjustment of the velocity of the circulating electron hub and interacting electrons in the spokes relative to the phase velocity of the RF wave on the slow wave circuit. It is well known that electrons located in the favorable phase region of the RF wave experience phase focusing forces as they traverse the interaction region from the hub to the anode. The magnitude of the RF fields from the circuit determine the magnitude of the phase focusing forces. The translational velocity of the electrons is determined by the ratio E/B in the interaction space. For RF power to be added to the slow wave it is necessary that the velocity of the circulating electrons be somewhat greater than the phase velocity of the RF wave; i.e., $E/B > v_p$. This allows current in the hub to move forward toward the base of the electron spoke to replenish current extracted by the RF wave and drawn up into the spoke. The basic idea is to have as large a value locally for E/B relative to v_p that will permit stable operation. If E/B becomes too large for the value of RF electric field that exists locally on the circuit, the phase focusing forces will not be adequate. Electrons within the spoke will begin to move forward too rapidly and the spoke pattern will begin to disintegrate. Therefore, a proper balance

must be maintained. It is desirable to have current move into the base of the spoke and be transported to the anode as rapidly as possible because this allows RF power to be generated in a shorter length of slow wave circuit. By minimizing the length of the circuit, RF losses are minimized and higher efficiency obtained. The approach, therefore, is based upon increasing the translational velocity of the electron stream relative to the phase velocity of the circuit wave in some optimum fashion as RF power is added to the slow wave circuit.

Several ways of achieving the desired effect are described in the patent, but no optimum profile for the changing interaction parameters is set forth. One of the goals of this present effort was to learn more about the method by which this should be done. One of the methods described was to alter the magnetic field along the interaction region so that the magnetic field decreased in the direction of power growth. This assumes that the cathode-anode space remains constant. This increases E/B and raises the translational velocity of the electrons as the RF power level is increased. This method of programmed interaction has been used with success on linear format CFA's. It is more difficult to apply to a reentrant CFA because the entire interaction region usually involves a relatively small volume. Attempts to adjust the value for B in one region can lead to changes in another that are difficult to control. For this reason magnetic field adjustment has not been used extensively for reentrant CFA's.

A second approach described in the patent involves changing the phase shift per section along the length of the slow wave circuit. The circuit dimensions are modified such that the phase shift per section increases in the direction of RF power growth. This decreases the phase velocity of the circuit wave from RF input to output. In this case, the cathode-anode spacing and magnetic field are uniform and E/B is constant. The desired relative change in velocity is obtained because the circuit wave slows down relative to the circulating electron stream.

This approach has been tested previously and found to have difficulties. Alteration of the mechanical dimensions along the length of the slow wave circuit to obtain a change in phase shift per section leads to a circuit with one passband at one end of the circuit and another passband at the other end. Therefore, the band over which the circuit is matched is not the same at both ends. This has been found to lead to oscillations. An alternate method for achieving this kind of programmed interaction is obtained by a tapered pitch circuit. This will be described.

The third method described by Feinstein for obtaining a programmed interaction space involved tapering the cathode-anode spacing. The cathode is brought closer to the anode as the RF power level grows along the circuit. At a fixed cathode voltage the electric field intensity increases as the spacing decreases and E/B changes accordingly. The magnetic field has a fixed value.

This method has been used often for a reentrant stream CFA. In many cases, such as the SFD-261, the cathode radius is different along the interaction region to provide this effect. In any case, such an effect can be produced by changing the cathode location relative to the anode. These effects have been clearly demonstrated with the instrumented tubes.

Tapering the cathode-anode spacing has one serious drawback. For a fixed peak power output at a specified voltage and slow wave circuit properties, the interaction space design near the output of the tube will be defined. Therefore, increasing the spacing near the input to provide programming results in the cathode surface and electron hub being moved further away from the circuit wave. The relative difference in velocities between the RF wave and the circulating electrons is decreased as desired. However, the RF electric field intensity near the hub surface is also decreased. Therefore, the phase focusing forces are decreased. This is not desired; hence, this appraoch to programmed interaction is a compromised solution. The alternative approach that attempts to preserve all of the advantage is the use of a tapered pitch, slow wave circuit. Obviously, various combinations of the above techniques could be employed.

For some slow wave circuits, such as the stub-supported helix, it is possible to alter the circuit pitch and, therefore, the phase velocity without much change in the phase shift per section.

The reason for this is that the phase shift is determined primarily by the geometrical distance around a helix turn from the center of one gap to the next. Increasing the pitch has only a small effect on the geometrical path length because the pitch of the helix is small compared to its circumference. Therefore, changing the pitch of such a circuit will not significantly alter the passband along the circuit length. This overcomes the disadvantage of using a change in phase shift per section to obtain a desired change in phase velocity that was described before. Difficulties due to circuit mismatches are minimized.

The peak power output, voltage and circuit characteristics will dictate the design of the cathode-anode spacing near the output of the tube. A uniform cathode-anode space and magnetic field can be employed. The desired change in relative velocity between the circuit wave and the circulating current is obtained by increasing the circuit pitch near the input to the tube. This has the effect of increasing the wavelength for the slow wave since there is no significant change in phase shift per section. The phase velocity for the circuit wave is, therefore, increased and the relative difference in velocity between the circuit wave and the circulating electrons is decreased as desired. However, this method has an added advantage over the tapered cathode-anode geometry. The cathode in this approach is located closer to the anode and, therefore, the hub is in a region of stronger RF electric fields for the same RF input power. Furthermore since the circuit pitch is larger, the propagation constant is

smaller and the fringing field decay away from the circuit is less rapid. This results in a still larger RF electric field intensity near the electron hub. Not only are the relative velocity differences optimized by this approach, but the phase focusing forces are also increased.

5.2.3.2 Circuit Modification to Obtain a Tapered Pitch Circuit

Based upon some computer simulations and examination of experimental data from CFA experiments, it has been estimated that the tolerable variation in synchronism between the circuit wave and electron stream near the output end of the tube would be in the region of 15-20%. This means that the ratio of applied voltage to Hartree voltage, V/V_H, would be in the area of 1.15-1.20. For a programmed interaction using a tapered pitch circuit and a symmetrical interaction space this ratio would be much closer to unity near the RF input. Since the amount of tolerable velocity variation along the circuit was not known accurately, it was decided to make a compromise. The design of the SFD-261 anode was changed from 62 to 59 active circuit sections. The angular distance allotted to the metal and space of the three sections removed was distributed over the remainder of the circuit sections. The spacing between the helix turns was kept constant and the thickness of the helix and stub support was increased by a constant amount per section toward the input of the tube. The RF input and output locations remained the same as for the circuit with the uniform pitch. The result was a linear variation in circuit pitch from input to output. The ratio of the pitch of the resulting input circuit section to the output circuit section was 1.102. Since the phase shift per section was essentially unchanged, this corresponds to a ten percent linear variation over the circuit length.

The matching characteristics of the tube with tapered pitch circuit (S/N J329T) is shown in Figure 36. By comparison it is seen that the matching characteristics are essentially the same as for the tubes with uniform pitch circuits.

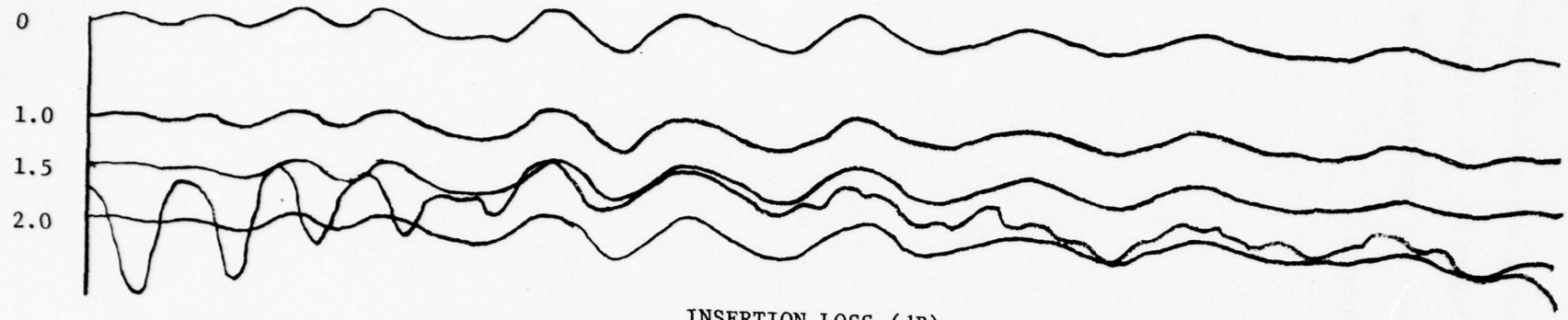

FIGURE 36

WAVEGUIDE MATCHING CHARACTERISTICS OF

INSTRUMENTED CFA, S/N J329T.

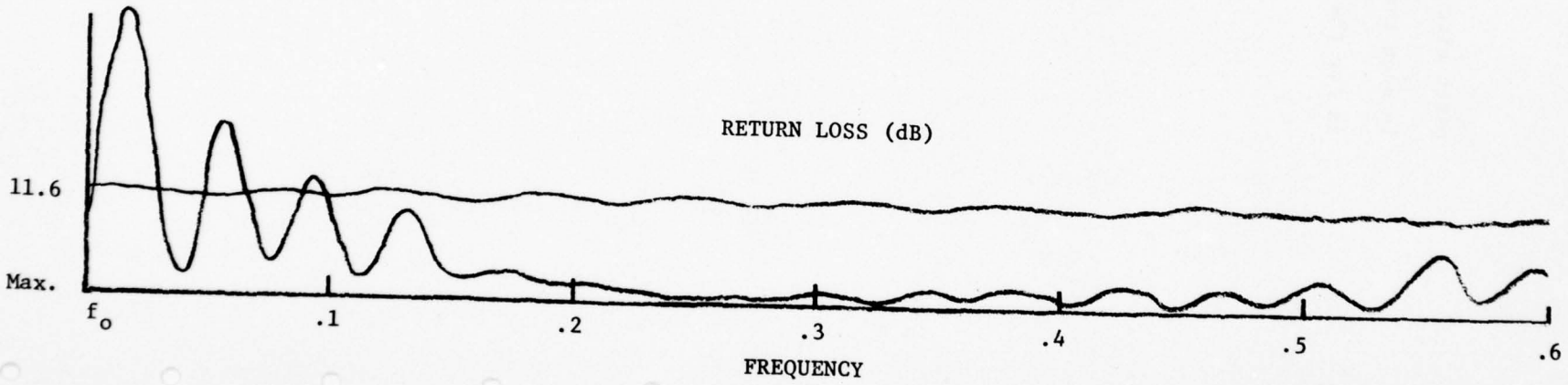

5.2.3.3 Cathode on Mechanical Center

The tube with the tapered pitch, slow wave circuit (S/N J329T) was tested first with the cathode located on mechanical center. This tube had a circular cathode and the cathode-anode spacing was increased to 93.5 mils. This was done because of preliminary results obtained previously on a similar tube that showed some tendency to oscillate when the cathode-anode spacing was only 90 mils. Several things were quickly evident from this new design. First, this tube would operate across the full operating band at rated input power and at rated cathode current. Also, the peak power output was nearly equal to or exceeded the rated peak power output for the SFD-261. Recall that the tube with the uniform pitch circuit and circular cathode would not operate under these conditions above mid band and operated poorly at mid band. Secondly, the signal-to-noise at the output of this tube was better with the cathode on mechanical center than for many SFD-261 tubes after the cathode position had been optimized. A signal-to-noise ratio of about 50 dB was obtained across the band. Both of these characteristics represent an improvement.

The power growth and vane tip temperature profiles are shown in Figures 37-39. Differences from B193T with the circular cathode on mechanical center are immediately obvious at the frequencies where data are available for comparison. First, the rate of power growth near the RF input is much faster for J329T even though

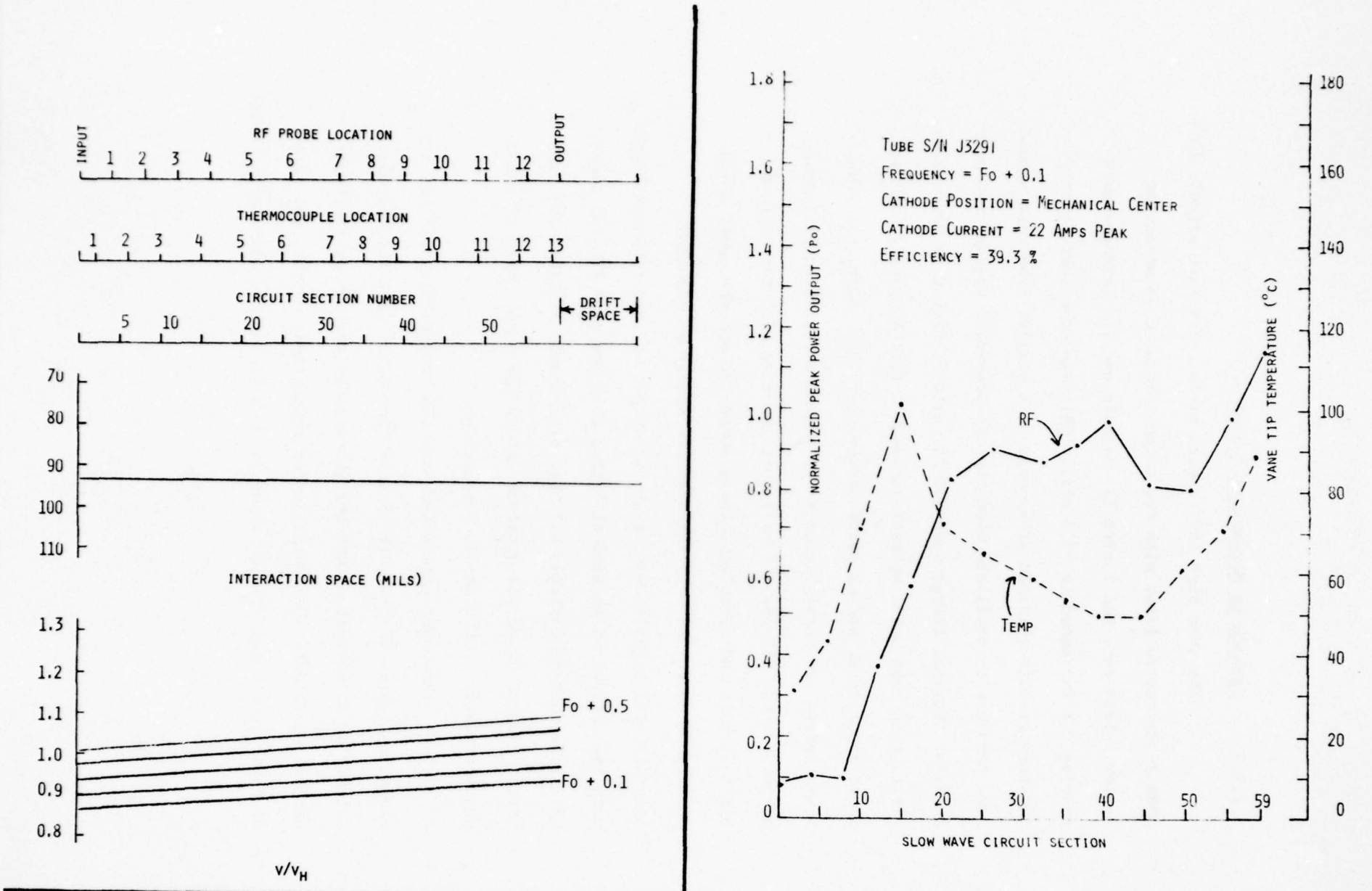

FIGURE 37

RF POWER AND VANE TIP TEMPERATURE PROFILES IN INSTRUMENTED CFA (S/N F376T) WITH CATHODE POSITION ON MECHANICAL CENTER.

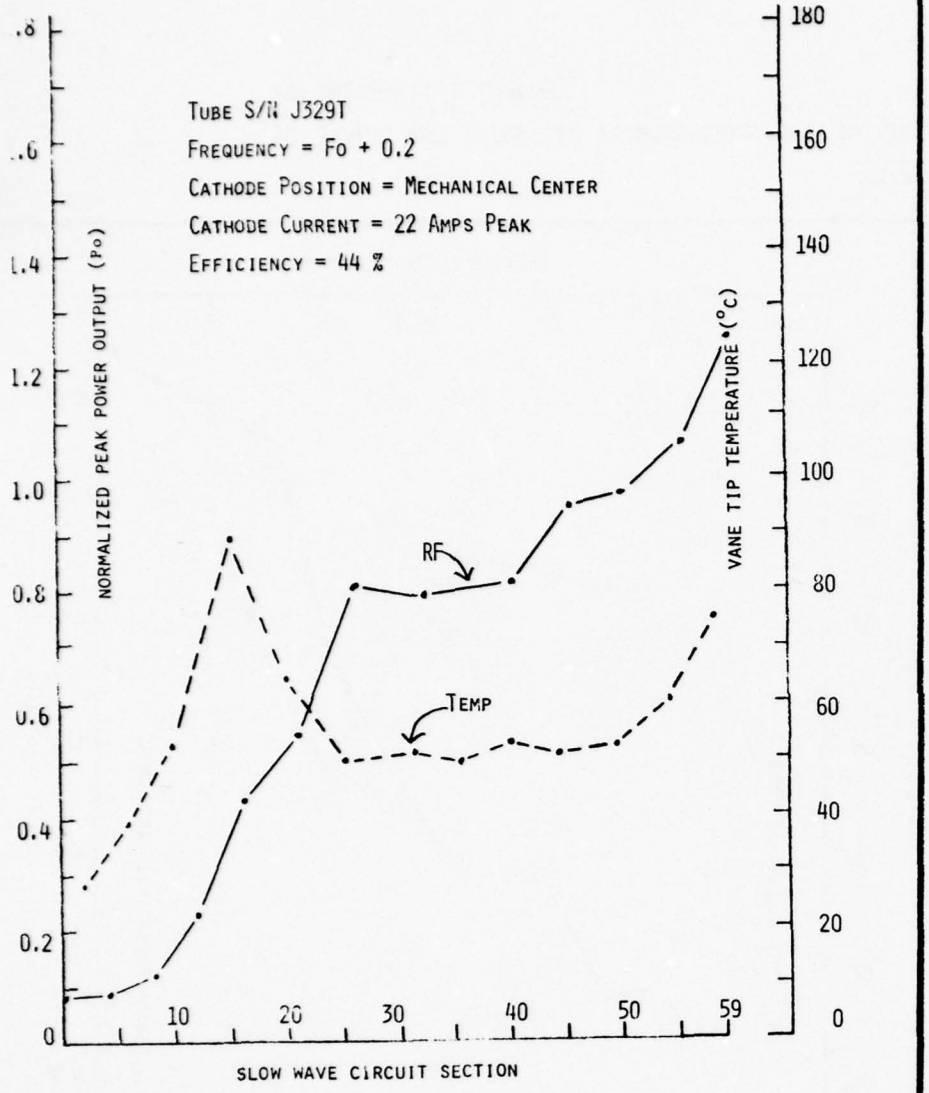

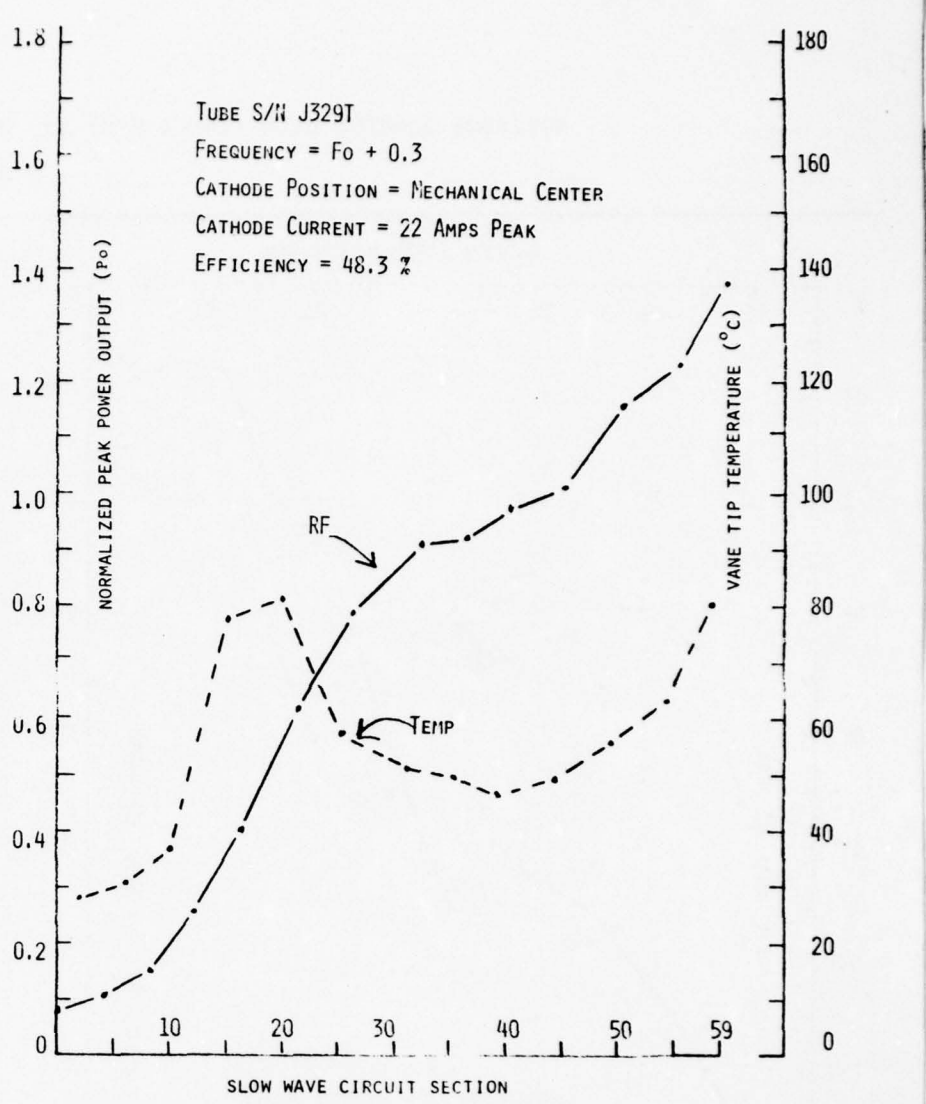

FIGURE 38

RF POWER AND VANE TIP TEMPERATURE PROFILES IN INSTRUMENTED CFA (S/N F376T) WITH CATHODE POSITION ON MECHANICAL CENTER.

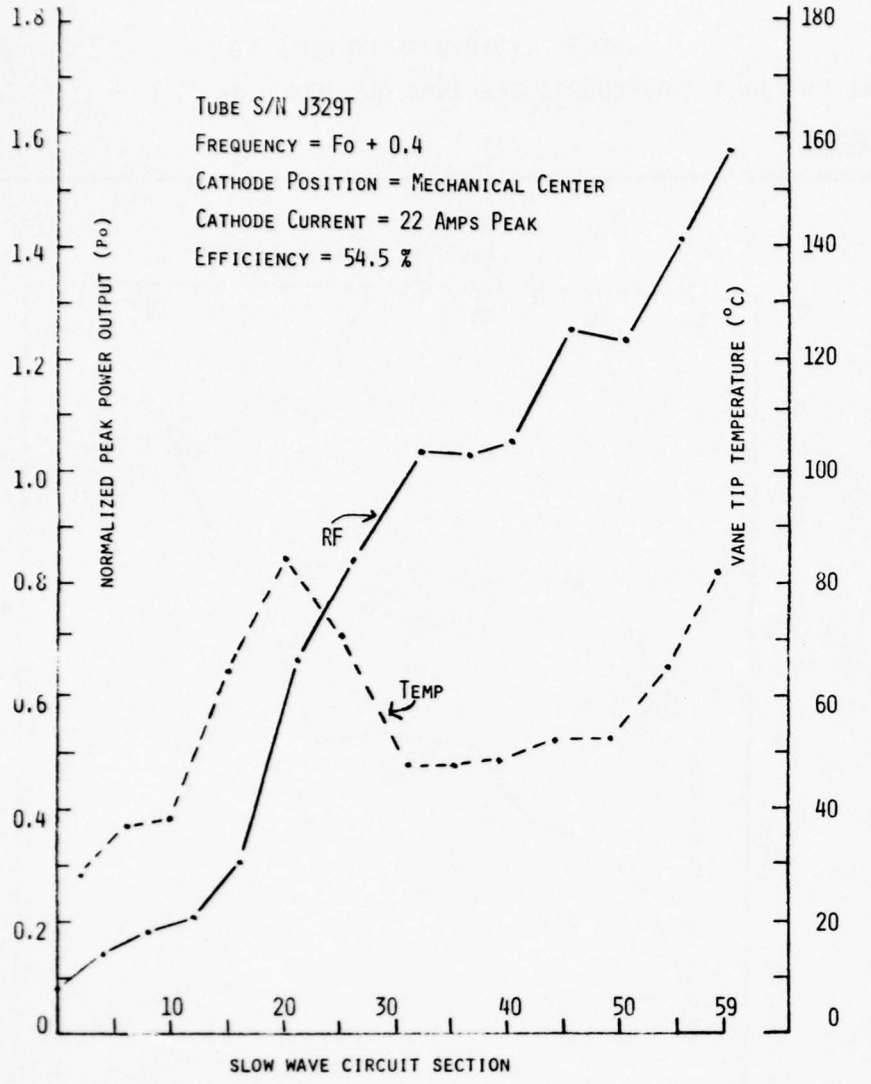

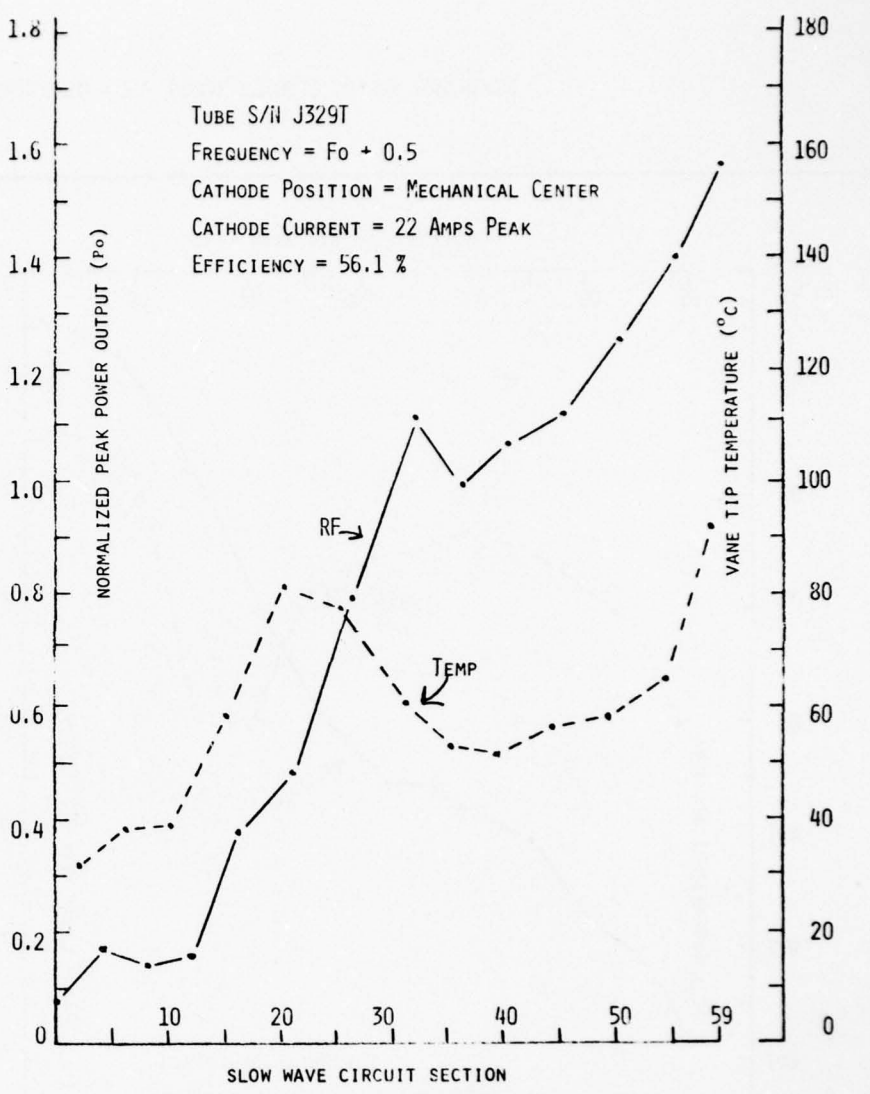

FIGURE 39

RF POWER AND VANE TIP TEMPERATURE IN INSTRUMENTED CFA (S/N F376T) WITH CATHODE POSITION ON MECHANICAL CENTER.

the cathode is further away from the circuit. Secondly, there is a peak in the temperature profile for J329T whereas there is not for B193T. On the other hand, the final peak power output at these frequencies is greater for B193T. These results imply that the programming near the input is better for J329T and better near the output for B193T. J329T utilizes the reentering space charge better, but B193T utilizes more favorably the current available from the cathode further along the interaction region. The existence of two regions of operation are quite evident in several of the power growth profiles for J329T. When first observed, it was suggested that the first part of the tube was utilizing the reentrant space charge in a fashion somewhat like an injected beam tube and was using current extracted from the hub for interaction further along. It seems reasonable to expect that if two types of interaction are possible in this tube, it should also be possible for similar effects to be occurring in a tube with a uniform pitch circuit. However, this was not quite so apparent from data obtained to date.

The efforts with the computer simulation will be discussed elsewhere. Nevertheless, it should be noted here that these phenomena were anticipated from that effort. The computer showed that much asynchronism existed between the space charge in the reentrant stream and the circuit wave. A lower limit existed for the RF field intensity at the hub that would be capable of extracting current. Furthermore, the computer showed that lowering the ratio of E/B by

moving the cathode away from the circuit made the situation even worse. Therefore, it was speculated that the effects actually obtained by programming the cathode-anode spacing near the RF input were the result of something different from what had been intended. It was thought that the increased cathode-anode spacing most likely led to more favorable conditions for interaction with the reentering space charge above the hub rather than improving conditions for removing space charge from the hub. It will be seen from the data obtained from J329T that this appears to be the correct interpretation. This result is very important for obtaining a high gain, reentrant stream CFA because it shows that the concept for proper programming must be revised. Efficient use of the current will require one kind of programming near the input for interaction between a low power input signal and the reentering space charge above the hub surface. A different type of programming will be required further along the interaction space when the RF power level has increased to a value high enough to extract current from the hub and maintain proper control of it during its transport to the anode.

Prior to performing experiments with J329T, the electromagnet was recalibrated so that the actual value of magnetic flux density in the interaction sapce for the CFA could be determined from the magnet current. This made it possible to calculate the Hartree voltage and subsequently the ratio of applied voltage-to-Hartree voltage. The value for the Hartree voltage, V_H, is

given by the familiar equation:[3,4]

$$\frac{V_H}{V_0} = 2\frac{B}{B_0} - 1$$

where

V_0 = synchronous voltage

$$= \frac{1}{2}\left(\frac{m}{e}\right)\left(\frac{2\pi c}{n\lambda}\right)^2 ra^2$$

B = applied magnetic field

B_0 = characteristic magnetic field

$$= 2\left(\frac{m}{e}\right)\left(\frac{2\pi c}{n\lambda}\right)\frac{1}{\left[1 - \left(\frac{r_c}{r_a}\right)^2\right]}$$

where

m = electron mass

e = electron charge

c = velocity of light

n = number of slow wavelengths around the anode

r_a = anode radius

r_c = cathode radius

These equations were developed for magnetrons where operation occurs in the pi mode standing wave for the slow wave circuit. The cathode is assumed to be circular and on mechanical center so that the

interaction space is uniform. For a magnetron with N (even number) resonators, there are n slow wavelengths around the tube where $n = N/2$.

Operation in a crossed-field amplifier uses the slow wave circuit in a travelling wave mode at other values of phase shift per section which varies with frequency. In addition, the cathode anode spacing can change along the interaction circuit and the circuit pitch can change as in the tapered pitch tube. Also, the slow wave circuit may employ any number of sections. Hence, these equations need to be modified for calculating properties for an amplifier. This can be done by noting that the quantity $(\frac{2\pi c}{n\lambda})$ is actually the angular velocity Φ for the circuit wave. For the general case, the angular velocity can be writte:

$$\Phi = \frac{vp}{r_a} = \frac{\omega}{\beta r_a} = \frac{2\pi fp}{\theta r_a} \quad \frac{rad}{sec}$$

where

β = propagation constant of the slow wave circuit

vp = phase velocity of the circuit wave

r_a = anode radius

f = operating frequency

p = circuit pitch

θ = phase shift per section for the circuit

By substitution we have:

$$V_0 = \frac{1}{2} \left(\frac{m}{e}\right) \left(\frac{2\pi fp}{\theta}\right)^2$$

The anodes for reentrant stream CFA's are always circular in format so that the anode has a fixed radius, r_a. The cathodes may be programmed so that they are non-circular and have different values for the radius. In addition, they may be adjusted in the actual tube so that the cathode-anode spacing may not be constant around the tube. Therefore, instead of using a value for the cathode radius in the equation for the characteristic magnetic field, we substitute $r_c = (r_a - d)$ where d is the cathode anode spacing. We then have:

$$B_0 = 2\left(\frac{m}{e}\right)\left(\frac{2\pi fp}{\theta r_a}\right) \quad \frac{r_a^2}{r_a^2 - (r_a - d)^2}$$

Using these equations a value for the Hartree voltage can be calculated at any position along the circuit. This is the value of voltage between anode and cathode that would provide exact synchronism between the circuit wave and the surface of an ideal Brillouin electron hub. From this and a value for the actual voltage applied to the cathode the ratio of V/V_H can be calculated. The values were calculated for each test frequency for J329T with a circular cathode on mechanical center. The results are shown in Figure 37. The values for V/V_H change linearly from input to

output in this case because of the linear change in circuit pitch.

Several things can be noted from these results. First these calculated values for V/V_H are lower than were anticipated for an emitting sole CFA. The simple theory for crossed-field tubes requires that a voltage greater than Hartree voltage must be applied to the tube to generate power. The results here show significant power at values of V/V_H less than unity. On the other hand, any inaccuracies in values for B, θ or d can lead to a wrong value for V_H. Also these tubes are known to differ significantly from the model used in the simple theory. For instance, magnetrons generate power at voltages below the calculated Hartree voltage. Therefore, these results should be used in a qualitative fashion to interpret the CFA operation rather than belaboring any questions about quantitative values.

With this point of view, other things can be noted. For instance, at the low frequency end of the band there is a rapid growth in power near the input of the circuit, a leveling off near the middle and a slight increase near the output. The calculated values for V/V_H are all less than unity, but do progressively increase with distance along the interaction region. This suggests that conditions near the input are correct for interaction with the reentering space charge, but that no new space charge is drawn up into the spoke for interaction until some larger value of V/V_H is reached near the output. On the other hand, at higher frequencies the rate of power growth near the input decreases, but significant power is added to the circuit near

the middle and towards the end. The calculated values for V/V_H increase progressively for this circuit. This suggests that the values for V/V_H may be a bit too large near the input, and the lower rate of power growth occurs because of some asynchronism between the circuit wave and the reentering electron stream. On the other hand, the larger values for V/V_H are appropriate for interacting with the hub current and this accounts for the higher rate of power growth near the output.

These specualtions should be verifiable with computer simulation when the programs for tapered interaction are perfected. If they prove to be correct, it seems to suggest a proper program for a very high gain CFA will be difficult over a broad bandwidth using a dispersive circuit.

The data for the vane tip temperature profiles are interesting for this tube. The peak in the curve near the input decreases in magnitude with increasing frequency just as the rate of power growth decreases. This may be due to the asynchronous condition that changes with frequency as described above or it may also be affected by the decrease in interaction impedance with increasing frequency. In general, however, the temperature profile is more nearly constant for this tube with the cathode on mechanical center than when the cathode was later adjusted for the best signal-to-noise ratio. This result is similar to those obtained with the uniform pitch circuits. It is also interesting to note that the tube efficiency increased progressively with frequency as follows

from fo+0.1 to fo+0.5: 39.3%, 44%, 48.3%, 54.5%, 56.1%. These values were obtained at rated RF input signal, rated constant current and very nearly the same cathode pulse voltage across the band.

5.2.3.4 Cathode Adjusted for Best Signal-to-Noise Ratio

For the next evaluation the cathode position for J329T was adjusted for best signal-to-noise ratio at the tube output across the band. The resulting profiles for rated RF input signal and constant current are shown in Figures 40-42.

It is seen that the final position for the cathode is again such that it is closer to the anode just before the output of the tube. A reverse taper is present at the output of the interaction region and through the drift space. There was essentially no change in the signal-to-noise ratio. It remained about 50 dB but more power output could be obtained from the tube. This was particularly true at the low frequency end of the band as can be seen from the power profiles. The efficiency increased significantly at the low frequency region. The efficiency values from fo+0.1 to fo+0.5 are: 47.5%, 48%, 51.3%, 53% and 58.1%.

Even with the cathode adjusted in this fashion there is still a region of no power growth at the low frequency end of the band at the mid portion of the interaction region. This region decreases in magntiude with increasing frequency. In fact the shape of the power growth profiles are not significantly different for the tube with the cathode in this position than for the cathode on mechanical center. The primary difference is higher peak power output, and this results from the larger values for V/V_H near the output of the tube. These are obtained because the cathode is

closer to the circuit in this region. These results suggest that it may be even more complicated to optimize the cathode-anode spacing contour for a tapered pitch CFA.

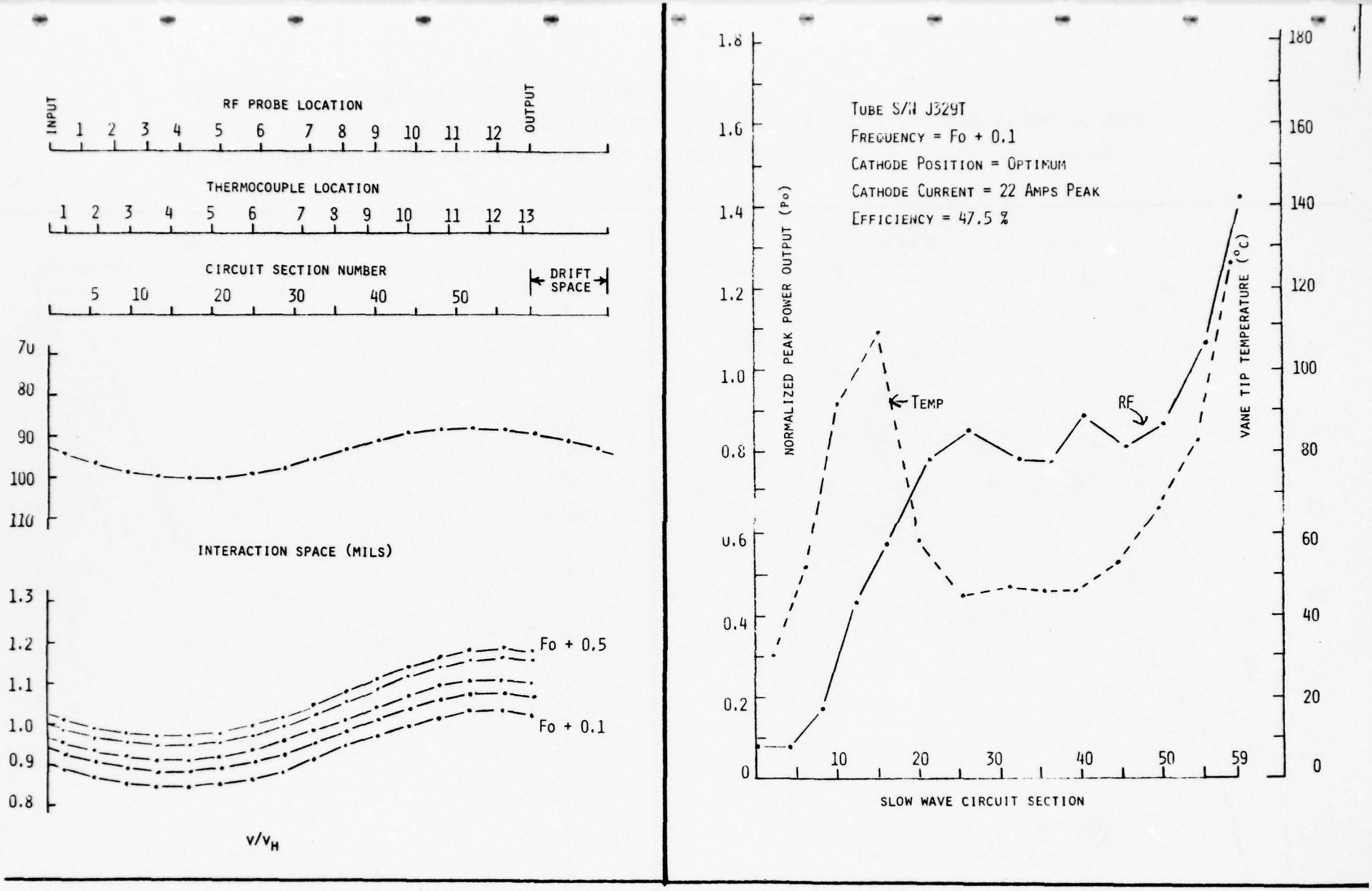

FIGURE 40

RF POWER AND VANE TIP TEMPERATURE PROFILES IN INSTRUMENTED CFA (S/N J329T) WITH CATHODE POSITION ADJUSTED FOR BEST COMPROMISE BETWEEN MAXIMUM POWER OUTPUT AND BEST SIGNAL-TO-NOISE RATIO ACROSS THE OPERATING BAND AT RATED RF INPUT.

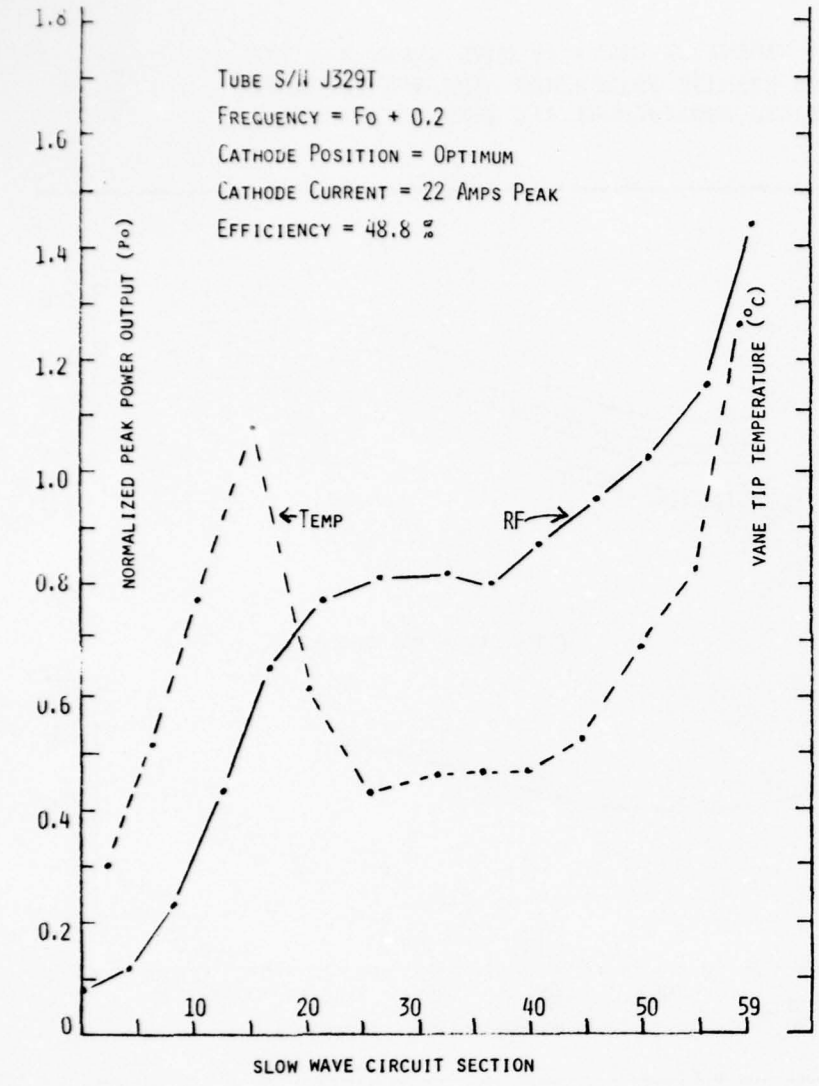

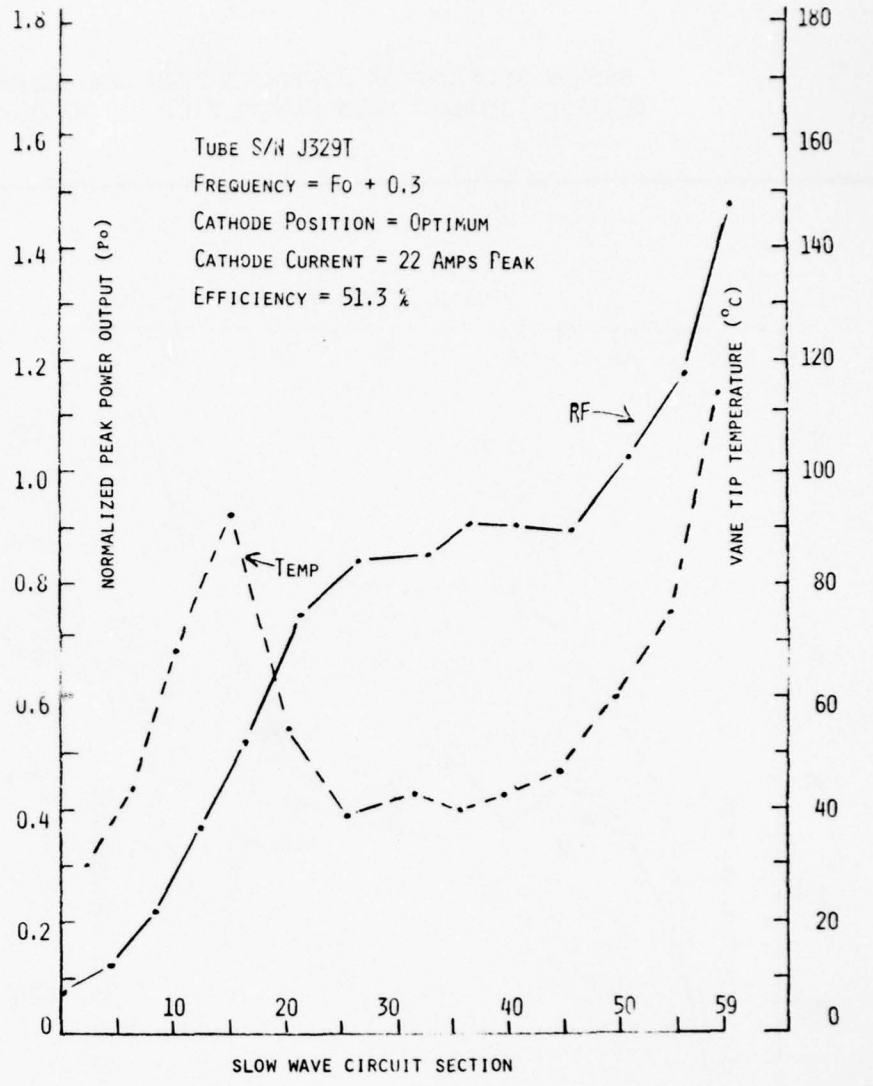

FIGURE 41

RF POWER AND VANE TIP TEMPERATURE PROFILES IN INSTRUMENTED CFA (S/N J329T) WITH CATHODE POSITION ADJUSTED FOR BEST COMPROMISE BETWEEN MAXIMUM POWER OUTPUT AND BEST SIGNAL-TO-NOISE RATIO ACROSS THE OPERATING BAND AT RATED RF INPUT.

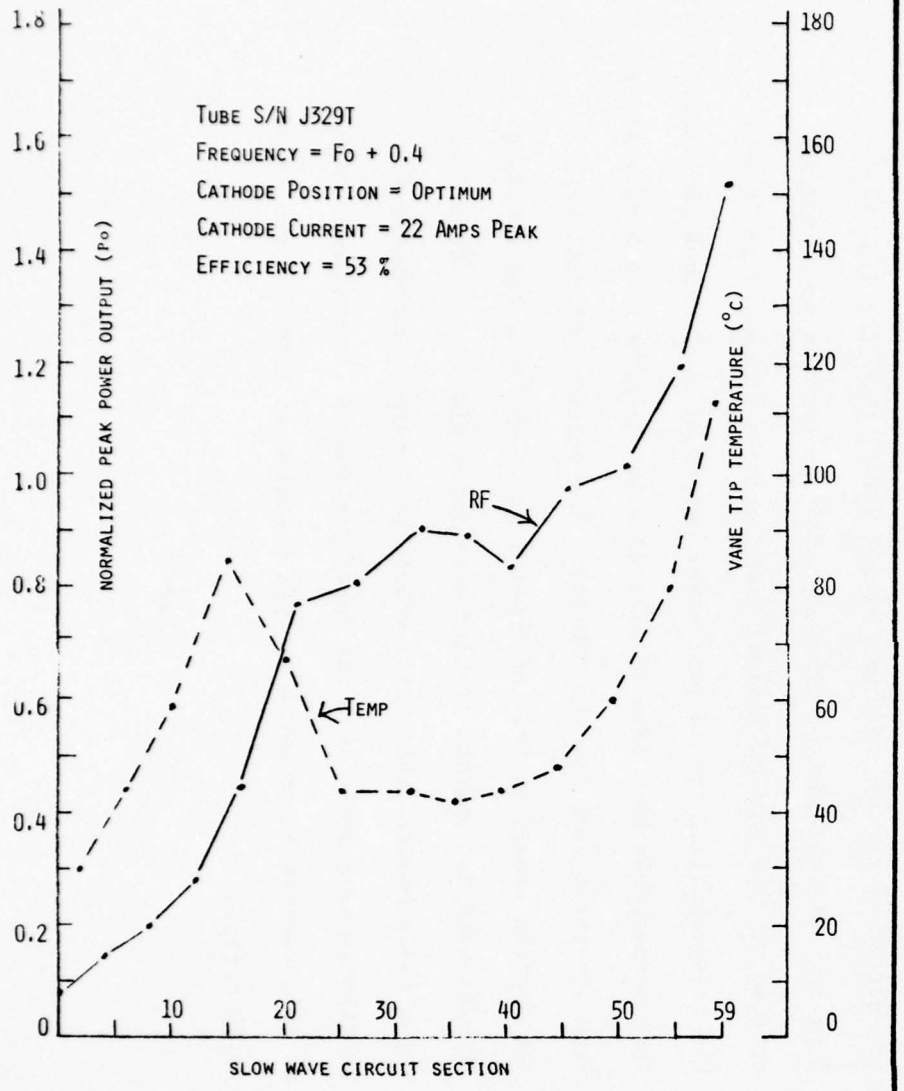

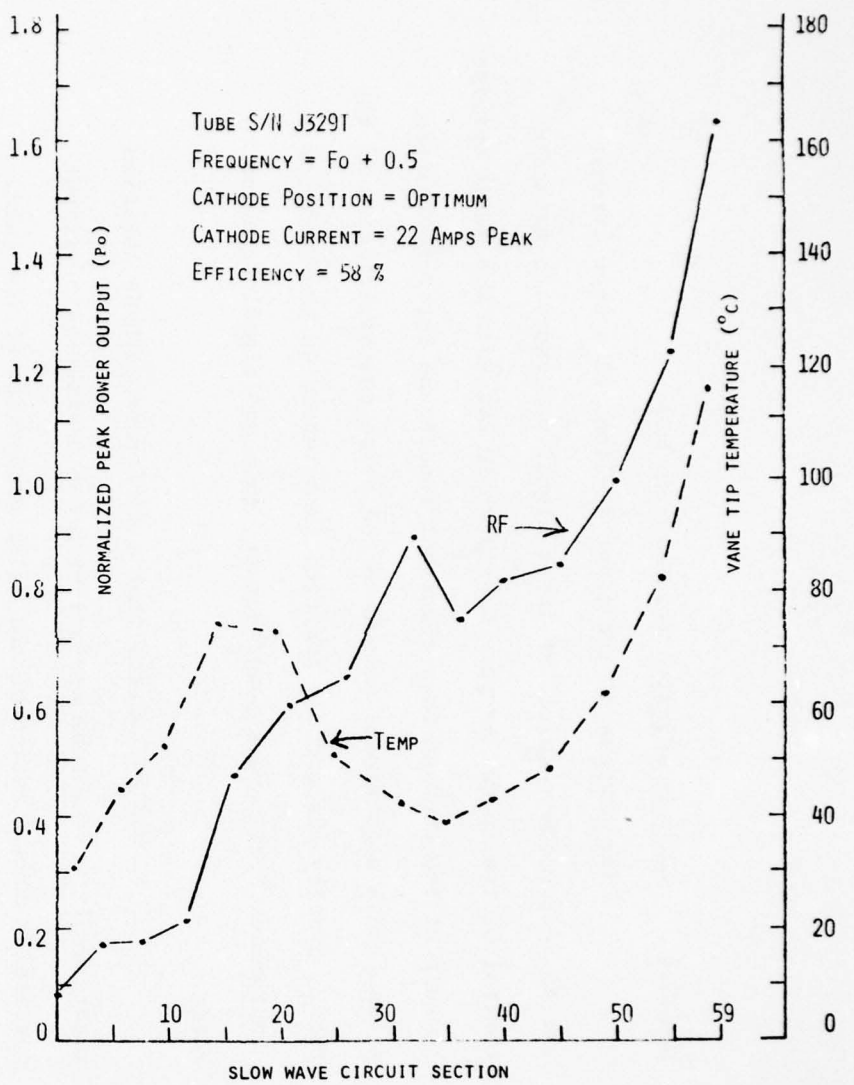

FIGURE 42

RF POWER AND VANE TIP TEMPERATURE PROFILES IN INSTRUMENTED CFA (S/N J329T) WITH CATHODE POSITION ADJUSTED FOR BEST COMPROMISE BETWEEN MAXIMUM POWER OUTPUT AND BEST SIGNAL-TO-NOISE RATIO ACROSS THE OPERATING BAND AT RATED RF INPUT.

5.2.3.5 Cathode Adjusted for Maximum Gain

The purpose of the tapered pitch, slow wave circuit was to reduce the required RF input signal necessary to maintain control of the space charge. Considerable evidence was being obtained to support the thought that reentrant conditions for the electron stream had a significant effect on the noise characteristics of the tube. Usually the cathode position is selected on the basis of a compromise between peak power output, gain and signal-to-noise ratio.

It was speculated that a different cathode position might result if the tube was adjusted for maximum gain without particular consideration of the noise properties of the tube. This idea was checked by reducing the RF drive to P_i' which is one-eighth of the normal input signal level, 0.08 Po; i.e., P_i' = 0.01 Po. The cathode was then adjusted for maximum power output at fo+0.3. The cathode current could only be increased to 20 amps for this condition, but a peak power output of 1.32 Po was obtained. This corresponds to a gain of 21.2 dB which is more than 9 dB greater than the rated gain for the SFD-261. The standard SFD-261 will not operate stably at this RF input level. In fact, the standard SFD-261 will not operate stably at an input signal of half of the rated input power. Therefore, the tapered pitch tube has much greater locking power near the input portion of the circuit. Even at this reduced drive level the CFA operated at this frequency with 49.5% efficiency.

The power growth and vane tip temperature profiles for this condition are shown in Figure 43. The power level grows monotonically from the input to the output. Note particularly the absence of the peak in the temperature profile near the input. This will be shown to be significant. Next the RF input signal level was increased in small increments up to 0.02 Po while maintaining the cathode current at 20 peak amperes. The RF drive was raised in steps from 0.03 Po to 0.08 Po (rated drive power) while maintaining the cathode current at 22 peak amperes (rated cathode current). The results are shown in Figures 43-46. At each value of cathode current the peak power output and efficiency tended to increase slightly with increased RF drive. The net gain progressively decreased. More significantly, however, as the RF drive level was increased a peak appeared in the vane tip temperature profile that grew in magnitude and moved closer to the RF input. This is interpreted as being the result of interaction with the reentrant space charge above the hub surface. At low RF drive levels, the current is not drawn up to the anode quickly enough and drifts further along the interaction region before collection over a broad range of the circuit. At increased drive power the collection becomes more concentrated and the temperature peak appears. At still higher RF drive level the collection occurs sooner and the peak moves toward the input. These data confirm quite clearly the earlier speculation that the temperature peak near the RF input is the result of localized collection of reentrant space charge. This is furter confirmed when the data

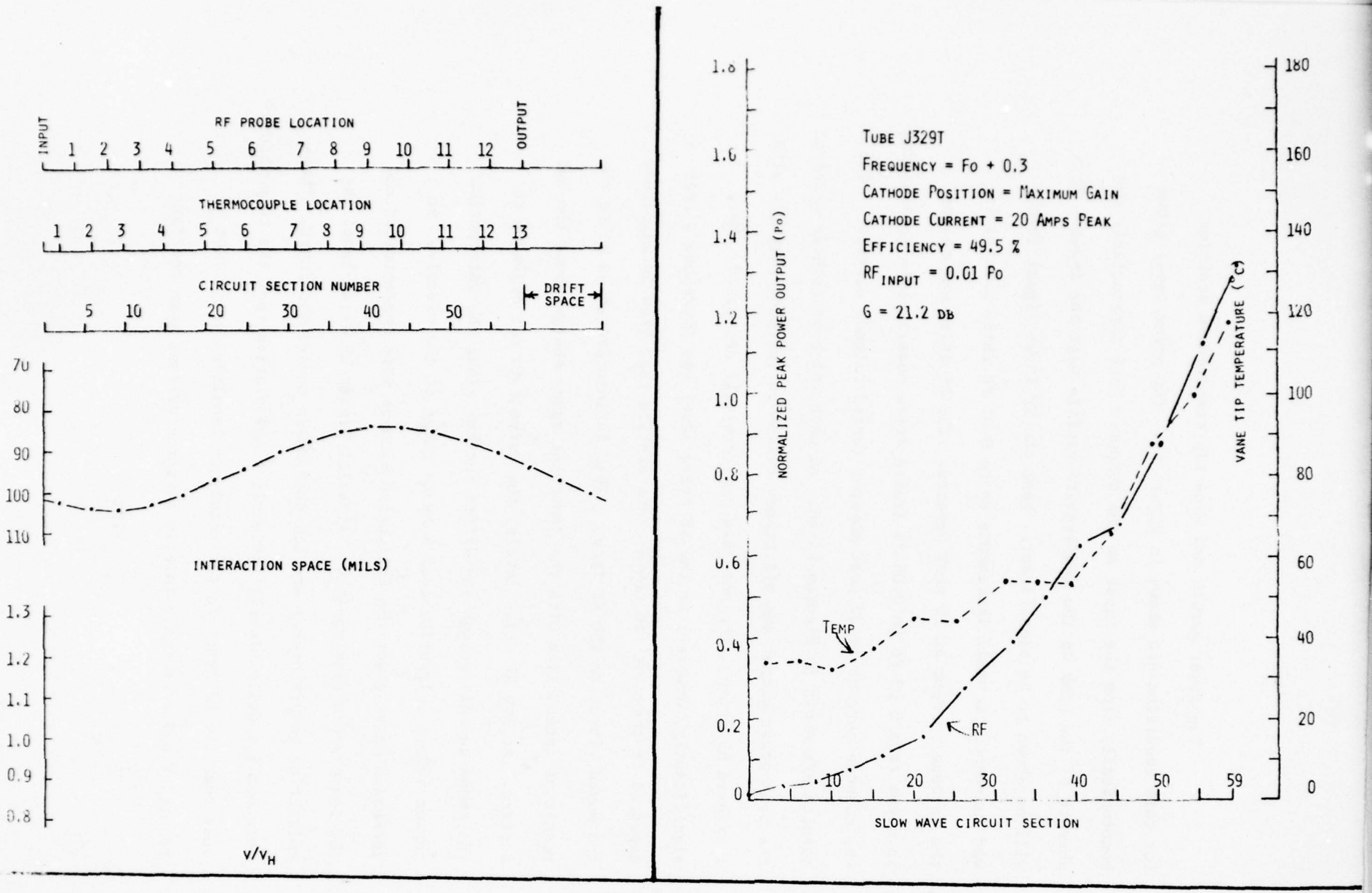

FIGURE 43

RF POWER AND VANE TIP TEMPERATURE PROFILES IN INSTRUMENTED CFA (S/N J329T) WITH CATHODE POSITION ADJUSTED FOR MAXIMUM POWER OUTPUT WITH RF INPUT SIGNAL EQUAL TO 0.01 Po.

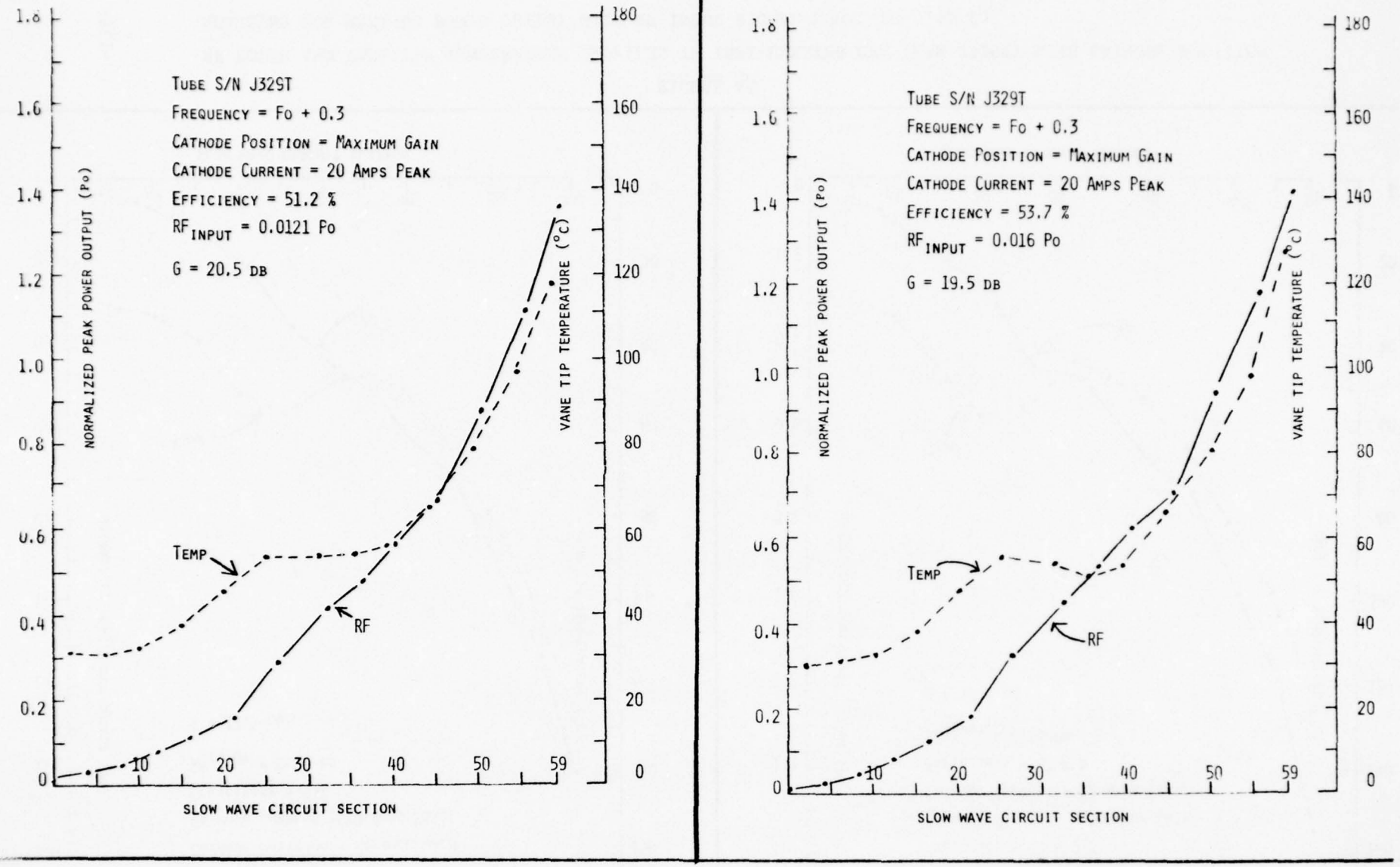

FIGURE 44

RF POWER AND VANE TIP TEMPERATURE PROFILES IN INSTRUMENTED CFA (S/N J329T) WITH CATHODE POSITION ADJUSTED FOR MAXIMUM POWER OUTPUT WITH RF INPUT SIGNAL EQUAL TO 0.01 Po.

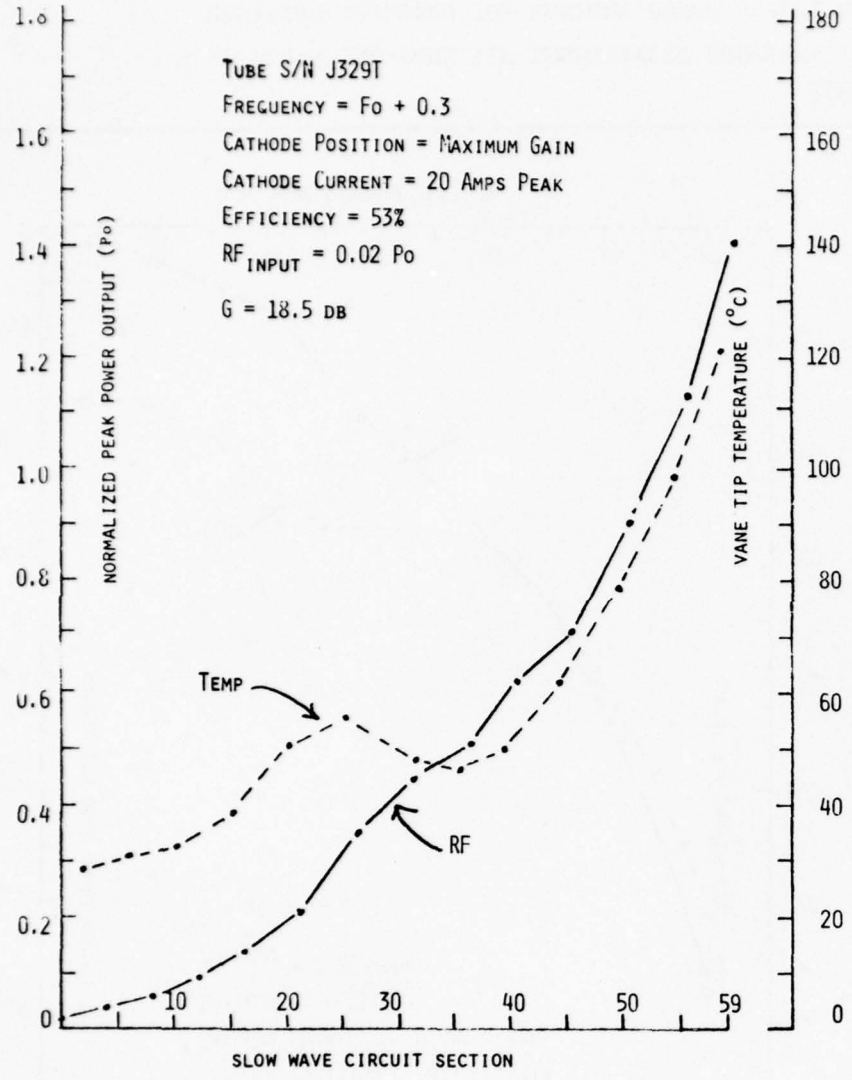

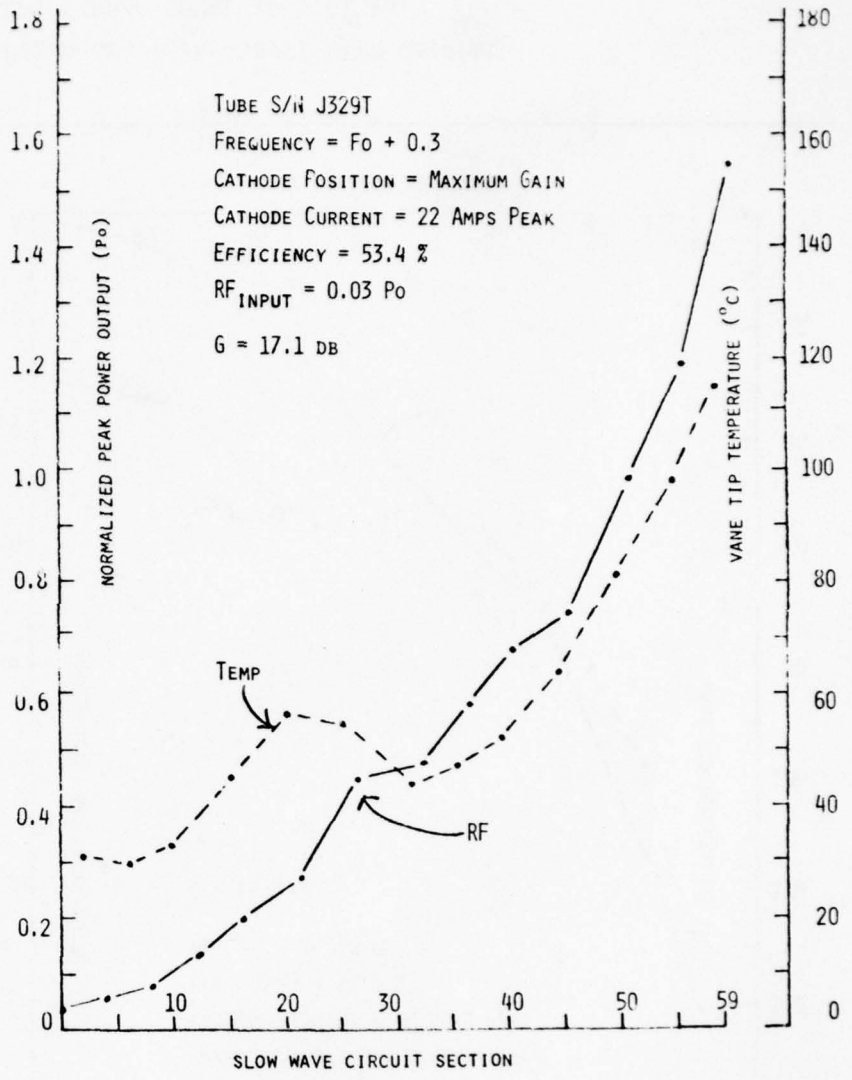

FIGURE 45

RF POWER AND VANE TIP TEMPERATURE PROFILES IN INSTRUMENTED CFA (S/N J329T) WITH CATHODE POSITION ADJUSTED FOR MAXIMUM POWER OUTPUT WITH RF INPUT SIGNAL EQUAL TO 0.01 Po.

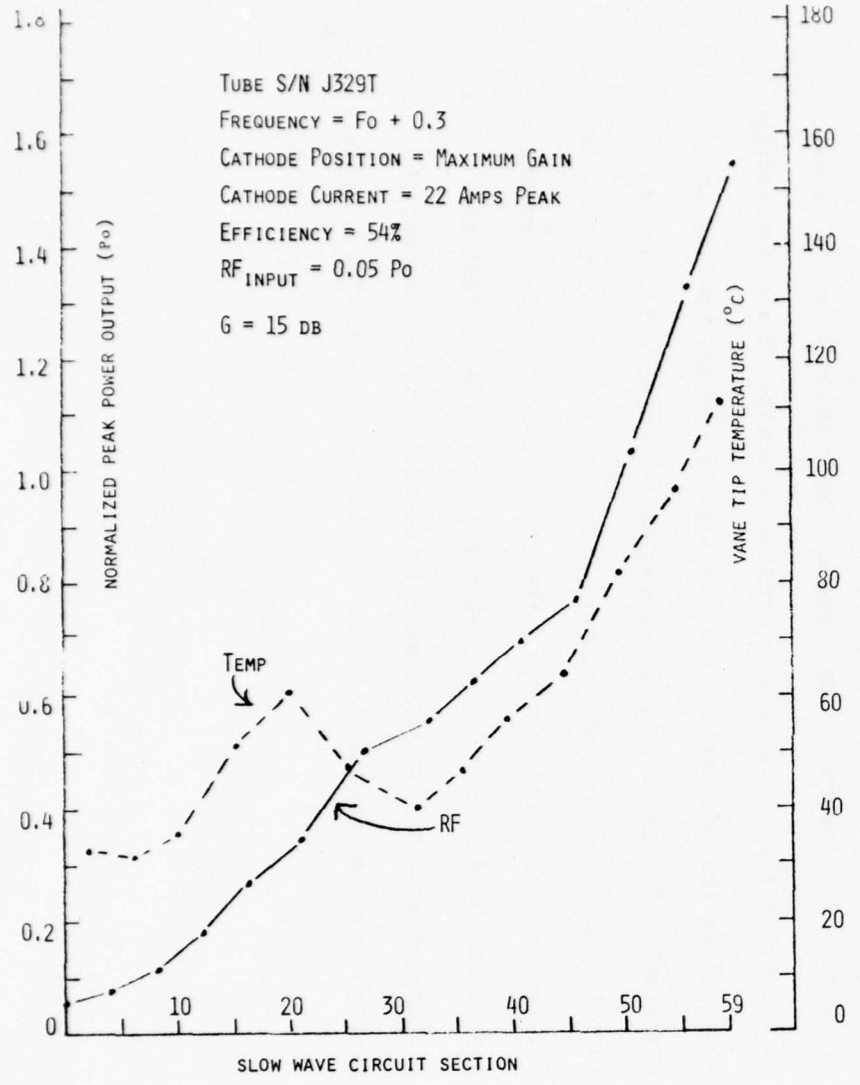

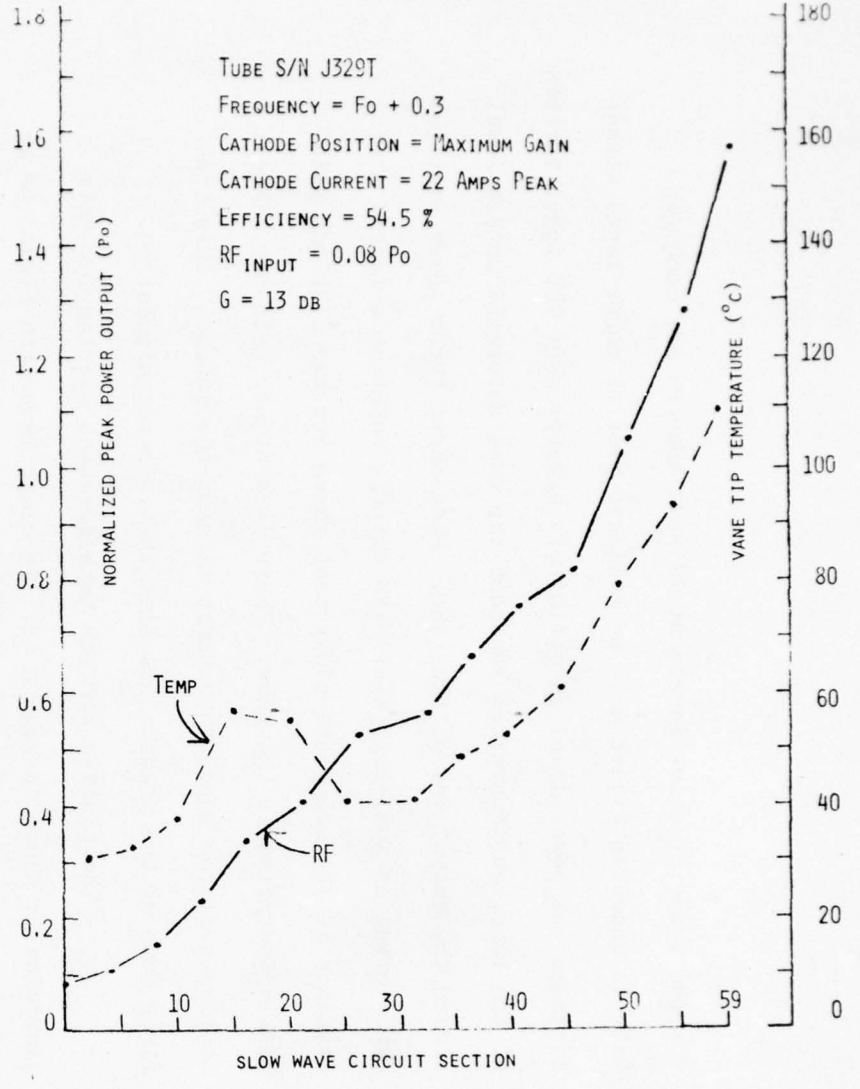

FIGURE 46

RF POWER AND VANE TIP TEMPERATURE PROFILES IN INSTRUMENTED CFA (S/N J329T) WITH CATHODE POSITION ADJUSTED FOR MAXIMUM POWER OUTPUT WITH RF INPUT SIGNAL EQUAL TO 0.01 Po.

for the three RF drive levels at 22 peak amperes are combined. This is shown in Figure 47. On a linear plot of power level versus distance the power level is definitely greater over the input portion of the tube, but converges to about the same saturated output level toward the output end of the tube. When these three power profiles are plotted on semi-log paper with circuit power as a function of distance it becomes quite clear that there are two distinct gain levels operating in the tube. There is a higher gain per circuit section near the input than there is near the output. This confirms some of the predictions from the computer simulation.

The profile for the cathode-anode spacing for this operation is shown in Figure 43. By comparison with Figure 40 it is seen that the cathode position is different from that which gave the best compromised performance across the band. The interaction space profiles for these two cases are superimposed in Figure 48. In the present case there is a greater variation in the interaction space along the circuit and the position of closest spacing is different. For the high gain operation the cathode is closest to the anode at about vane number 40 as opposed to vane number 52 for the configuration that gave the best compromised performance across the band. This lends credence to the concept that the programmed interaction might need to be optimized in one way to maximum gain and another approach may be needed to minimize noise.

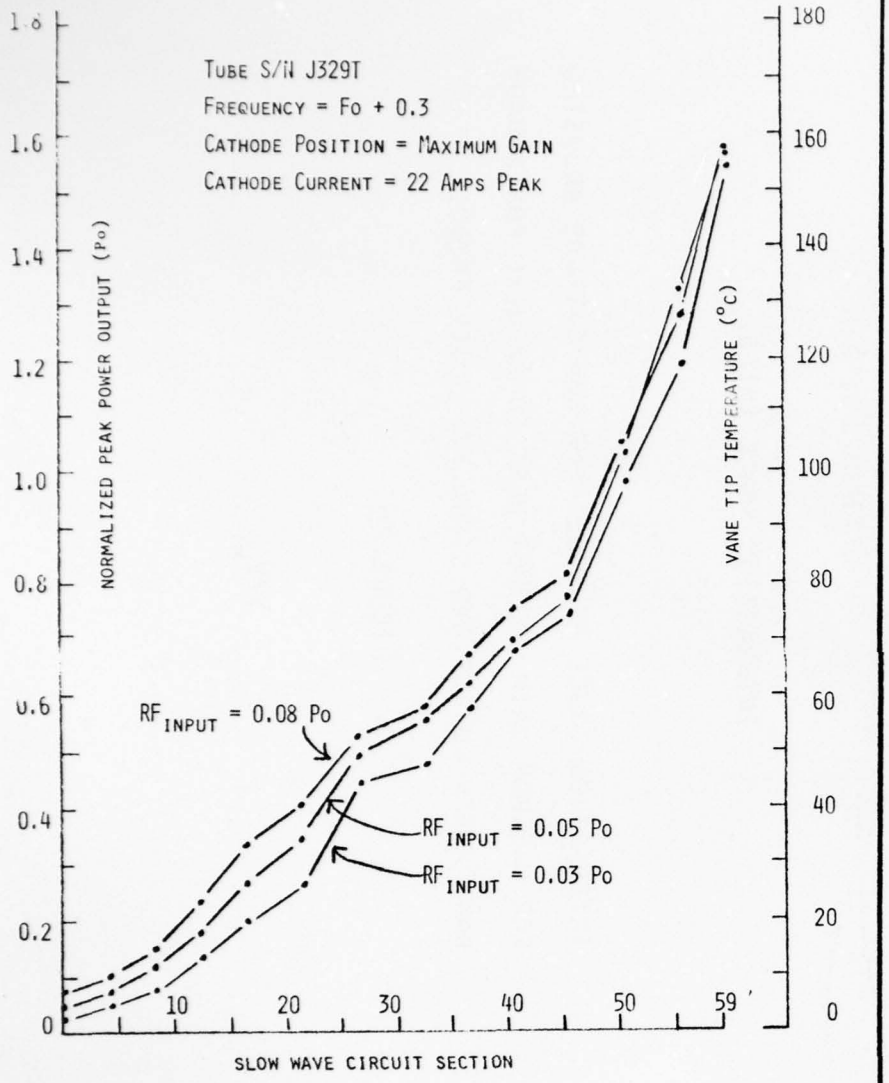

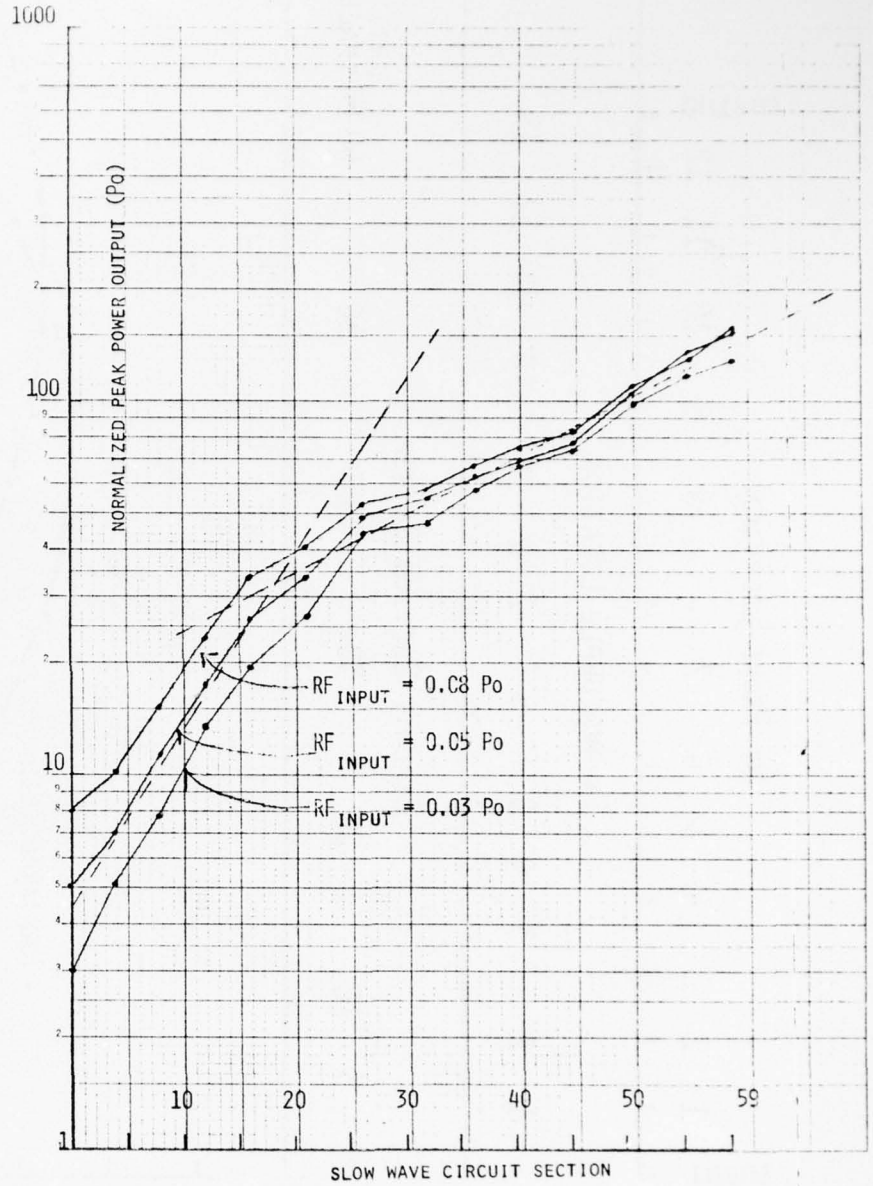

FIGURE 47

RF POWER PROFILES IN INSTRUMENTED CFA (S/N J329T) PLOTTED TO EMPHASIZE THE EXISTENCE OF TWO REGIONS OF DIFFERENT VALUES OF GAIN PER CIRCUIT SECTION.

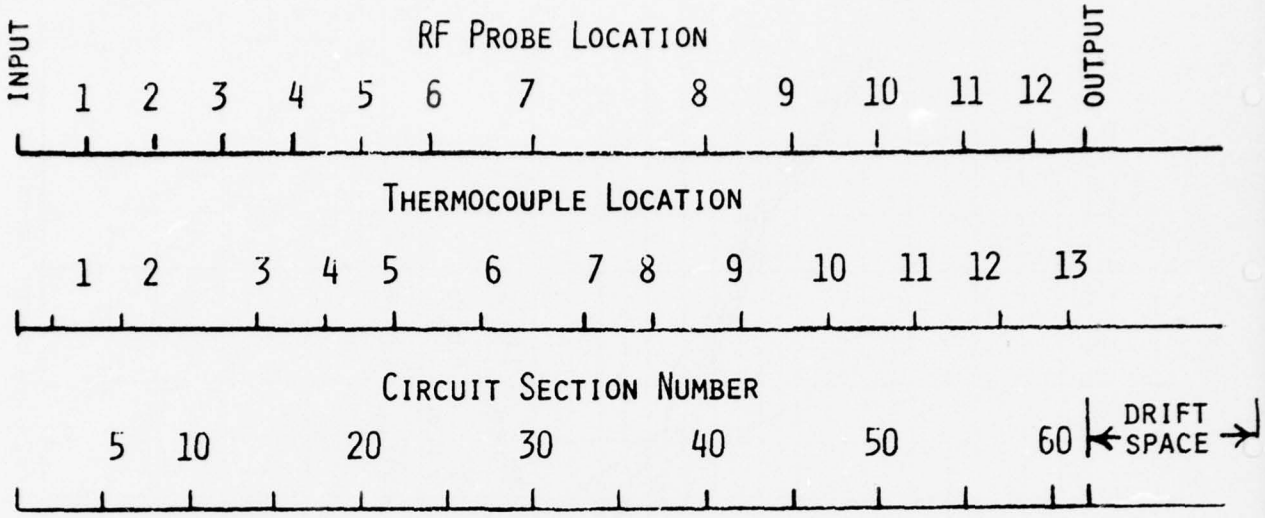

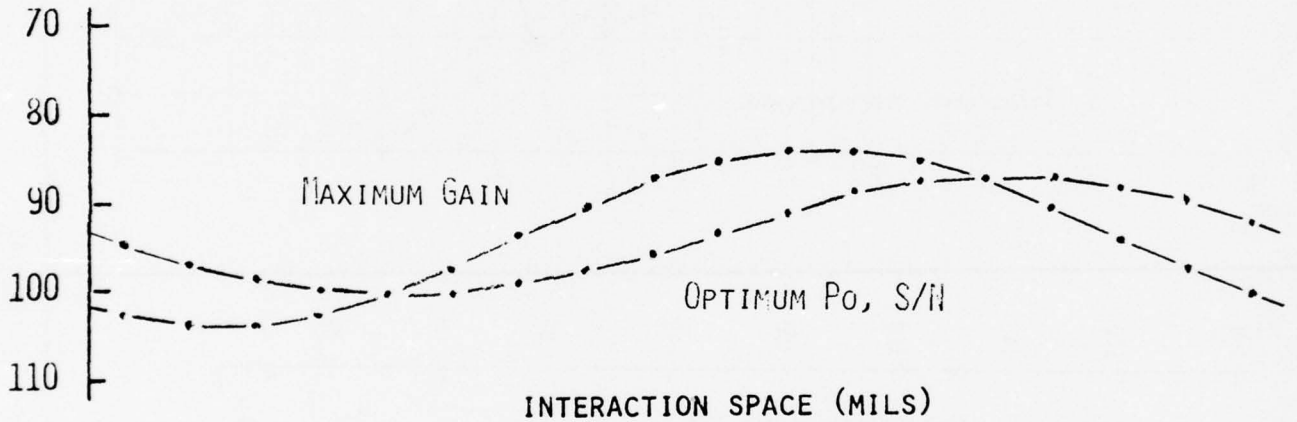

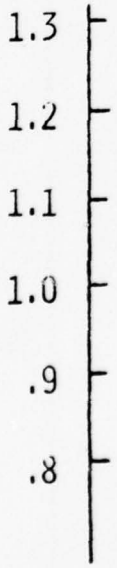

INTERACTION SPACE PROFILES FOR NEW CATHODE ADJUSTED FOR MAXIMUM GAIN AND FOR BEST COMPROMISE FOR BROAD-BAND POWER OUTPUT AND SIGNAL-TO-NOISE RATIO.

FIGURE 48

These data showed that a low drive signal allowed reentrant current to drift further along the slow wave circuit before collection. It has been speculated previously that much of the noise in a reentrant stream CFA is contributed by interaction with uncontrolled space charge near the slow wave circuit. This suggests that the tube with low drive power might be noisier than with rated drive power. To check this, the spectrum of the output signal was photographed for each of the drive signal levels for the high gain CFA. The results are shown in Figure 49. At a drive level of 0.01 Po, the signal-to-noise ratio was about 35 dB. This progressively improved with increased RF drive power until a signal-to-noise ratio of 50 dB was obtained at rated drive power of 0.09 Po. The reason for this progressive improvement is that the noisy reentrant space charge is collected more rapidly as the drive signal is raised and removed from circuit interaction. These results support the model for operation as described.

Tests were made next to determine the ability to maintain high gain across the operating band. Tests were made for a constant current of 20 peak amperes. The results are shown in Figures 50-52. Operation was obtained over the lower half of the band at drive signals of the order of 0.01 Po, and at gain levels of 20 dB or more. At the upper half of the band it was necessary to increase the drive signal to 0.02 Po for stable operation. Gain levels of greater than 18 dB were obtained. The peak power output at fo+0.2 is significantly higher than at the other frequencies. This was not noted until after the experimental arrangement was changed. There may have been an

experimental error or this may have been a frequency favorable to electronic feedback regeneration. In any case, operation across the band was obtained at an efficiency of the order of 50%.

The results obtained to date with the tapered pitch, slow wave circuit indicate that this approach to programmed interaction for obtaining high gain in a reentrant stream CFA is superior to others that have been tried.

FIG 49

NOISE PROPERTIES OF CFA (S/N J329T) AS A FUNCTION OF RF DRIVE LEVEL.

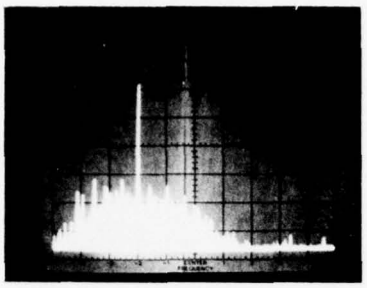

001 Po

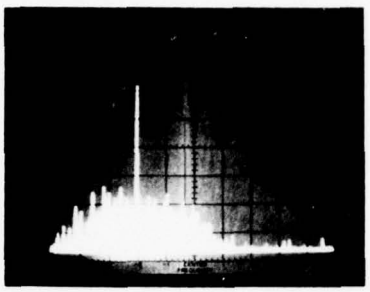

0.012 Po

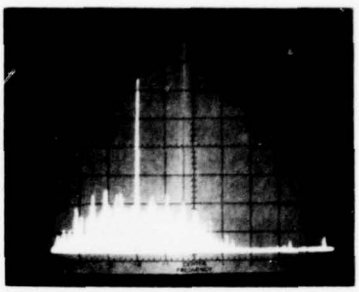

0.016 Po

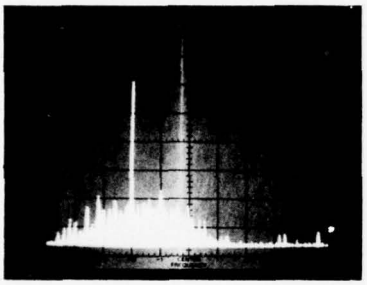

0.02 Po

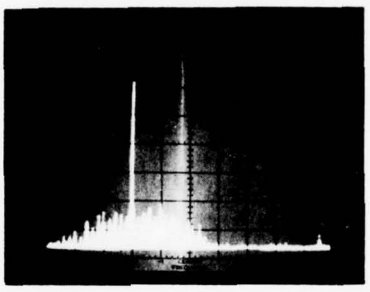

0.03 Po

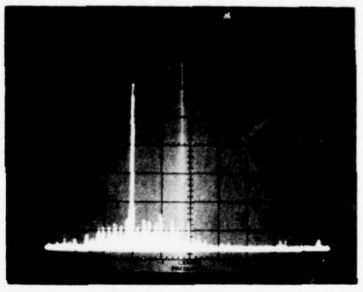

0.05 Po

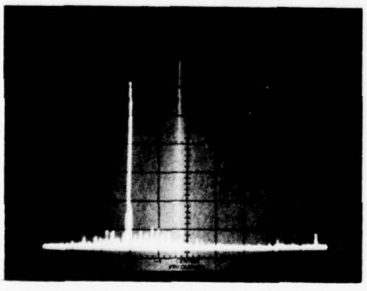

0.08 Po S/N 50 dB

THE SPECTRUM PHOTOGRAPHS SHOW THE EFFECT OF NOISE REDUCTION AT THE OUTPUT OF THE HIGH GAIN CFA WITH TAPERED PITCH, SLOW WAVE CIRCUIT. THE IMPROVED SIGNAL-TO-NOISE RATIO IS PRODUCED BY INCREASING THE RF INPUT SIGNAL. A TUBE WITH ONLY A TAPER HAS A SIGNAL-TO-NOISE RATIO OF 50 DB WHERE A TUBE WITH A TAPER PLUS BEAM SKIMMER HAS A SIGNAL-TO-NOISE RATIO OF 55 DB. THE SPECIFIED SIGNAL-TO-NOISE RATIO FOR THE SFD-261 IS 42 DB.

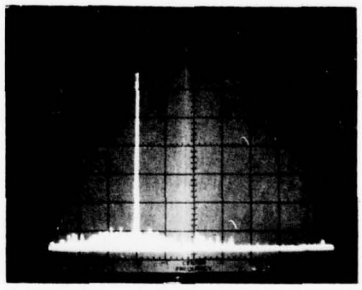

Tapered Circuit & Skimmer
0.08 Po S/N 55 dB

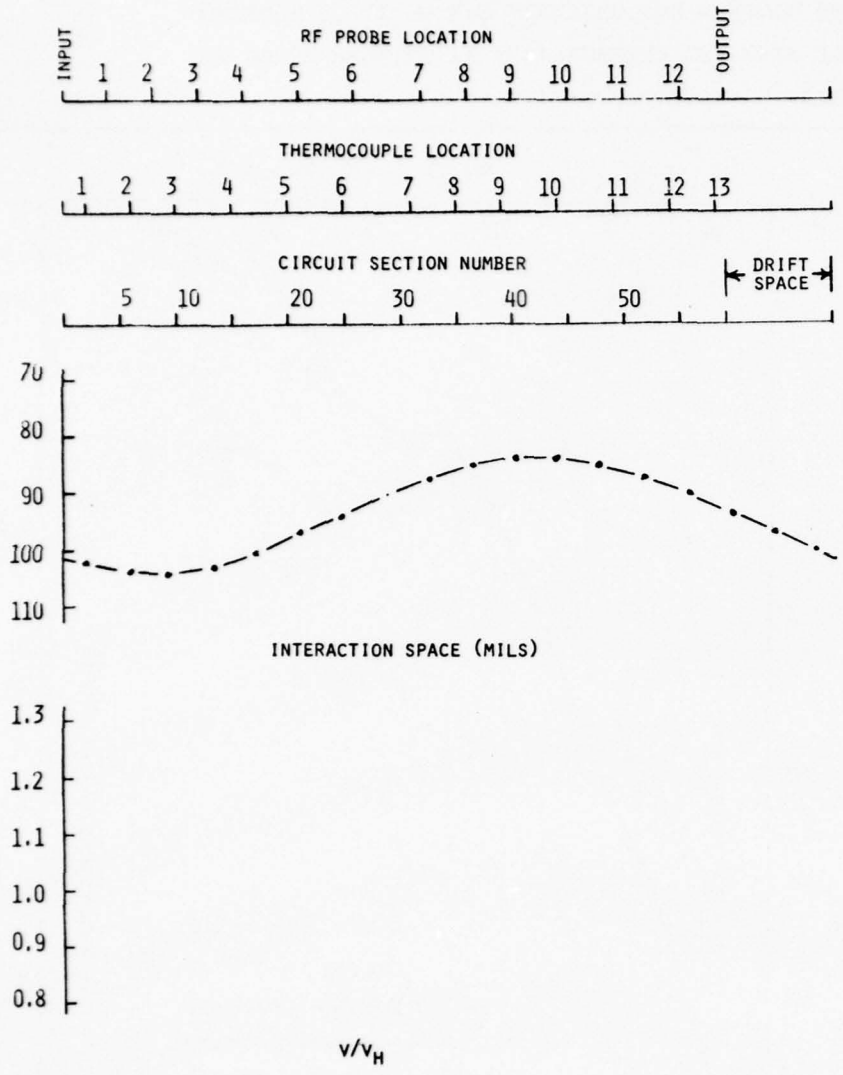

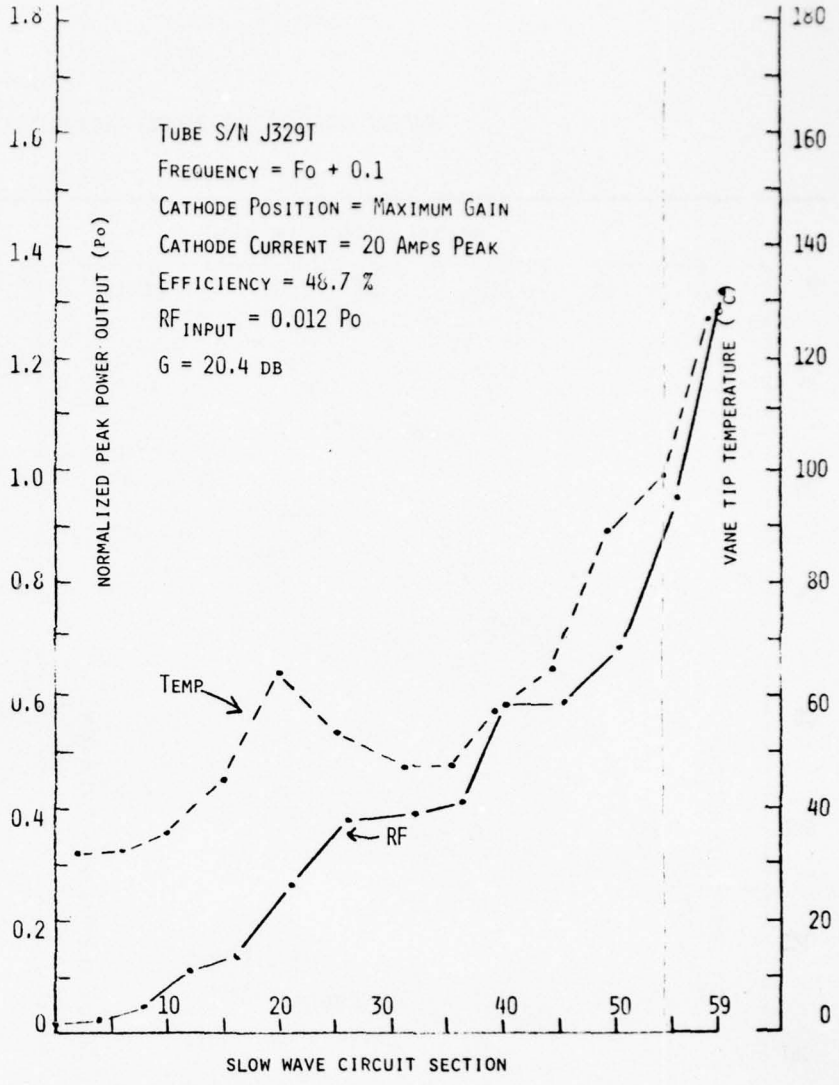

FIGURE 50

RF POWER PROFILE IN INSTRUMENTED CFA (S/N J329T) AT SPECIFIED INPUT FREQUENCY AFTER CATHODE POSITION WAS ADJUSTED FOR MAXIMUM GAIN AT Fo + 0.3.

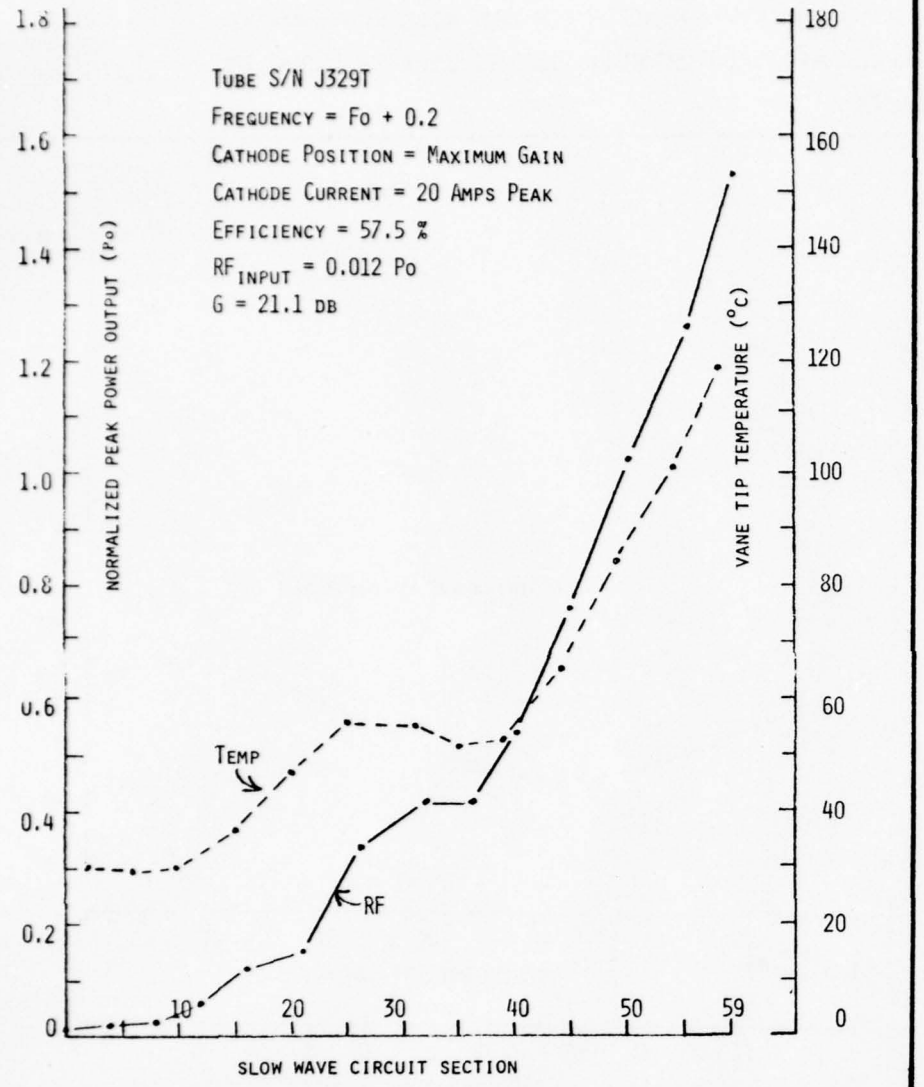

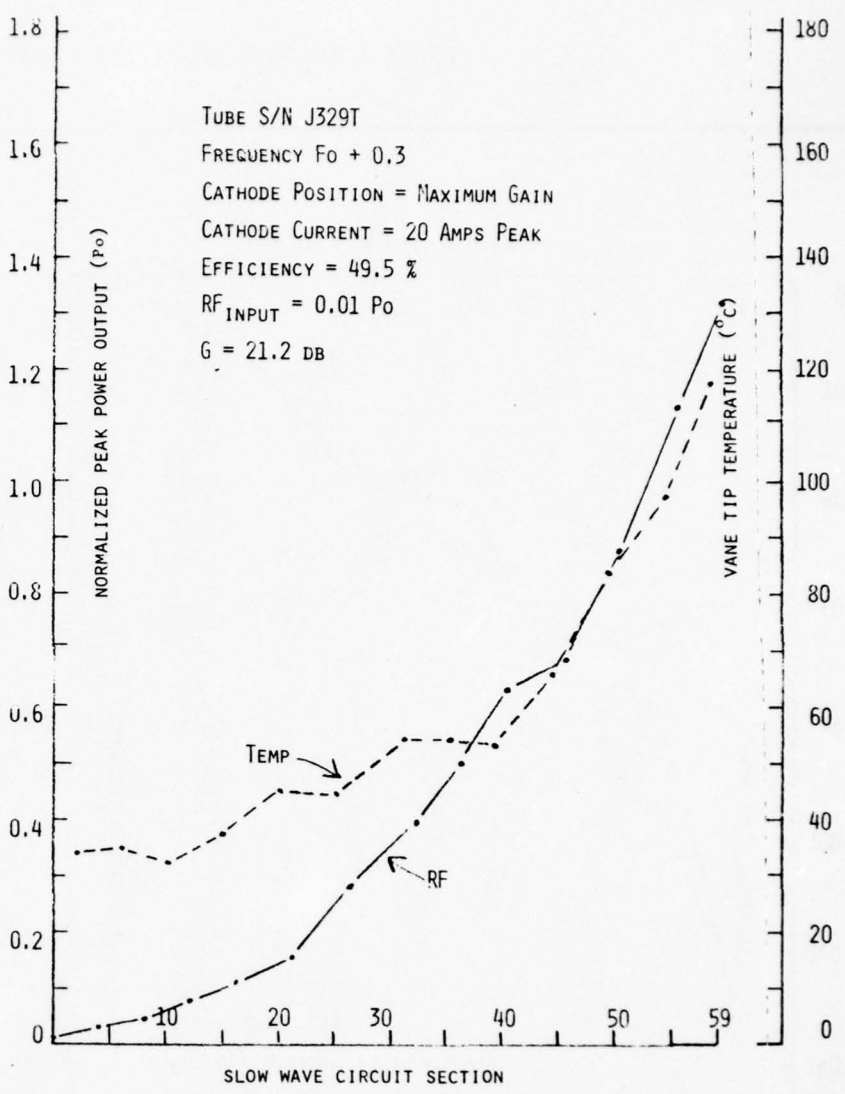

FIGURE 51

RF POWER PROFILE IN INSTRUMENTED CFA (S/N J329T) AT SPECIFIED INPUT FREQUENCY AFTER CATHODE POSITION WAS ADJUSTED FOR MAXIMUM GAIN AT Fo + 0.3.

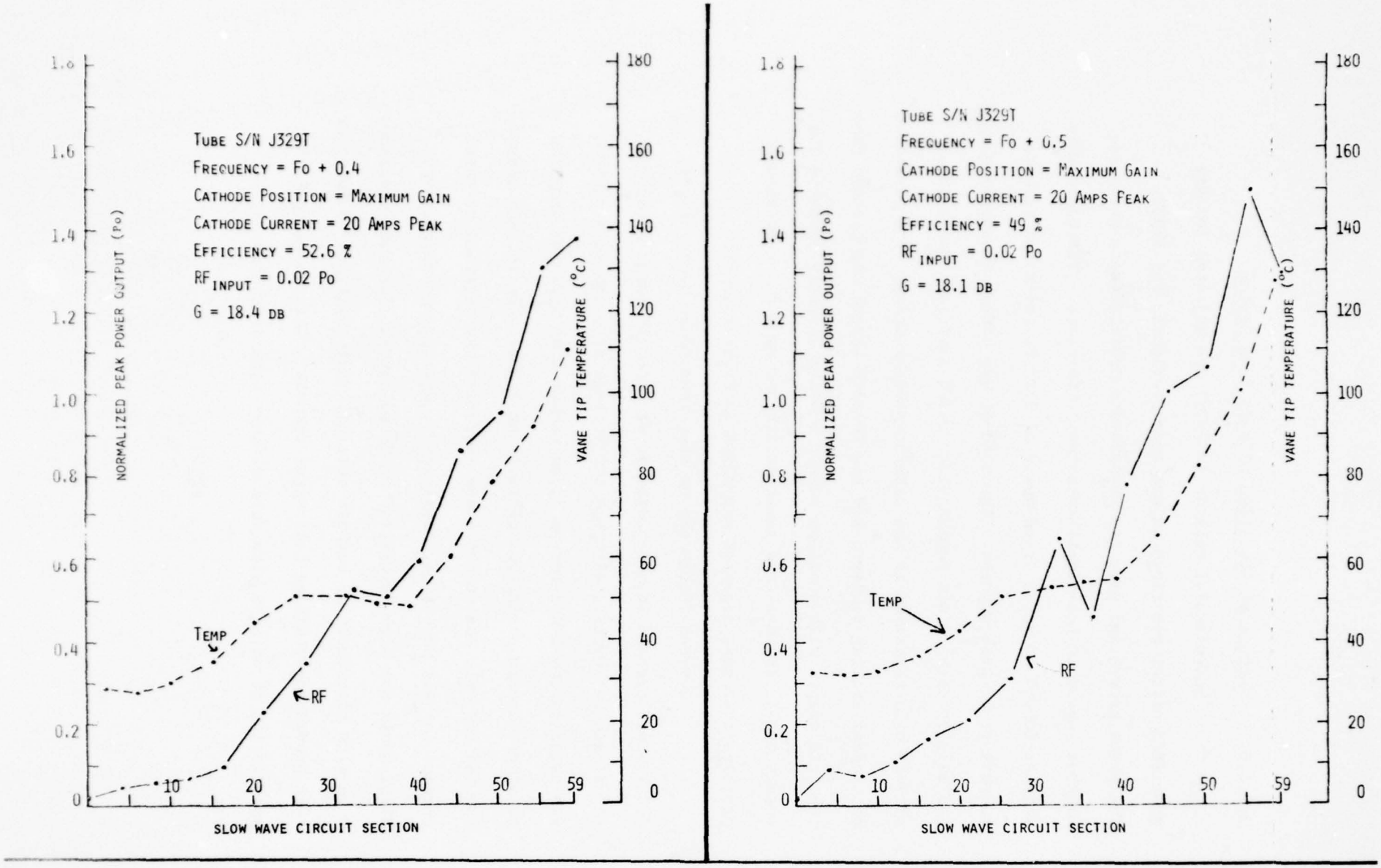

FIGURE 52

RF POWER PROFILE IN INSTRUMENTED CFA (S/N J329T) AT SPECIFIED INPUT FREQUENCY AFTER CATHODE POSITION WAS ADJUSTED FOR MAXIMUM GAIN AT Fo + 0.3.

5.2.3.6 Cathode at Specified Offsets from Center

The circular cathode in J329T was adjusted for six specified offset positions as was done previously for B193T. The power growth and vane tip temperature profiles were obtained without regard to the signal-to-noise performance. The tests were made at fo+0.3 at rated drive power of 0.08 Po and rated cathode current of 22 peak amperes. The cathode was offset by approximately 4.5 mils in each of six equiangular spaced positions for a total of 9-10 mils variation in the cathode-anode spacing. The positions of closest spacing numbered 1-6 are located around the circuit from input to output with position number 6 being directly opposite the output vane. The measured power growth and vane tip temperature profiles that were measured are shown in Figures 53-58.

Several things can be seen from these data. First, J329T would operate in all positions at rated RF input power and rated cathode current, although the voltage at which this current was obtained was lower for position number 1 by 2-2.5 KV compared to other cathode positions. This is an appreciable voltage change for the SFD-261, but nevertheless operation was obtained at rated current for all positions. Contrarily, similar experiments with B193T would not yield operation at rated current for some positions even with adjustment of cathode voltage. Instabilities would occur that prevented obtaining full rated current. This shows again the superiority of using a slow wave circuit with a tapered pitch.

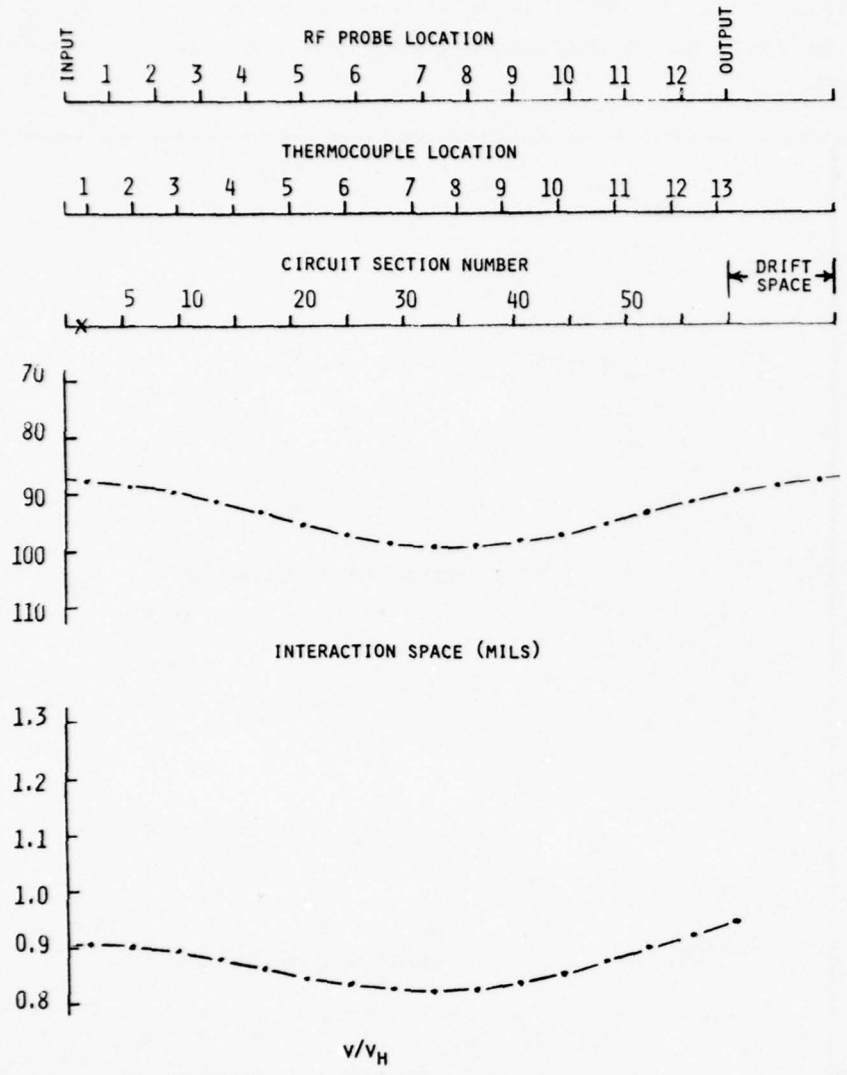

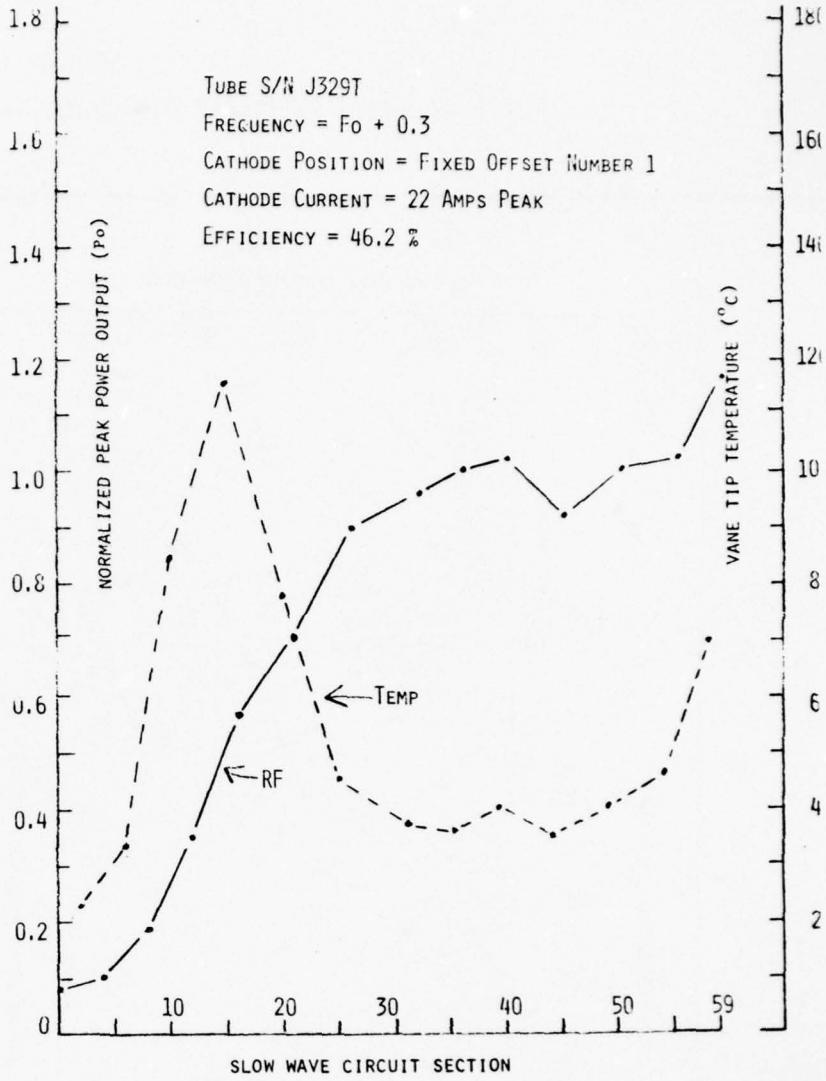

FIGURE 53

RF POWER AND VANE TIP TEMPERATURE PROFILES IN INSTRUMENTED CFA (S/N J329T) AT RATED RF INPUT (0.08 Po) WITH CATHODE ADJUSTED TO FIXED OFFSET POSITION NUMBER 1.

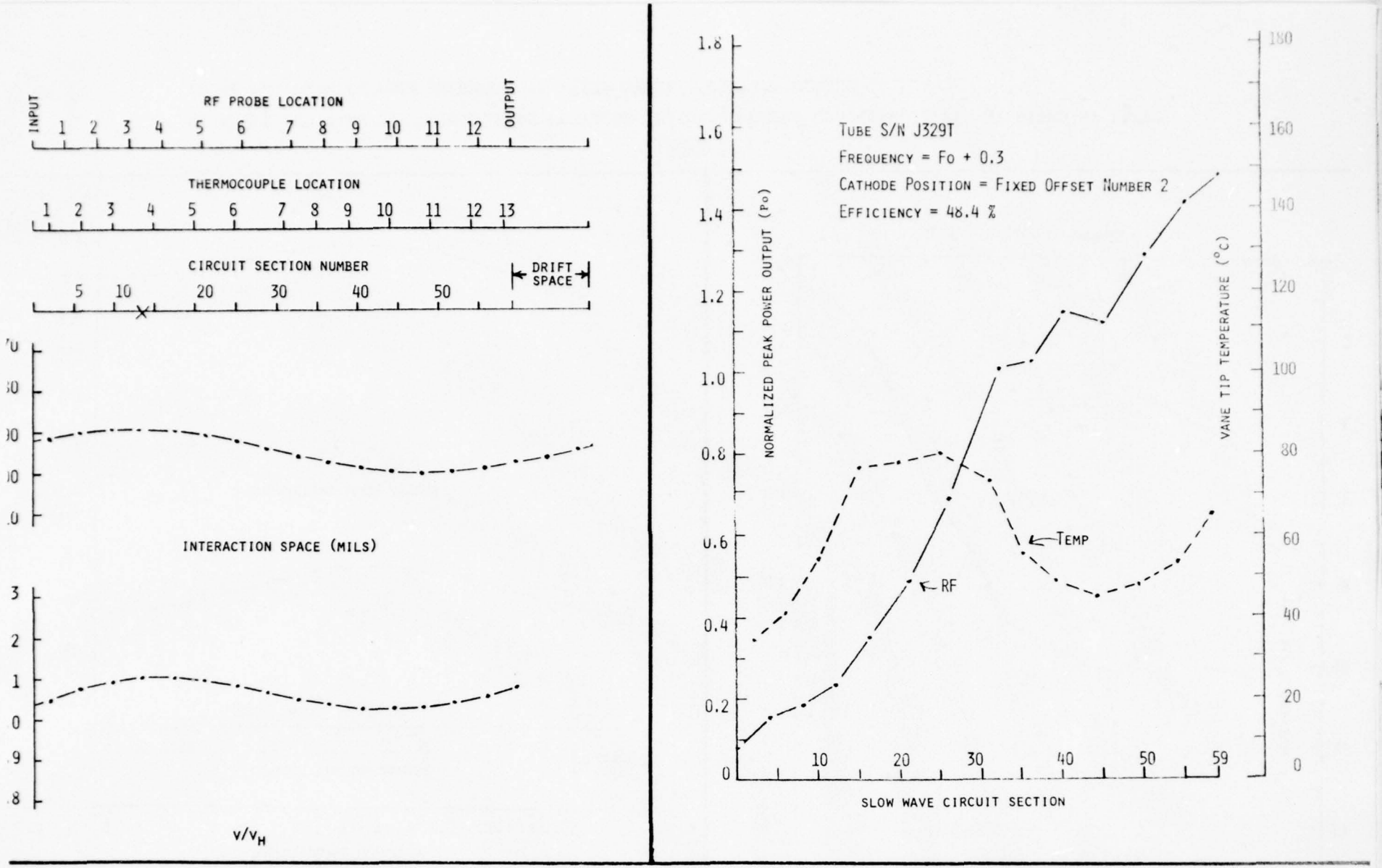

FIGURE 54

RF POWER AND VANE TIP TEMPERATURE PROFILES IN INSTRUMENTED CFA (S/N J329T) AT RATED RF INPUT (0.08 Po) WITH CATHODE ADJUSTED TO FIXED OFFSET POSITION NUMBER 2.

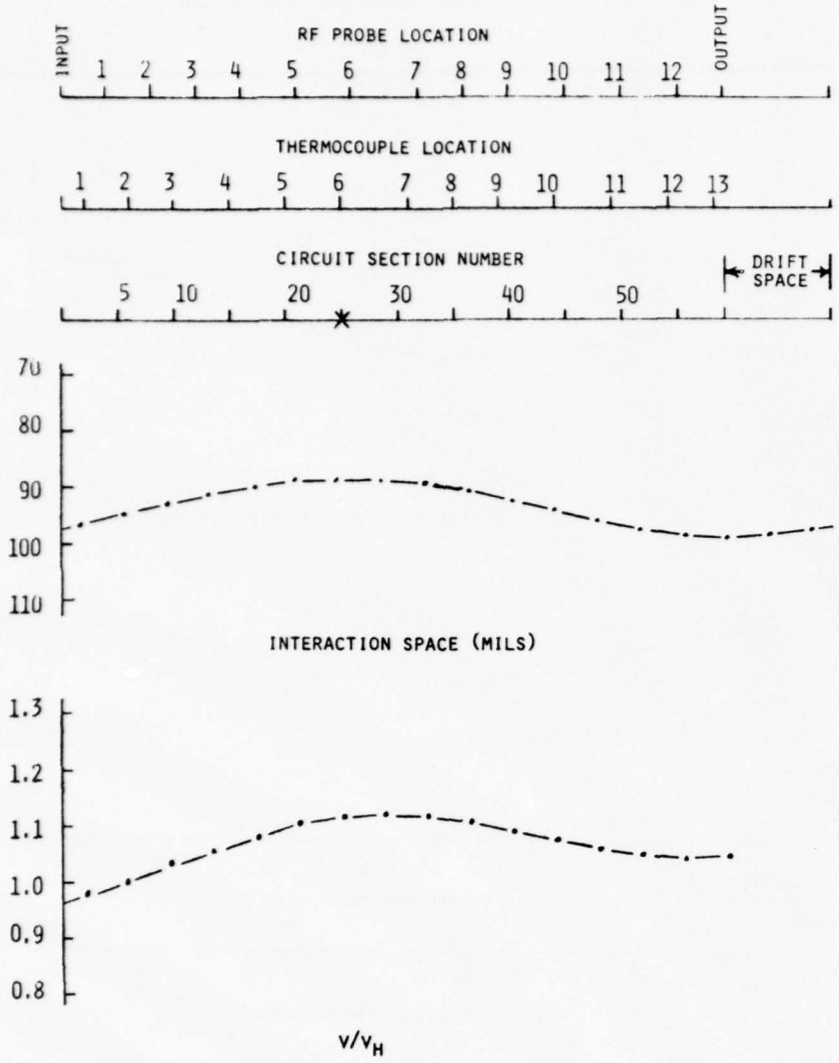

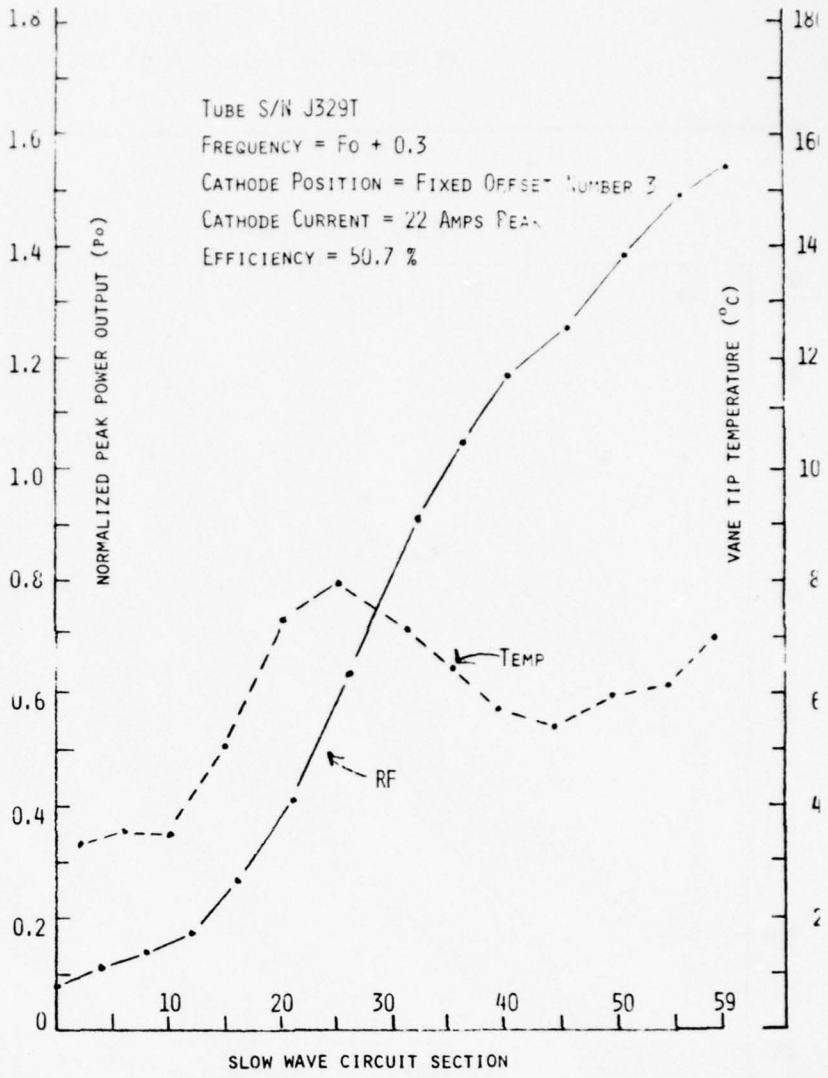

FIGURE 55

RF POWER AND VANE TIP TEMPERATURE PROFILES IN INSTRUMENTED CFA (S/N J329T) AT RATED RF INPUT (0.08 Po) WITH CATHODE ADJUSTED TO FIXED OFFSET POSITION NUMBER 3.

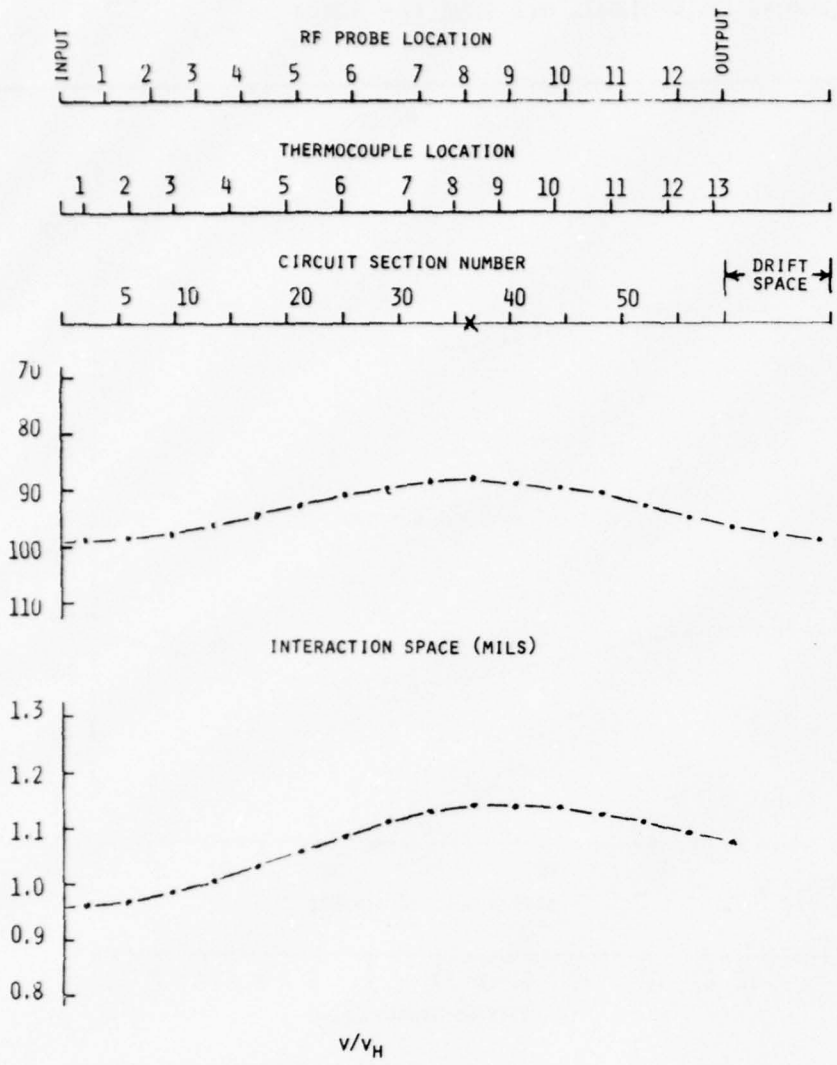

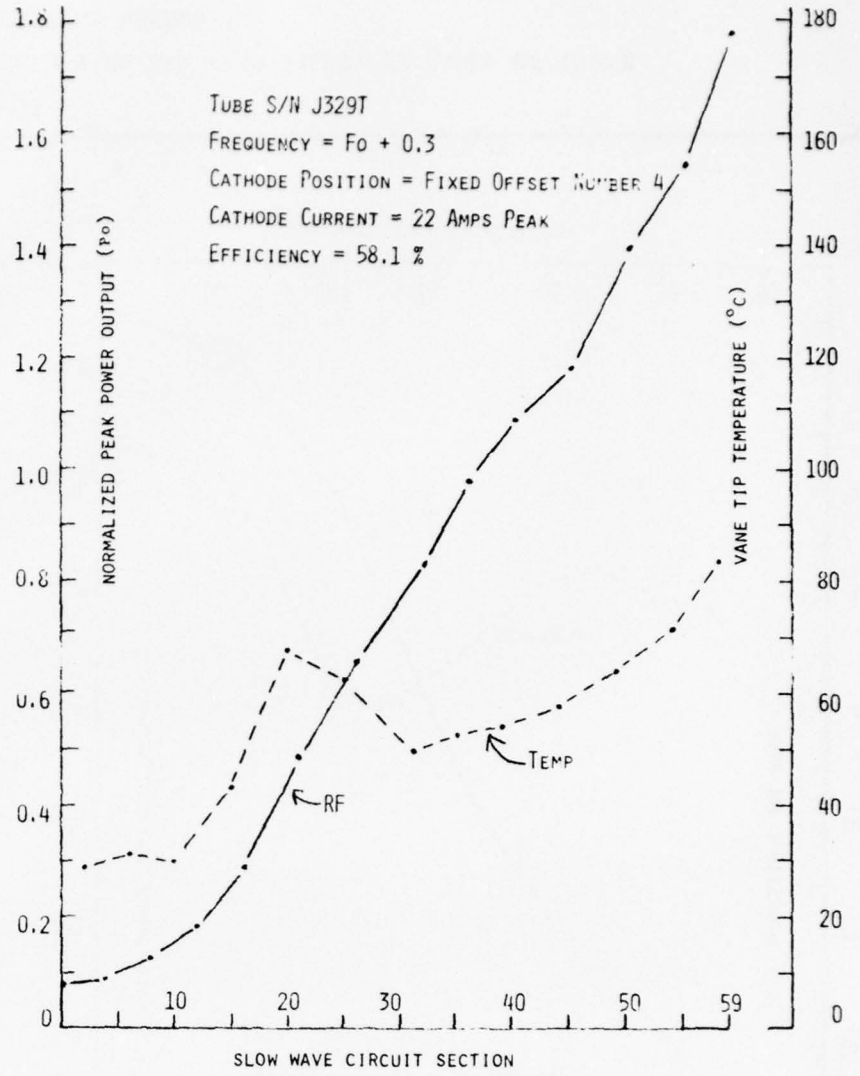

FIGURE 56

RF POWER AND VANE TIP TEMPERATURE PROFILES IN INSTRUMENTED CFA (S/N J329T) AT RATED RF INPUT (0.08 Po) WITH CATHODE ADJUSTED TO FIXED OFFSET POSITION NUMBER 4.

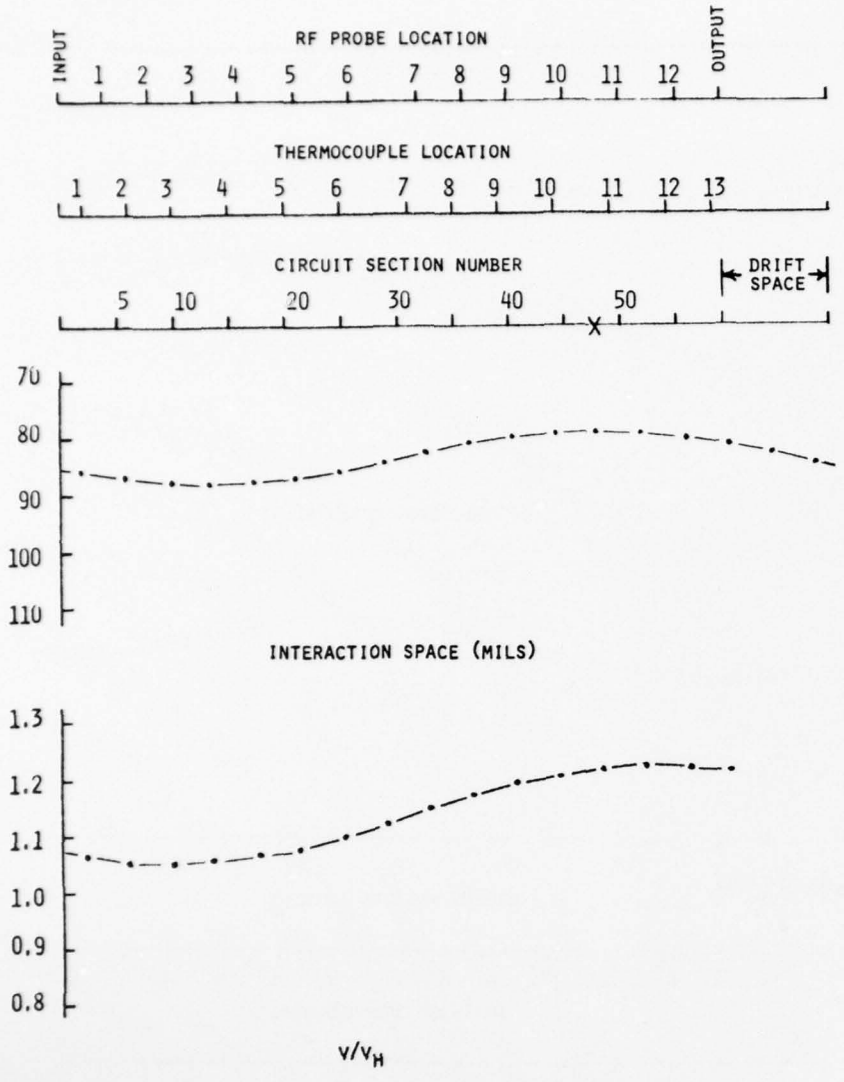

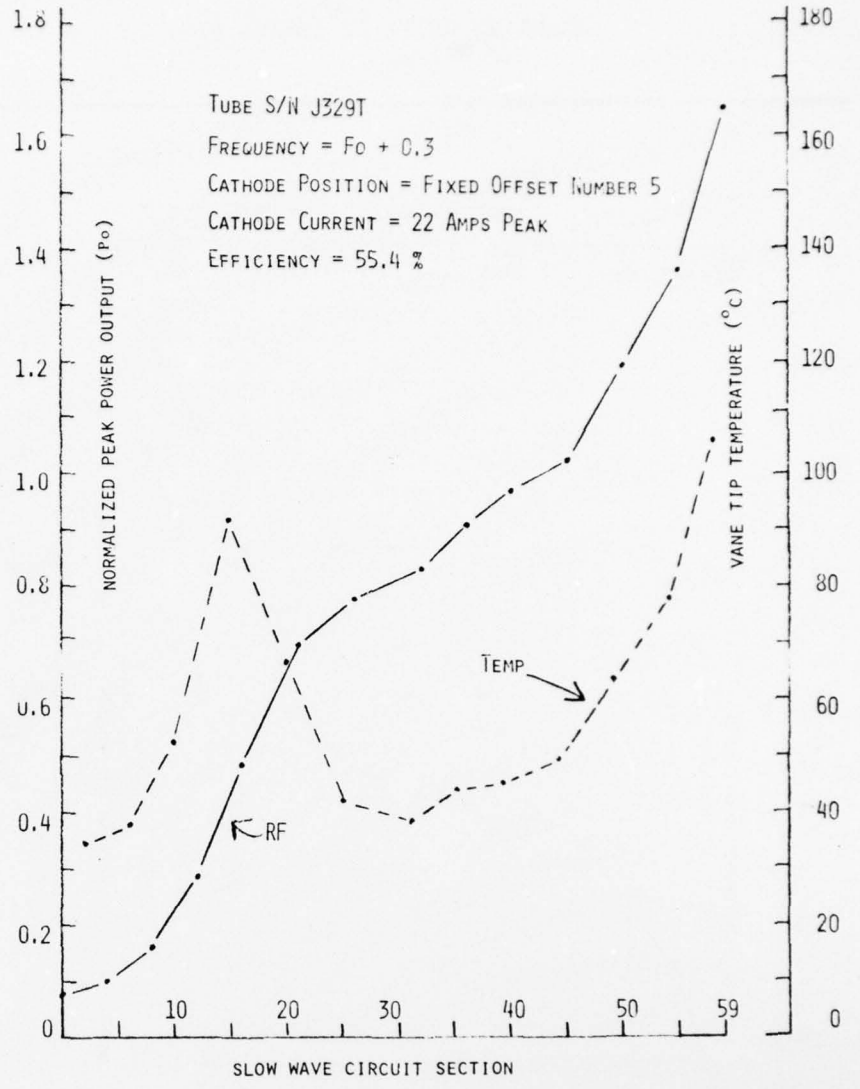

FIGURE 57

RF POWER AND VANE TIP TEMPERATURE PROFILES IN INSTRUMENTED CFA (S/N J329T) AT RATED RF INPUT (0.08 Po) WITH CATHODE ADJUSTED TO FIXED OFFSET POSITION NUMBER 5.

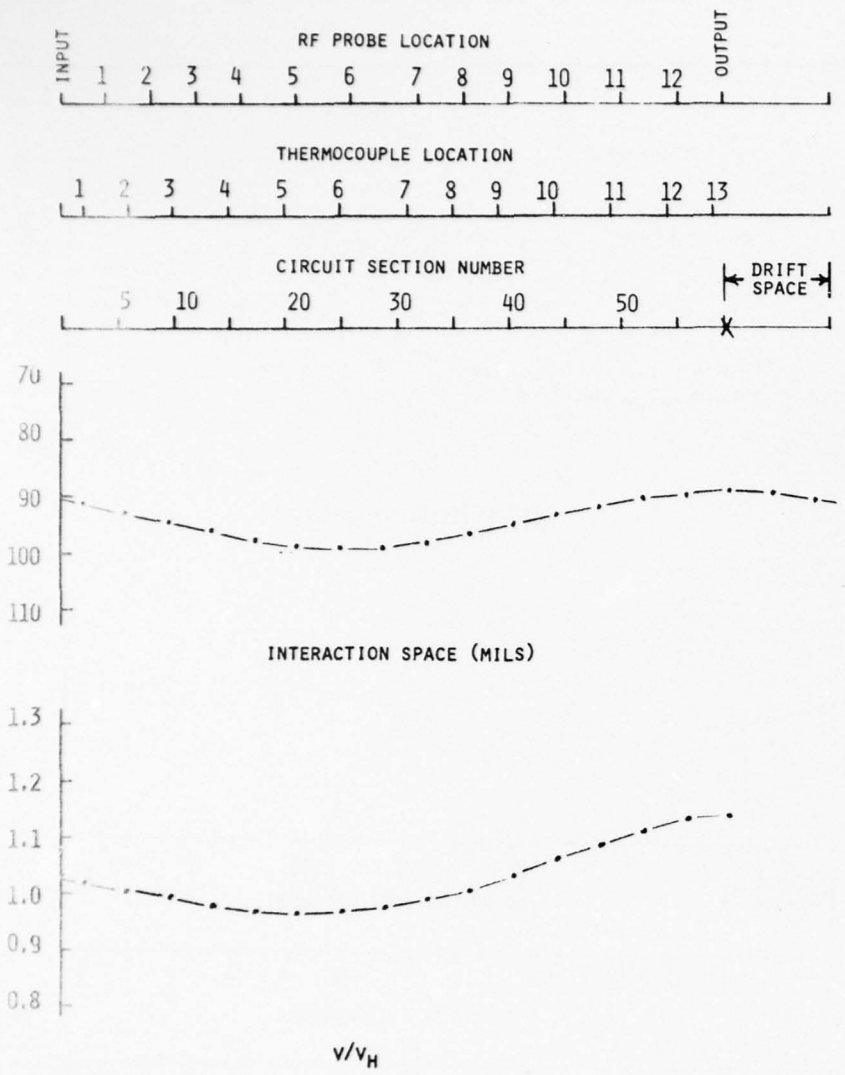

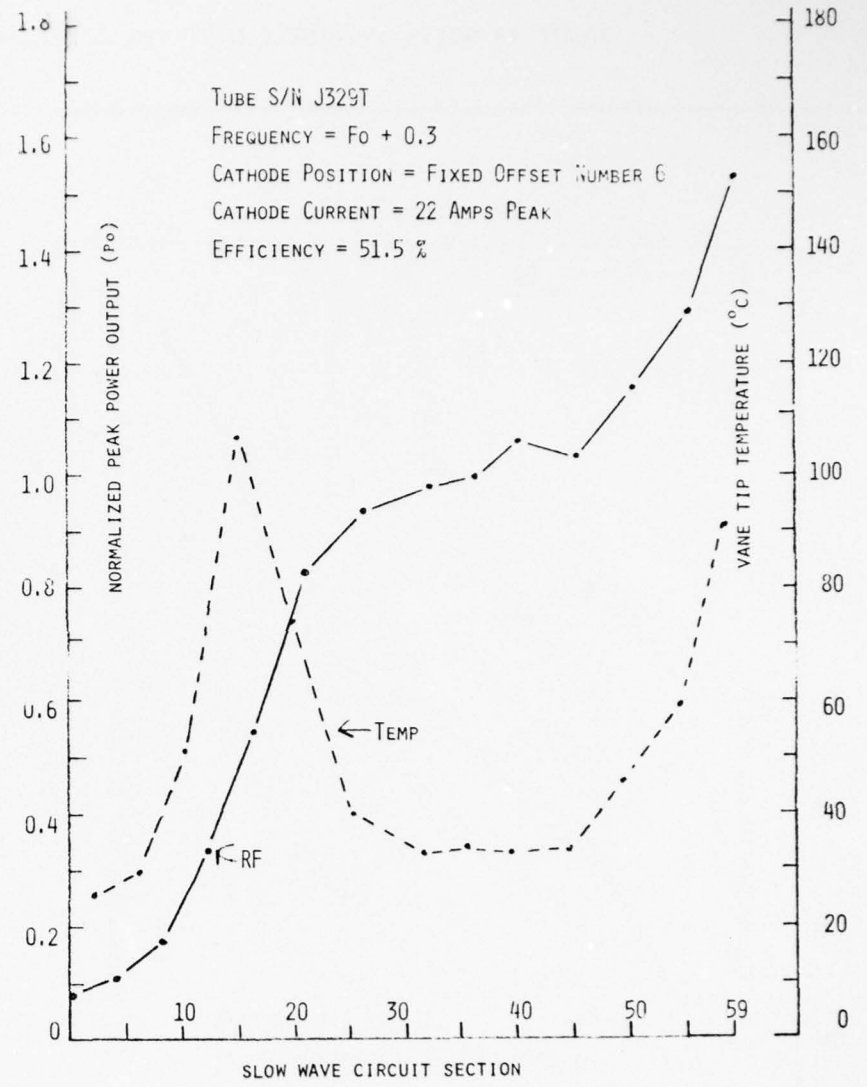

FIGURE 58

RF POWER AND VANE TIP TEMPERATURE PROFILES IN INSTRUMENTED CFA (S/N J329T) AT RATED RF INPUT (0.08 Po) WITH CATHODE ADJUSTED TO FIXED OFFSET POSITION NUMBER 6.

Another noteworthy feature is the change in the magnitude of the peak in the vane tip temperature profile as the cathode position changed. In the first position, the temperature peak has the highest value and decreases progressively to position number 4, and then continues to increase through position number 6. This behavior is explicable by use of the spoke current depletion model described previously. We assume that current is fed from the circulating hub into the spoke near the output by a diminishing cathode-anode space and that all of that current could not be transported to the anode. Under these conditions much reentrant space charge would be available near the input position of the circuit and a normal RF drive signal could capture it and transport it to the anode for local collection and heating. These are the conditions that are present in position number 1. For positions number 2, 3, and 4 there is a gradual change in geometry to one at the output that has a marked reverse taper near the output. This means that progressively less current was fed into the spoke and more of that within the spoke was transported to the anode. Progressively less current about the hub was available for reentrancy, and the localized current collection and heating near the input region of the circuit diminished. Hence, the vane temperature peak decreased. For positions 5 and 6 the interaction space geometry is changing back toward that of position number 1 so the trend reverses.

It is also interesting to note the change in overall efficiency with change in geometry. The efficiency is highest at

position number 4 where the temperature peak at the input is lowest and degrades progressively with departure from it. This suggests that the decrease in efficiency is due to lack of optimized use of the reentering space charge in a CFA with a drift space. Space charge dispersal can occur in the drift space and much current could reenter the interaction region in unfavorable phase conditions.

The power growth profile at position number 4 is reasonably constant across most of the interaction region. In addition, the vane tip temperature profile is relatively uniform over most of the circuit. These conditions are thought to be a desirable goal for the CFA for reliability and long operating life provided they can be obtained while maintaining or improving other properties of the tube. Therefore, some other tests were made with the interaction space profile of this position. For a first test the RF drive power was reduced 3 dB to 0.04 Po. The power growth and temperature profiles for this condition and rated drive are shown in Figure 59. The results are similar to those obtained with cathode adjusted for maximum gain. The power level is higher over the first portion of the circuit for the higher drive level, but both profiles converge toward the same saturated power output near the end. Again, the thermal peak is larger and closer to the RF input for the larger RF drive power.

Measurements were made for position number 4 at fo+0.1, fo+0.3, and fo+0.5. The profiles are shown in Figures 60-62. The tube operated across the band with the general shapes of the power growth and temperature profiles remaining about the same. Efficiency

increased with frequency. Stable operation at the upper end of the band was limited to 19 peak amperes for cathode current. Even so, the efficiency was in excess of 60%. These results suggest that proper programming can, indeed, lead to a broadband, forward wave CFA with 20 dB gain and with efficiency in the 50-60% range.

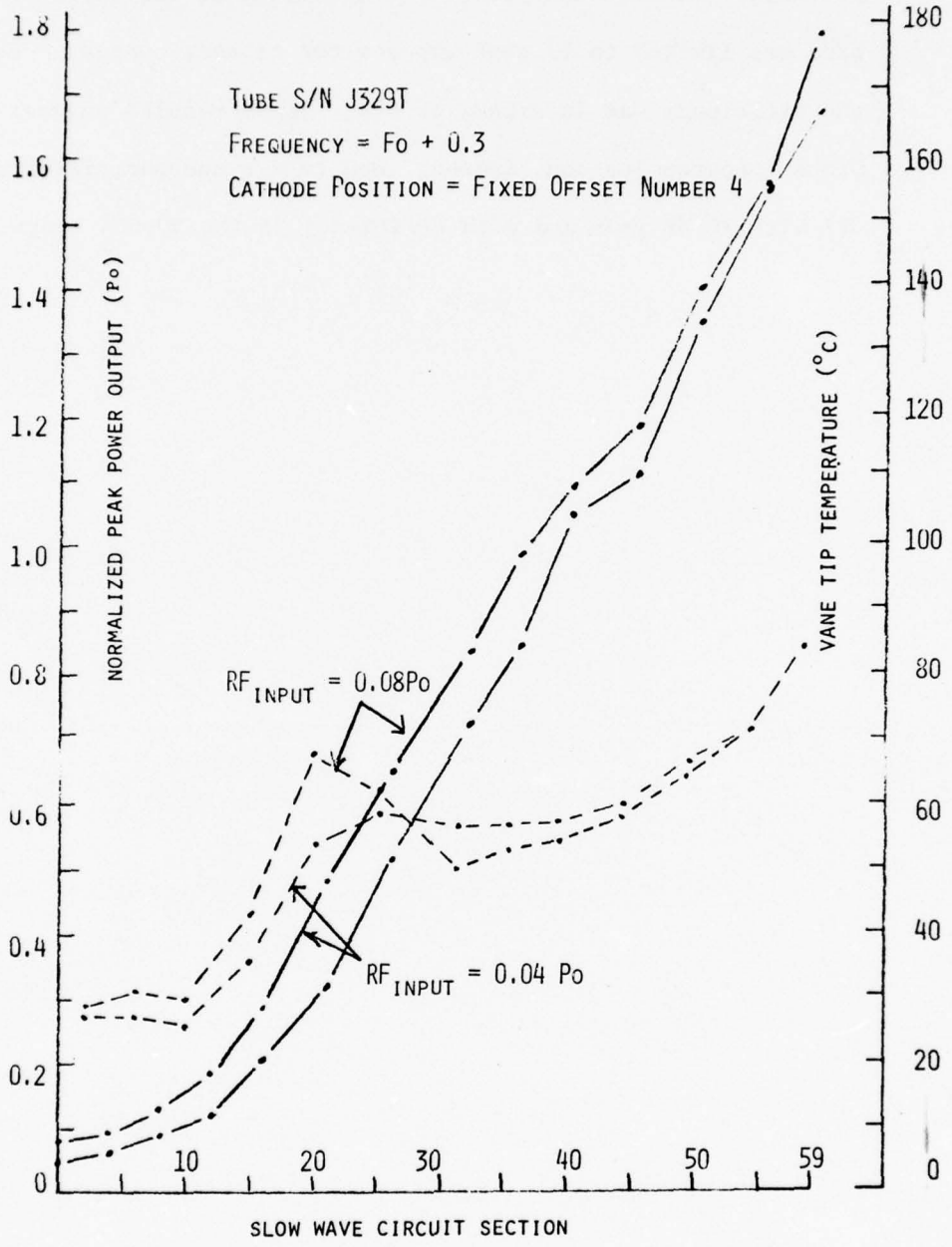

FIGURE 59

RF POWER AND VANE TIP TEMPERATURE PROFILE AS A FUNCTION OF RF DRIVE LEVEL WITH CATHODE IN FIXED OFFSET POSITION NUMBER 4.

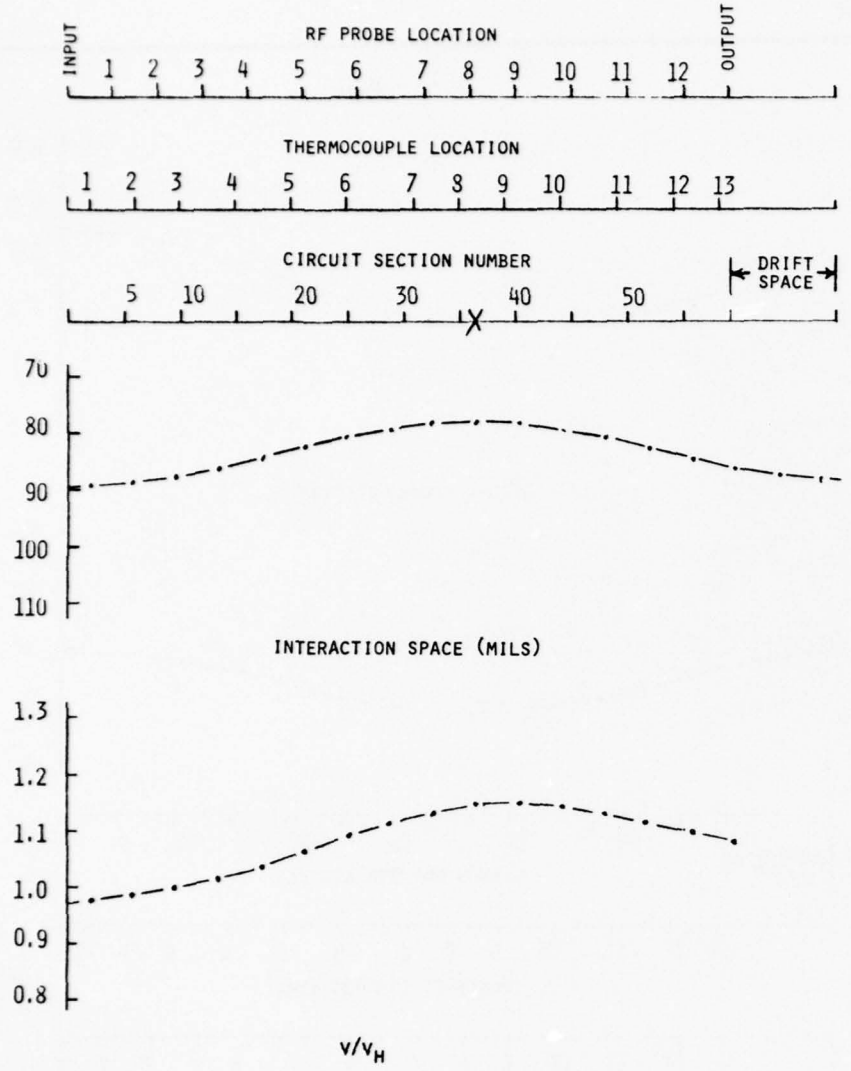

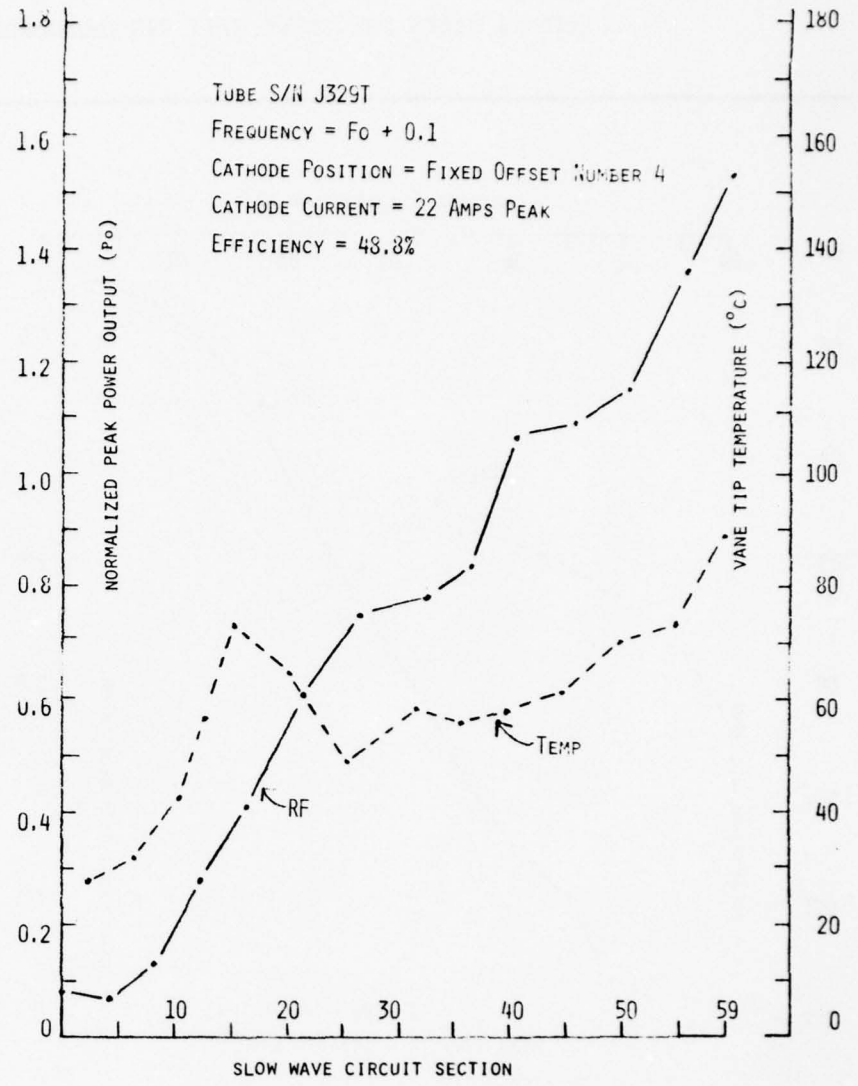

FIGURE 60

RF POWER AND VANE TIP TEMPERATURE PROFILES IN INSTRUMENTED CFA (S/N J329T) AT RATED RF INPUT LEVEL (0.08 Po) AND SPECIFIED FREQUENCY WITH CATHODE IN OFFSET POSITION NUMBER 4.

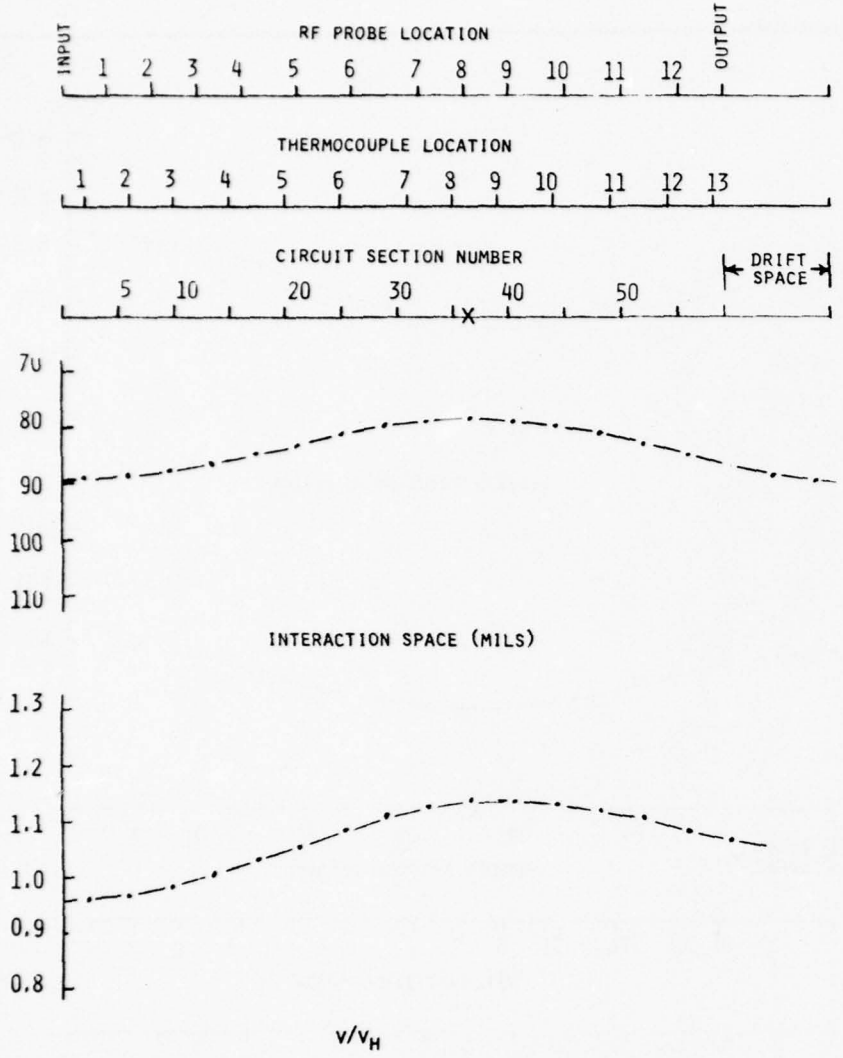

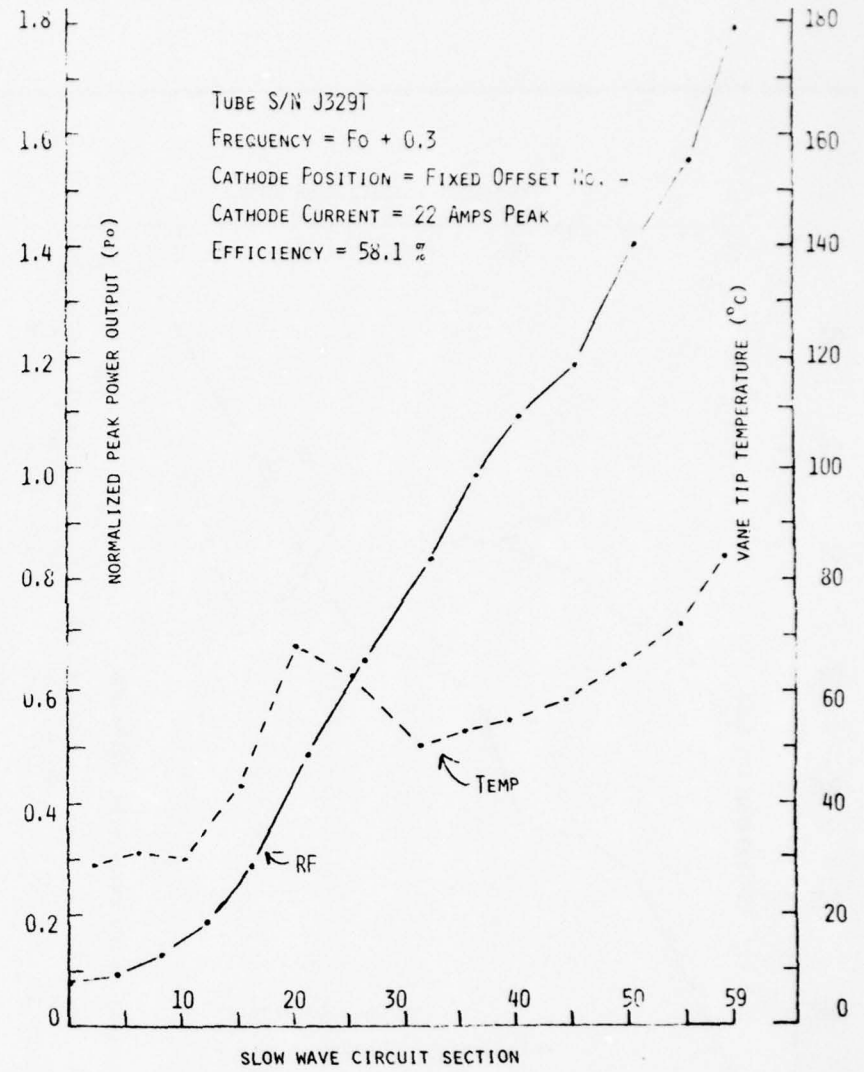

FIGURE 61

RF POWER AND VANE TIP TEMPERATURE PROFILES IN INSTRUMENTED CFA (S/N J329T) AT RATED RF INPUT LEVEL (0.08 Po) AND SPECIFIED FREQUENCY WITH CATHODE IN OFFSET POSITION NUMBER 4.

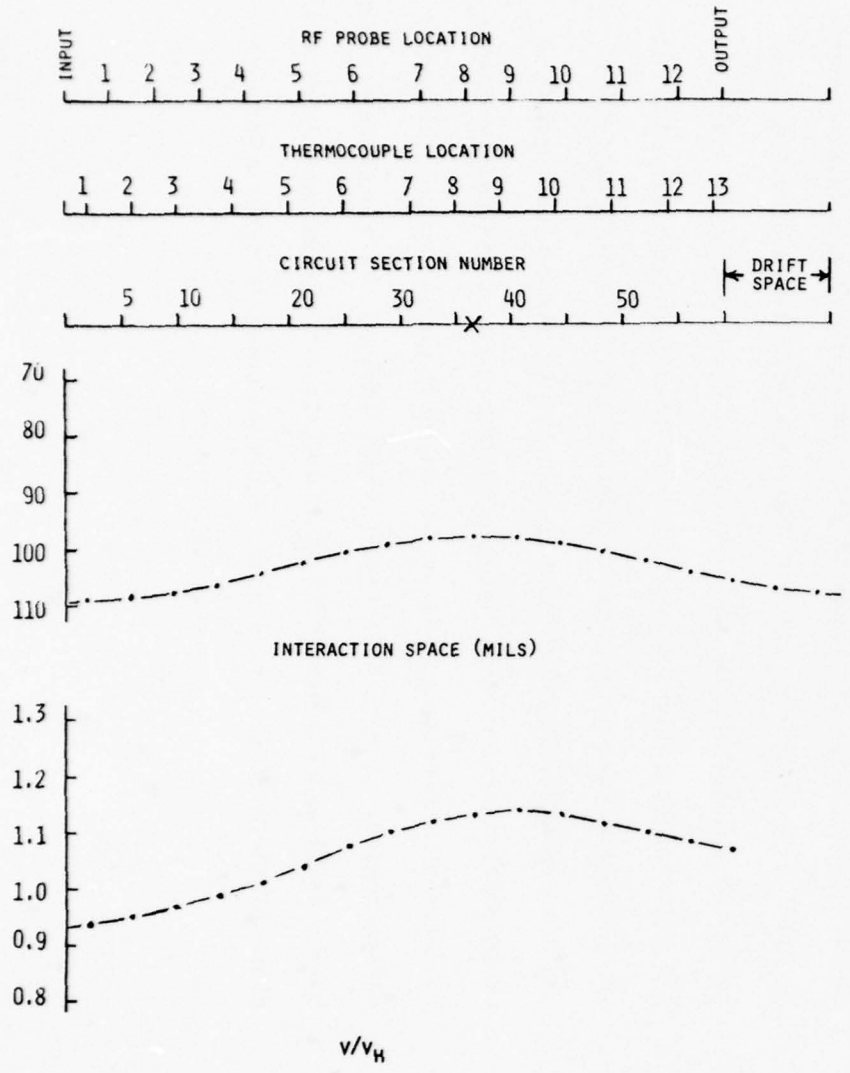

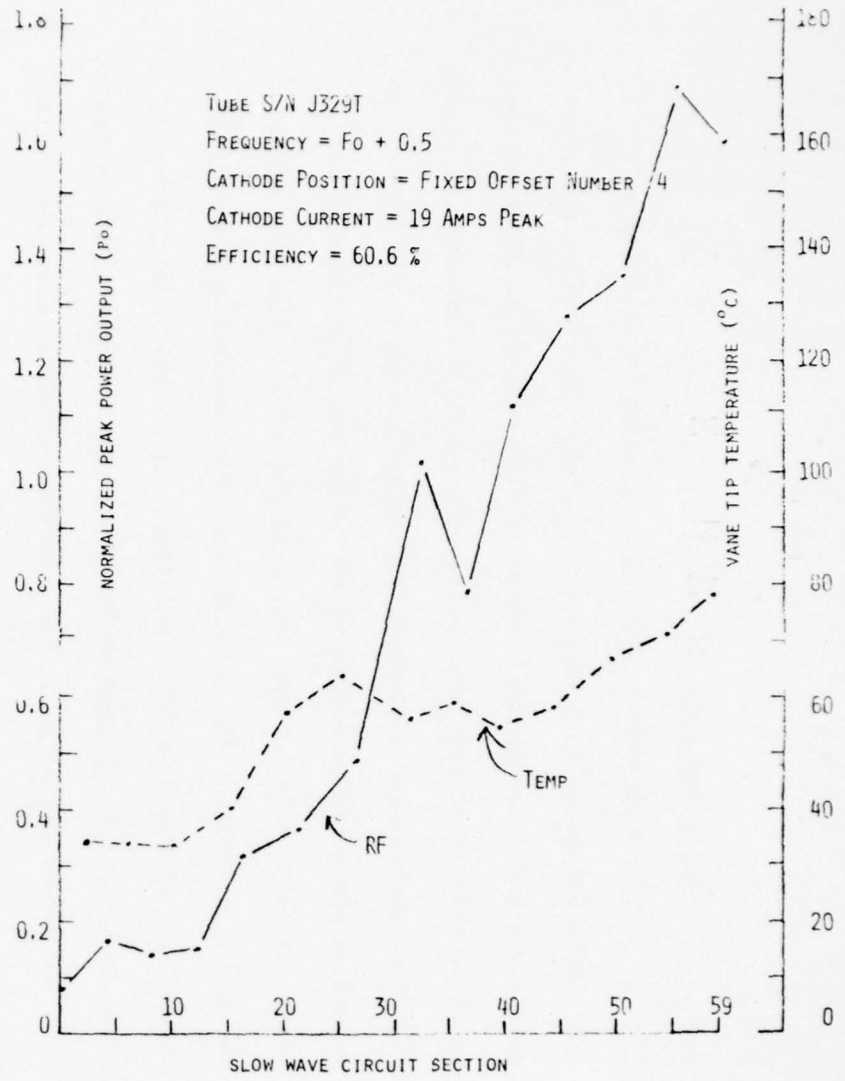

FIGURE 62

RF POWER AND VANE TIP TEMPERATURE PROFILES IN INSTRUMENTED CFA (S/N J329T) AT RATED RF INPUT LEVEL (0.08 Po) AND SPECIFIED FREQUENCY WITH CATHODE IN OFFSET POSITION NUMBER 4.

5.3 Noise Reduction

Several methods for reducing noise in emitting sole CFA's were suggested earlier in this report. They can be separated into three broad categories. These include methods in which attempts would be made to control the source of current to minimize the sources of noise, methods for minimizing the amplification of the noise, and method of preventing coupling of the noise out of the tube. The first category could include use of shaped cathode surfaces and/or the magnetic field at the cathode surface to control emission processes. In addition, cathode materials, fabrication and processing procedures could be changed to improve the uniformity of the secondary emission properties since it has been speculated by some that surface variability of emission could be a source of noise. The second category could inlcude the use of shaped end hats and magnetic fields to modify the range of values of E/B that exist in the interaction region. It has been speculated that this wide range of values that currently exists permits amplification of broadband noise within the interaction region without the need of a slow wave circuit. It is speculated that potential resonant or near resonant conditions exist because of the electron reentrancy. An alternate approach or supportive action might include the use of d.c. biased electrodes to interupt the noise growth during multiple passes around the interaction region. The third category might include the use of beam scrapers in the drift space to remove from circulation the reentrant space charge close to the circuit. This would allow a strong RF input signal to

the CFA to more properly phase lock the circulating space charge to the RF wave while it is remote from the circuit. Noise in the stream ordinarily close to the circuit would not be coupled to the circuit. Alternatively, a d.c. biased electrode might be used to interrupt the coupling process somewhere in the interaction region.

None of these procedures were investigated on this program directly. However, several of the experimental results showed that improved control of the reentering space charge could lead to reduced output noise. The interpretation of these experiments is that a reverse taper in the output region of the tube tended to reduce the recirculating space charge and that stronger RF fields at the input to the circuit provide rapid collection of noisy current. The net result is an improved signal-to-noise output from the tube. These experiments lend support to the concept of a beam scraper to remove recirculating space charge near the circuit.

A beam scraper consists of a protrusion from the anode in the drift space that decreases the cathode-anode spacing. This causes an increase in the d.c. electric field intensity. Electrons are drawn toward the anode and collected. The scraper configuration should be such that only a portion of the recirculating electrons near the anode are collected and the remainder is allowed to reenter the interaction region. Two possible configurations for achieving this are shown in Figure 63. Figure 63A shows a chord skimmer in which the electric field intensity is gradually increased and then

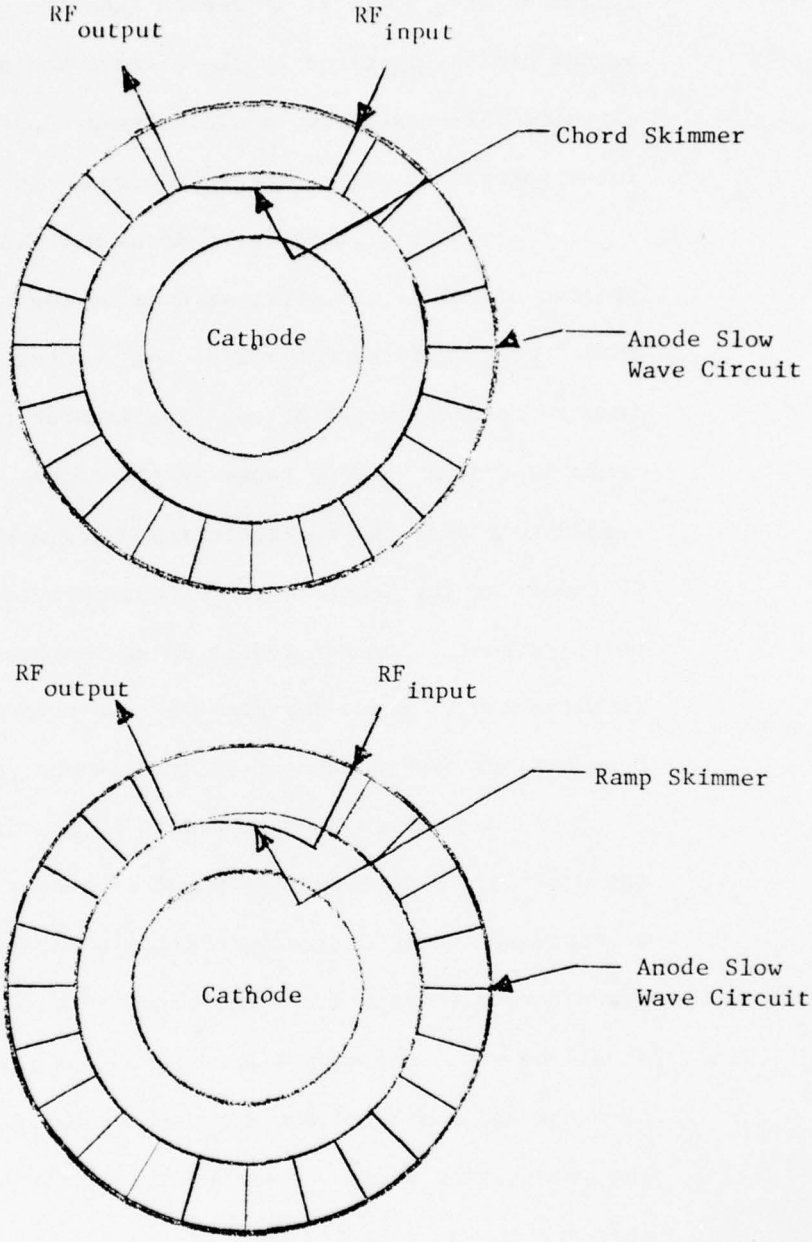
RF output
RF input
Chord Skimmer
Cathode
Anode Slow
Wave Circuit
RF output
RF input
Ramp Skimmer
Cathode
Anode Slow
Wave Circuit

FIGURE 63

gradually decreased to the original value. This is intended to pull all of the current toward the anode, collect a portion of the anode, and allow the remainder to move away from the anode as the d.c. electric field returns to its original value. This is intende to leave a space charge-free region near the circuit while maintaining the same interaction condition at the input to the interaction region. Figure 63B shows a ramp skimmer. In this case, the cathode-anode spacing is progressively decreased and then abruptly returned to its original value. This is intended to more nearly assure a space charge-free region near the anode at the RF input. However, this may be at the expense of possible marked perturbing effects on the reentrant hub and remaining space charge at that point. Clearly, other variations could be used that might be more effective. Computer simulations may be useful in optimizing the geometry.

Current collection that is not productive in generating microwave power will obviously lead to a reduction in efficiency. However, the reduction in efficiency due to a skimmer or scraper is not as large might be envisioned initially. Although an effective skimmer might remove 20-40% of the reentering space charge, this is only that portion of the total cathode current flowing through a single spoke at any one time. Since a CFA may have a circuit length of about fifteen wavelengths, it means that the total cathode current at any one time is divided among fifteen spokes, although probably not equally. Furthermore, the current that is being collected is above the hub surface so that it will have already been transported

across a large portion of the cathode-anode space and will not strike the anode at full voltage. For purposes of illustration, assume that the total cathode current is divided equally among fifteen spokes (although not likely to be true) and assume that all of this current is collected at an effective potential equal to half of the anode-cathode voltage (although the space charge is spread over many potential levels). This implies a reduction in efficiency due to heating of the skimmer with dissipated power equal to $\frac{I}{15} \times \frac{V}{2}$. This is about three percent of the total d.c. power into the tube. This approximation indicates only a small reduction in efficiency regardless of whatever is the actual current in the spoke and at whatever potential difference they are collected.

Control of the reentrant space charge by use of a skimmer to produce a reduction of noise had been successfully demonstrated prior to this program on another tube type. However, it was not examined in a fully-instrumented tube. On the other hand, Varian/Beverly had another contract from the Naval Sea Systems Command (No. N00024-76-C-5102) to explore methods for reducing noise in forward wave crossed-field amplifiers similar to the SFD-261. These experiments used a tube with a tapered pitch similar to J329T, but without any thermocouples or RF probe sensors. The tube was fabricated with a removable drift block that was screwed into place in the tube. The tube could be opened and the drift block changed to provide different skimmer geometries.

The tube was assembled first with a drift block insert that simulated the standard tube; i.e., the drift block face matched the circular anode contour. The tube also had a circular cathode. The signal-to-noise ratio at the output of the tube exceeded the specification value across the band for the SFD-261 even when the cathode was on mechanical center. Recall that the standard SFD-261 with a circular cathode would not even operate across the full operating band. Next the cathode position was adjusted and the S/N ratio improved such that performance exceeded that of the standard tube with tapered cathode even after cathode adjustment by 3-5 dB across the band.

Next this test vehicle was modified by using a different drift block that produced a chord skimmer that reduced the cathode-anode spacing by 20% at the point of closest spacing. This tube with cathode on mechanical center had an S/N ratio that exceeded the optimized standard tube by 2-8 dB across the band. When the cathode position was optimized this difference increased to 5-12 dB.

Next the tube was again modified to inlcude a different drift block that formed a chord skimmer that reduced the cathode-anode spacing by 40% at the point of closest spacing. The performance for this tube was best when the cathode was on mechanical center. This tube has an S/N ratio that was 10-13 dB better than the standard optimized SFD-261. These results show that the skimmer drift blocks produce a definite reduction in noise power output from these tubes.

It is interesting to note that the cathode-pulsed tubes did not arc even though the interaction space was markedly reduced in the drift space. This had been a point of concern prior to the experiments because the spacing between end hats and the drift block were significantly reduced from that in a standard tube.

It would be extremely interesting to investigate the effect of drift space skimmers in a fully instrumented tube to determine exactly what is occurring. It is speculated, of course, that the peak in the vane tip temperature profile near the input will not be present.

6.0 CONCLUSIONS FROM THE EXPERIMENTAL EFFORTS WITH THE FULLY-INSTRUMENTED TUBES

Many interesting things have been learned about reentrant steam, emitting sole, forward wave, crossed-field amplifiers from the experiments using the fully instrumented tubes. Some of these represent new information about these tubes and some confirm things that were only speculation heretofore. Other things are not yet fully understood, but have provided insight into other approaches for improving these tubes. These have all been discussed previously in this report and the earlier ones submitted on this program. However, it is believed to be worthwhile to summarize them here.

1. The use of fully-instrumented, crossed-field amplifiers employing RF and thermal sensors has proved to be a very useful technique for identifying power growth and vane tip temperature profiles within the tube without introducing perturbing influences. Further instrumentation such as a segmented cathode to determine secondary emission yield as a function of position is feasible. The data obtained are satisfactory for comparison with computer simulations.

2. It was demonstrated that a cathode-pulsed tube employing a dispersive, uniform pitch, slow wave circuit, such as in the SFD-261, will not function properly across a wide bandwidth with a circular cathode located on mechanical center. Wider bandwidth operation was achieved by altering the cathode position showing that a programmed interaction space improves tube RF performance.

3. Disregarding RF performance of the amplifier, it was shown that the most uniform profiles for the vane tip temperatures were obtained with the cathodes located on mechanical center.

4. It was demonstrated that the present tapered cathode profile and adjustment procedure do not produce what is believed to be an optimum power growth and vane temperature profile for the SFD-261. The present profile was developed for d.c. operation of this tube. Cathode-pulsed operation offers additional considerations. A change in cathode geometry might lead to a more uniform vane temperature for the same output power.

5. It was demonstrated that the final positioning of the cathode for overall optimized RF performance was not extremely critical with regard to radial positioning of the cathode, but the increase in the vane tip temperature was very sensitive. This lead to modified procedures for cathode adjustment in the SFD-261.

6. The waveguide-to-slow wave circuit matching technique effects the broadband noise output from the tube as well as the reflected noise internal to the tube. Very broadband matching configurations are desirable if the tube outline specifications will permit their use.

7. It was shown that harmonic signals and spurious peaks may be present internally for the tube, but not apparent in the output signal.

8. Feedback effects due to electronic reentrancy and circuit reflection exist internal to the tube and are detectable. Electronic feedback is present even in a CFA with a drift space.

9. The existence of two gain mechanisms in the reentrant stream CFA has been verified. The amplification process near the RF input occurs primarily because of utilization of reentrant

space charge above the circulating electron hub and amplification near the output utilizes current extracted directly from the hub. This is confirmed by computer simulation.

10. It has been demonstrated that noise power from a CFA is caused, in part, by recirculating space charge near the anode. Noise can be reduced by use of a beam skimmer to partially remove this current.

11. Data was obtained which indicate that a reverse taper in the cathode-anode spacing near the output of the tube reduces the recirculating space charge. This may be responsible for reducing noise output from reentrant crossed-field amplifiers. This effect has been partially confirmed by computer simulation.

12. Cathode-anode space profiles that result from empirical adjustment of the cathode position have greater variation along the interaction space than anticipated based upon the original concepts of programmed interaction. It is believed that this results because of the existence of two gain mechanisms in the tubes. The empirical adjustment tends to accommodate both.

13. It is known that a small reduction in cathode voltage often leads to a small reduction in output power, but a much better improvement in signal-to-noise ratio. It is now thought that this may be the result of improved interaction at the input with recirculating current at the expense of interaction near the tube output. An improved programmed interaction geometry may lead to reduced noise without degradation of output power. Computer simulation may lead

to a better design configuration.

14. Use of a tapered pitch, slow wave circuit has been demonstrated to provide a better method for programmed interaction than use of a tapered cathode profile. Combinations of the two are expected to provide even better performance.

15. The broadband gain of a tube similar to the SFD-261 was increased from 12 dB to a value of 18-21 dB by use of a tapered pitch circuit. High gain was produced at an efficiency of 50% or more across the band.

APPENDIX A

INTRAPULSE NOISE (IN-BAND) MEASUREMENTS

THIS MEASUREMENT METHOD IS TAKEN FROM THE ACCEPTANCE TEST PROCEDURE FOR THE SFD-261 CFA. SPECIFIC CLASSIFIED PARAMETERS HAVE BEEN OMITTED.

INTRAPULSE NOISE (IN-BAND)

Test conditions are as follows:

A. Frequency: As specified.

B. Pulse Length: As specified.

C. Duty: As specified.

D. Cathode voltage rate of rise shall be between 120 and 160 kV/μsec. measured at the 70% point and shall be verified by viewing the rise time on an oscilloscope using a Tektronix P6015 high-voltage probe connected directly to the cathode lead. A time mark generato shall be used to calibrate the time base. High-voltage probe compensation shall be verified by viewing the full voltage pulse.

E. Cathode voltage fall time shall be between 100 and 200 nanoseconds and shall be verified by viewing the fall time on an oscilloscope using a Tektronix P6015 high-voltage probe connected directly to the cathode lead. Fall time is measured from the 100% voltage level to the 80% voltage level, where 0% voltage level is established as the level at the start of the voltage pulse.

Figure 1 is a diagram of the test set-up used to make the measurements. A sample of the RF pulse is applied to the spectrum analyzer which is used in this measurement as a tunable receiver. It should be noted that neither the leading nor the trailing edge of the pulse will be clipped. An output is taken from the IF test point at the rear of the analyzer and amplified. The amplified output is gated and measured by an rms meter and an oscilloscope. A pulse generator drives the modulator so as to gate on only the peak of the analyzer's response to the input pulse. Analyzer noise in the interval between pulses is gated off to improve sensitivity. The detailed procedure for making the measurement is described below:

1. The test equipment shown in Figure 1 will be located in a screen room.

2. When making the measurment, the transmitter will be run with the maximum duty available from the test station.

3. The measurement should be repeated for the drive pulse only to be sure that its noise is lower than that seen at the amplified output. Note that when this measurement is made for a CFA, the CFA should be turned off or disconnected from the drive pulse to avoid noise emanating from the CFA input.

4. Tune the analyzer to the center frequency of the pulse spectrum. This is found by watching the display while adjusting the IF gain to keep the signal amplitude in the display range. Test will be conducted at F1, F2, F3, F4 and F5.

5. Set the analyzer bandwidth to 1/10T, where T is the pulse width, or to the nearest available bandwidth.

6. Adjust the input attenuator of the analyzer for a maximum input wihtout amplitude compression. This is done by observing the pulse spectrum on the analyzer display and reducing attenuation in 10 dB steps. When a step is reached where the peak of the spectrum does not increase by 10 dB in the display, 10 dB attenuation is added and the input attenuator left at that setting.

7. Change the vertical display from log to linear.

8. Stop the analyzer sweep by disconnecting the coaxial cable carrying the sweep signal from the display to the analyzer.

9. Synchronize the oscilloscope and display the pulse as seen at point "A" with the modulator bypassed.

10. Observe the pulse generator output with the oscilloscope and position the output pulse to be in time coincidence with the analyzer output pulse as seen at point "A".

11. Connect the pulse generator and modulator and adjust the pulse generator amplitude so that the pulse peak is not attenuated at point "A".

12. Retune the analyzer to maximize the pulse seen at point "A". Also, reduce IF gain to prevent saturation as seen on the oscilloscope.

13. Adjust the range of the rms voltmeter so that the meter reads near the 0 dB mark on the scale.

14. Record the meter reading and IF attenuator setting in the log.

15. Retune the spectrum analyzer to a point in the RF band where noise is to be measured (usually 150 MHz away from the carrier frequency on high or low). This point should be selected while the analyzer is sweeping to be sure that the pulse spectrum has dropped below the amplifier noise level at the selected point.

16. Increase the IF gain to obtain a reading on the rms voltmeter. Do not change the meter scale. Check the oscilloscope to be sure that the pulse at point "A" is not in saturation.

17. Record the meter reading and IF attenuator setting in the log.

18. When the meter is reading the noise level, Step 17, increase the attenuation of the input attenuator on the spectrum analyzer by 10 dB. This should cause the meter reading to drop, thus proving that the meter is reading the noise on the input pulse rather than analyzer noise.

19. Convert the spectral density ratio of the above measurements to a CW signal-to-noise ratio as follows:

The measured ratio, R, is...

$$R = \frac{\text{Spectral density at the peak of the pulse spectrum}}{\text{Noise spectral density outside the signal spectrum}} \quad (1)$$

Rewriting this ratio in terms of the pulse parameters...

$$R = \frac{\hat{S}(\tau f_m)^2/f_m}{N_o(\tau f_m)} = \frac{\hat{S}}{N_o(1/\tau)} \quad (2)$$

where

$\hat{S}$ is the peak pulse power

τ is the pulse width

f_m is the pulse repetition frequency

N_o is the noise spectral density during the pulse

The desired CW signal-to-noise ratio is....

$$\frac{S}{N} = \frac{\hat{S}}{N_o B} \quad (3)$$

where B is the bandwidth in which the noise is measured.

Comparing equations (2) and (3), we see that R = S/N when $B = 1/\tau$. For example, if R is measured using a 1 μs pulse, this is equivalent to the CW signal-to-noise ratio where

the noise power has been measured in a 1 MHz bandwidth. Scaling the result to other bandwidths simply requires multiplying by the bandwidth ratio. Record the calculated values of in-band intrapulse noise on the data sheet for each operating frequency.